AFGHANISTAN

Multi-hazard risk assessment

THE WORLD BANK
IBRD • IDA | WORLD BANK GROUP

GFDRR
Global Facility for Disaster Reduction and Recovery

AFGHANISTAN

Multi-hazard risk assessment

THE WORLD BANK
IBRD • IDA | WORLD BANK GROUP

GFDRR
Global Facility for Disaster Reduction and Recovery

1818 H Street NW
Washington, DC 20433
Telephone: 202-473-1000
Internet: www.worldbank.org

Citation
Please cite the report as follows: Afghanistan—Multi-hazard risk assessment. Washington, DC: World Bank.

Cover photo: Raisa Jorge / Rumi Consultancy / World Bank.

Design: Ultra Designs, Inc.

Notes
1. All dollars ($) indicated are in United States dollars.

Acknowledgments

Prepared in collaboration between the Government of Afghanistan and the World Bank.

This report was prepared in response to a growing demand from the Government of Afghanistan to better understand and integrate risk information in policy planning and investments across various economic sectors. The Multi-Hazard Risk Assessment and Risk Profiles are a result of extensive research, analysis, and close collaboration between the Afghanistan National Disaster Management Authority (ANDMA), the Ministry of Rural Rehabilitation and Rural Development (MRRD), the Water Resource Department (WRD) of the Ministry of Energy and Water (MEW), the Ministry of Agriculture, Irrigation and Livestock (MAIL), and the World Bank.

This report is based on a national level risk assessment conducted by an international consortium, using data from national and international sources. The consortium was led by Deltares and included Global Risk Forum Davos, the Karlsruhe Institute of Technology, the Omran Technical Company, and the Italian National Agency for New Technologies, Energy and Sustainable Economic Development (ENEA).

The World Bank team was led by Federica Ranghieri, Senior Urban Specialist and Ditte Fallesen, Senior Operations Officer, and Task Team Leaders, including: Brenden Jongman, Young Professional; Guillermo Siercke, Disaster Risk Management Specialist; Abdul Azim Doosti, Disaster Risk Management Specialist Consultant; Julian Palma, Disaster Risk Management Specialist Consultant; Simone Balog, Disaster Risk Management Analyst; Sayed Sharifullah Mashahid, Disaster Risk Management Specialist Consultant; and Erika Vargas, Senior Knowledge Management Specialist. The editorial technical lead was Pasquale Franzese, Senior Energy Specialist Consultant.

The report could not have been developed without the guidance and support of World Bank management and advisors. We especially thank: Sameh Wahba, Director, Social, Urban, Rural and Resilience Global Practice (GSURR); Robert Saum, Director, South Asia Regional Programs and Partnerships (SARRP); Bernice K. Van Bronkhorst, Director, Climate Change Group; Christoph Pusch, Practice Manager South Asia DRM and Climate Change Unit (GSURR); Vladimir Tsirkunov, Lead Specialist; and Makoto Suwa, Sr., Disaster Risk Management Specialist (GFDRR).

Above all, we would like to thank and recognize our partners for their financial support, including Global Facility for Disaster Reduction and Recovery (GFDRR), and in particular, the Government of Japan under the Japan-World Bank Program for Mainstreaming Disaster Risk Management in Developing Countries. Without their generous support, the preparation of this report would not have been possible.

Photo: MivPiv

Foreword

In a country that is severely affected by natural hazards and climate change, the Afghanistan *Multi-Hazard Risk Assessment* and the accompanying *Afghanistan Risk Profile* showcase how risk information can be generated in a fragile and low capacity context, and how it can be used to inform development efforts across sectors to ensure greater resilience and sustainability.

Afghanistan is highly prone to intense and recurring natural hazards such as flooding, earthquakes, avalanches, landslides, and droughts due to its geographical location and years of environmental degradation, resulting in the frequent loss of lives, livelihoods, and property. Ranked 8th out of 170 countries for its vulnerability to climate change over the next 30 years, Afghanistan has a high poverty rate, limited coping mechanisms and protective capacity, and reliance on flood/ drought prone agricultural land. All of these factors increase the likelihood that when hazard events happen, they turn into disasters with large humanitarian and economic consequences. It is anticipated that current climate change conditions will increase the incidence of extreme weather events, including heat waves, floods, and droughts, creating climate-induced disasters such as Glacial Lake Outburst Floods, avalanches, and rainfall-induced landslides.

Until now information regarding current and future disaster and climate risk has been extremely limited in Afghanistan. Aside from providing essential data and information for decision-making, the Multi-Hazard Risk Assessment has enabled the Government to mainstream risk information in key economic sectors—including Education, Energy, Social Development, Transport, and Urban Development—thereby facilitating the integration of risk considerations into development planning, public policy, and overall investments. The World Bank has supported these mainstreaming efforts through community level activities, pilot projects to foster resilience, as well as ongoing training of different agencies on basic principles of disaster risk management and the use of the Afghanistan Disaster Risk Info GeoNode, an online tool that visualizes the results of the risk assessment.

We believe that this Risk Assessment provides a useful reference for policy makers to lay the building blocks of effective disaster risk management by 1) providing an analytical framework for understanding disaster risk, in accordance with the Sendai Framework for Disaster Risk Reduction (2015-2030); and 2) identifying opportunities in building resilience across all sectors.

We greatly appreciate the collaboration between the Government of Afghanistan, the World Bank Group, and the Global Facility for Disaster Risk Reduction (GFDRR), with funding from the Government of Japan, to bring together multi-disciplinary expertise in support of improved risk information for Afghanistan.

Ede Ijjasz-Vasquez
Senior Director
Social, Urban, Rural and Resilience Global Practice
The World Bank Group

Shubham Chaudhuri
Country Director
Afghanistan, South Asia Region
The World Bank Group

Kabul. Photo: Ahmet Erkan Yigitsozlu

Introduction

The impacts of natural hazards are increasing around the world due to population growth, urbanization, globalization, and climate change-induced changes in extreme weather (UNISDR and CRED, 2016). Poor and fragile countries are hit hardest by disasters, since the population has less ability to respond to and recover from such shocks (Hallegatte et al., 2015; Jongman et al., 2015). In addition, there is a strong relationship between fragility, conflict, and disasters. On the one hand, disasters caused by natural hazards can result in resource scarcity and social grievances, and are shown to significantly increase the risk of violent conflicts (Nel and Righarts, 2008; Xu et al., 2016). On the other hand, conflict and fragility increases social vulnerability and may therefore intensify disaster impacts.

Being both a natural hazard and conflict prone country, Afghanistan is highly exposed and vulnerable to disasters, including floods, earthquakes, droughts, avalanches, and landslides. An estimated 59 percent of the population is affected by climate shocks, whereas 19 percent suffers security-related shocks (The World Bank, 2016), with over 16,000 fatalities from floods and earthquakes since 1990. In addition to the impact on the population, natural hazards frequently affect economic sectors and major infrastructure. Prolonged droughts strongly affect agricultural production, especially since irrigation infrastructure is often lacking. Some of the major road transport corridors, such as the Salang Pass connecting Kabul to the northern regions, are closed off on an annual basis due to avalanches and landslides. Strong earthquakes occur every few years around Afghanistan—there have been around 100 damaging earthquakes since 1900 according to the CATDAT database (Daniell et al., 2011). In 2015, a Mw 7.5 earthquake in the Hindu Kush mountains caused 117 fatalities and destroyed over 7,000 houses (IFRC, 2015).

The effective management of disaster risk is therefore increasingly important to support the development and stability of Afghanistan. Over the past decades, disaster risk management in Afghanistan has been focused on response (Shroder and Shroder, 2014) and recovery (Sadiqi et al., 2017) to events. Recently, the Government of Afghanistan has started working more intensively with development partners—including the World Bank, United Nations organizations, and various NGOs—on prevention and preparedness activities. This includes construction of physical flood, landslide, and avalanche protection measures, as well as the implementation of community-based early warning systems.

However, the nationwide scale-up of disaster risk management has been hampered by a lack of consistent national-level information on hazard, exposure, and risks. The approaches that can be used to assess hazards and risks are limited by the lack of data, and by security issues preventing field observations and data collection. Due to these limitations, limited information is available on, for example, rainfall statistics, river levels, and infrastructure typologies. There is a general gap in data availability between 1980 and 2000, when ongoing conflict virtually stopped all data collection. However, advancing methodologies using remote sensing information and global models offer new opportunities for quantitative risk assessment in data-scarce areas (e.g., Fraser et al., 2016) and even on a global scale (e.g., Ward et al., 2015).

This is the first comprehensive national-level multi-hazard risk assessment for a fragile country. With funding from the Government of Japan and the GFDRR, and in close cooperation with the ANDMA, the MRRD, the WRD of the MEW, and the MAIL, the World Bank has produced a comprehensive multi-hazard risk assessment at the national level, including in-depth assessments for selected geographic areas. The analysis covers flood, flash flood, drought, earthquake, snow avalanche, and landslide hazards, as well as detailed asset and exposure modelling. The results of this assessment provide a nationwide overview of risk and are being used by the Government of Afghanistan and its development partners to design local-level risk reduction measures. The availability of risk information is key for effective management of disaster and climate risk. Integrating risk information into development planning, public policy, and investments and assuring the resilience of new and existing reconstruction to natural hazards and climate change, is critical to secure both lives and livelihoods.

This publication describes the applied methods and main results of the assessment. Namely, Chapter 1 provides a risk analysis for both fluvial floods and flash floods. The fluvial flood modeling framework consists of a hydrological analysis, a hydrodynamic analysis, and a flood impact analysis. The flash floods risk analysis is based on susceptibility indicators, based on topographic and land use maps. Chapter 2 is devoted to drought risk analysis based on a distributed rainfall-runoff model and a water-balance model. Chapter 3 analyzes the landslide risk. Landslide susceptibility hazard maps are obtained from historical inventories of past events combined with the analysis of slope angle, bedrock lithology, geomorphological, morphometric, geological, geotechnical, hydrogeological, and land use factors. Chapter 4 includes an assessment of snow avalanche risk based on historical avalanche data and numerical modeling of the avalanche runout potential and dynamics. Chapter 5 focuses on the risk of ground shaking caused by seismic activity. The seismic risk analysis is based on historic earthquake data, a model for zones and faults, and numerical modeling combining hazard, exposure, and vulnerability to create the risk assessment.

References

Daniell, J. E., Khazai, B., Wenzel, F., and Vervaeck, A. 2011. The CATDAT damaging earthquakes database. *Nat. Hazards Earth Syst.* Sci. 11, 2235–2251. doi:10.5194/nhess-11-2235-2011

Fraser, S., Jongman, B., Balog, S., Simpson, A., Saito, K., and Himmelfarb, A. 2016. Making a Riskier Future: How Our Decisions Are Shaping Future Disaster Risk. Washington, D.C.

Hallegatte, S., Bangalore, M., Bonzanigo, L., Fay, M., Kane, T., Narloch, U., Rozenberg, J., Treguer, D., and Vogt-Schilb, A., 2015. Shock Waves: Managing the Impacts of Climate Change on Poverty. The World Bank. doi:10.1596/978-1-4648-0673-5

IFRC. 2015. DREF Final Report: Afghanistan Earthquake. Geneva.

Jongman, B., Winsemius, H. C., Aerts, J. C. J. H., Coughlan de Perez, E., van Aalst, M. K., Kron, W., and Ward, P. J. 2015. Declining vulnerability to river floods and the global benefits of adaptation. Proc. Natl. Acad. Sci. USA 112, 201414439. doi:10.1073/pnas.1414439112

Munich Re, 2016. NatCatSERVICE Database. Munich Reinsurance Company Geo Risks Research, Munich.

Nel, P., Righarts, M., 2008. Natural Disasters and the Risk of Violent Civil Conflict. *Int. Stud.* Q. 52, 159–185. doi:10.1111/j.1468-2478.2007.00495.x

Sadiqi, Z., Trigunarsyah, B., and Coffey, V. 2017. A framework for community participation in post-disaster housing reconstruction projects: A case of Afghanistan. I*nt. J. Proj. Manag.* 35, 900–912. doi:10.1016/j.ijproman.2016.11.008

Shroder, J. F., and Shroder, J. F. 2014. 8 Hazards and Disasters in Afghanistan, in *Natural Resources in Afghanistan,* pp. 234–275. doi:10.1016/B978-0-12-800135-6.00008-8

UNISDR, and CRED. 2016. The human cost of weather-related disasters 1995–2015. Geneva.

Ward, P. J., Jongman, B., Salamon, P., Simpson, A., Bates, P., De Groeve, T., Muis, S., de Perez, E. C., Rudari, R., Trigg, M. A., and Winsemius, H. C. 2015. Usefulness and limitations of global flood risk models. *Nat. Clim. Chang.* 5, 712–715. doi:10.1038/nclimate2742

Xu, J., Wang, Z., Shen, F., Ouyang, C., and Tu, Y. 2016. Natural disasters and social conflict: A systematic literature review. *Int. J. Disaster Risk Reduct.* 17, 38–48. doi:10.1016/j.ijdrr.2016.04.001

Aerial view of the Hindu Kush mountain range Photo: Goddard Photography

List of Acronyms and Abbreviations

AAD	annual average number of deaths
AAL	average annual loss
ANDMA	Afghanistan National Disaster Management Authority
CBA	cost-benefit analysis
CSO	Central Statistics Organization of Afghanistan
Delft-FIAT	Flood Impact Assessment Tool
DMI	domestic, municipal, and industrial
DTM	digital terrain model
EAD	expected annual damages
EMIS	Ministry of Education
ENEA	Italian National Agency for New Technologies, Energy and Sustainable Economic Development
EP	expected loss
FFSI	Flash Flood Susceptibility Index
GCMs	global climate models
GDP	gross domestic product
GFDRR	Global Facility for Disaster Reduction and Recovery
GIS	geographic information system
GMPE	ground motion prediction equation
GSHAP	Global Seismic Hazard Assessment Program
GSURR	Social, Urban, Rural and Resilience Global Practice
HDX	Humanitarian Data Exchange
I-DPC	Italian Department of Civil Protection
IPCC	Intergovernmental Panel on Climate Change
IRD-EQ	International Relief and Development, Inc. - Engineering Quality Assurance and Logistical Support
IRR	internal rate of return
kPa	kilo Pascal
MAIL	Ministry of Agriculture, Irrigation and Livestock
MDR	mean damage rate
MEW	Ministry of Energy and Water
MRRD	Ministry of Rural Rehabilitation and Rural Development
NIBS	National Institute of Building Sciences
NPV	net present value
OCHA	United Nations Office for the Coordination of Humanitarian Affairs
OEP	occurrence exceedance probability
P	precipitation
PET	(potential) evaporation transpiration
PGA	peak ground acceleration
PGD	permanent ground displacement
PMD	probable maximum deaths
PML	probable maximum loss
RC	reinforced concrete
RCP	Representative Concentration Pathway
RPs	return periods
SARRP	South Asia Regional Programs and Partnerships
SPI	Standardized Precipitation Index
SSP	Shared Socio-Economic Pathway
SWE	snow water equivalent
T	temperature
TDaR	tail deaths at risk
TVaR	tail value at risk
URM	unreinforced masonry
US$	United States Dollars
WRD	Water Resource Department

Table of Contents

Irrigation Restoration and Development Project. An adjustable gate which allows water distribution and division in the canal. Intifat Village,shakardara, Kabul. Afghanistan. 13/1/2015. Photo: Ghullam Abbas Farzami / World Bank

CHAPTER 1

Fluvial and Flash Floods

1.1 Introduction

Fluvial flood risk is developed using a flood modeling framework that consists of three components:

- **Hydrological analysis** models how much precipitation comes to runoff.
- **Hydrodynamic analysis** translates runoff into river flow and inundation, and flow over floodplain areas.
- **Flood impact analysis** calculates the impacts of a flood to areas with high damage potential.

Flash flood risk is calculated deriving susceptibility indicators based on topographic and land use maps.

1.2 Brief summary of the approach

1.2.1 Fluvial floods

The EUWATCH meteorological time series is used as the basis for the simulations. It includes rainfall and snowfall data on a 0.5-degree Lat-Long spatial scale, and a daily and 3-hourly temporal scale. The workflow is summarized as follows:

1. A hydrological and flood model is used to simulate the hydrological response of the river basins to the precipitation input of the EUWATCH series. The model dynamically estimates discharge, average water levels in the river bed, inundation depths in surrounding floodplains, snow cover accumulation, and snowmelt for the entire country for the time period 1958–2001.
2. The combined EUWATCH rainfall series and snowmelt series are stochastically extrapolated to several return periods, and simulated with the combined hydrological and flood model.
3. The results for historical and stochastic events were downscaled into high resolution flood maps. The simulation results of the stochastic events provide flood hazard maps for a range of return periods.

Meteorological data of rainfall, snowfall, and evaporation were used to validate, calibrate, and downscale the EUWATCH meteorological time series. The hydrological model was validated and calibrated using observations of snow cover and stream flow. Figure 1-1 presents the implemented workflow for the fluvial flood hazard model.

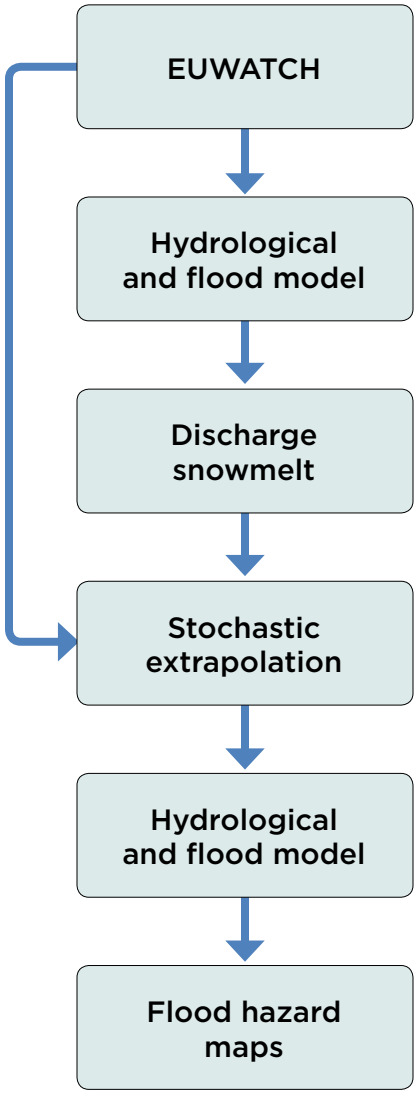

Figure 1-1
Workflow for the probabilistic model for fluvial floods.

1.2.2 Flash floods

There are a number of ways to estimate the potential hazard of an area to flash floods. Although many hybrid systems exist, the following broad subdivision can be made based on the type of approach:

1. Flash Flood Potential Index or Flash Flood Susceptibility Index. These indexes are based on a combination of catchment physiographic factors and soil properties (e.g., Smith, 2003, Jacinto et al., 2015).
2. The Flash Flood Guidance System (Stewart, 2007) and other systems that use some sort of hydrological modelling.

Based on the available information and the scale of the project, we used drainage network and soil information to derive a Flash Flood Susceptibility Index (FFSI) based on catchment physiographic factors and soil properties (Jacinto et al., 2015). The FFSI is a number between 0 and 1, with 0 meaning no risk and 1 meaning high risk. The final maps were classified in five categories as shown in Table 1-1:

Table 1-1

Flash Flood Susceptibility Index Categories.

Category	Range
No risk	0–0.15
Very low risk	0.15–0.25
Low risk	0.25–0.45
Considerable risk	0.45–0.55
High risk	0.55–1

1.3 Fluvial flood hazard model

1.3.1 Processing of EUWATCH data

For the hydrological modelling, three meteorological input variables are needed: precipitation, temperature and (potential) evaporation transpiration. These variables are imported from the EUWATCH dataset. With the calibrated model, the entire EUWATCH period (1959–2002) was simulated to derive the statistics that were needed to generate the stochastic events.

1.3.2 Hydrological modelling and flood modelling

1.3.2.1 The WFLOW hydrological model concept

A WFLOW model was set up to cover all the river basins of Afghanistan. The WFLOW-HBV hydrological model concept (based on the HBV model concept developed by SMH (Linström et al., 1997) was chosen, because this model concept had already been successfully applied in similar contexts.

The WFLOW-HBV model is a completely distributed conceptual model which includes the following processes (see Figure 1-2):

- Rainfall interception;
- Snow accumulation and snowmelt (not included in Figure 1-2);
- Soil processes;
- Unsaturated zone;
- Saturated zone; and
- Channel and overland flow modelled with the kinematic wave model.

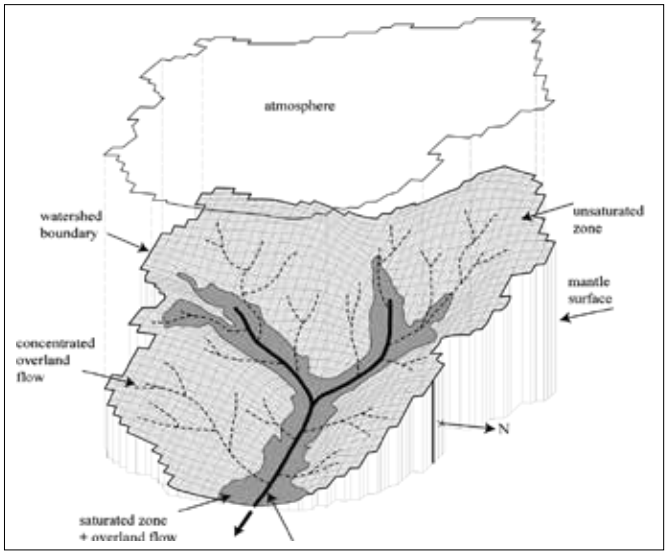

Figure 1-2

General representation of the distributed WFLOW rainfall runoff model.

1.3.2.2 Hydrological model results for risk analysis

The output of the hydrological model was used for several risk analyses:

- The time series of precipitation and simulated snowmelt over 44 years (1958–2001) was used to derive statistics on which stochastic events were based. The stochastic events were simulated as well with the hydrological model to derive T-year flood maps for a range of return periods.
- The time series of snowpack simulation over 44 years was used to derive nationwide annual maximum snow heights.

The precipitation and simulated snowmelt results were also used as input for the drought risk analysis, whereas snowpack simulation results were used as input for the avalanche risk analysis.

1.3.3 Climate change impacts on flood hazards

For the flood risk assessment in 2050 the future climate conditions under the Representative Concentration Pathway RCP6.0 scenario were calculated in a way similar to present day impacts. Climate projections for 2050 were drawn from an ensemble of global climate models (GCMs) in accordance with Hempel et al. (2013). The climate projections will help determining how precipitation and snowfall may increase or decrease.

The hydrological model was also used to simulate 40 years of synthetic input data from five GCMs, which can essentially be considered as five climate scenarios for the year 2050. Three GCMs (GFDL, HadGEM, and NorESM) indicate an increase in rainfall plus snowmelt, and two GCMs indicate a decrease in rainfall plus snowmelt (IPSL and Miroc). In other words, there does not appear to be a clear concept of climate change impacts on the Afghanistan hydrometeorology. In order to be conservative, the risk analysis for the year 2050 was conducted taking a relatively "dry" GCM (IPSL) for drought risk analysis and a relatively "wet" GCM (NorESM) for flood risk analysis.

1.3.4 Flood map generation

The stochastic events (rainfall plus snowmelt) simulated by the hydrological model were downscaled into four different higher resolution spatial scales. Combined with nine return periods (2, 5, 10, 20, 50, 100, 250, 500 and 1,000 years), this produced 36 nationwide flood mapping simulations.

1.4 Resulting flood hazards

1.4.1 Fluvial floods

As an example, Figure 1-3 and Figure 1-4 show the flood map over the East of Afghanistan, which is a flood-prone area, for a 5-year and a 100-year return period, respectively. The 100-year return period map clearly shows much more severe flooding, with both flood extent and water zdepth much greater than in the 5-year map.

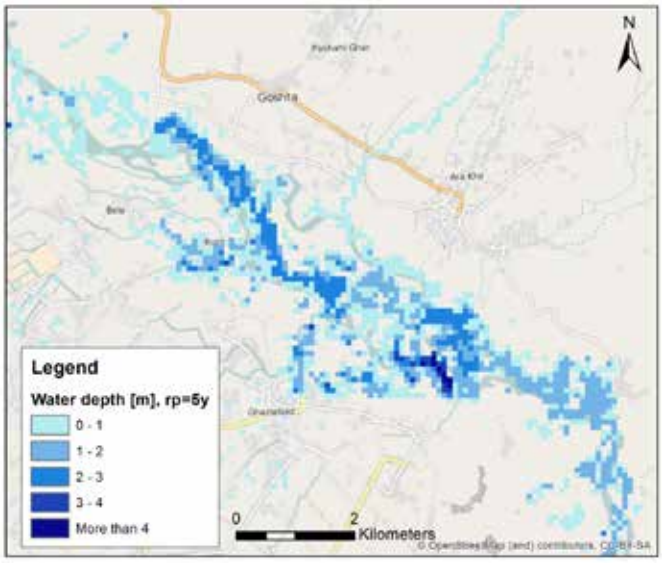

Figure 1-3

5-year return period flood map (combined events of all spatial scales).

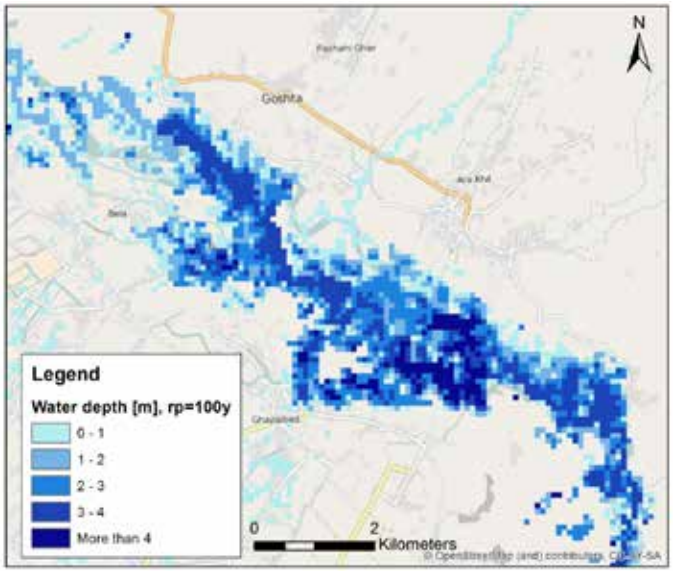

Figure 1-4

100-year return period flood map (combined events of all spatial scales).

1.4.2 Flash flood hazards

The Flash Flood Susceptibility Index (FFSI) calculated using the methodology for flash flood hazard susceptibility described in section 1.2.2 is shown in Figure 1-5. Figure 1-6 shows the results per district.

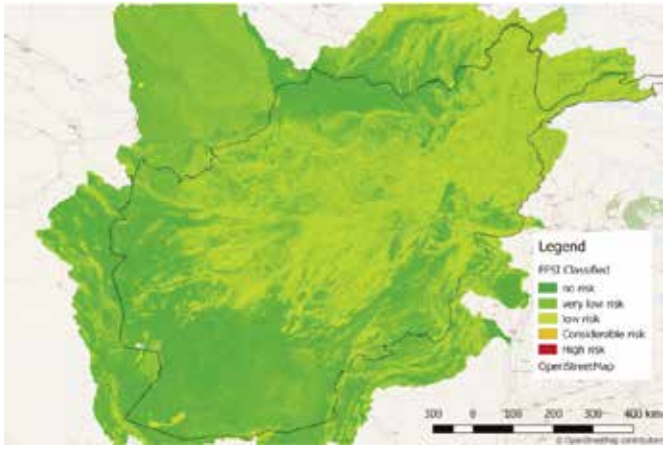

Figure 1-5

FFSI derived for the whole country.

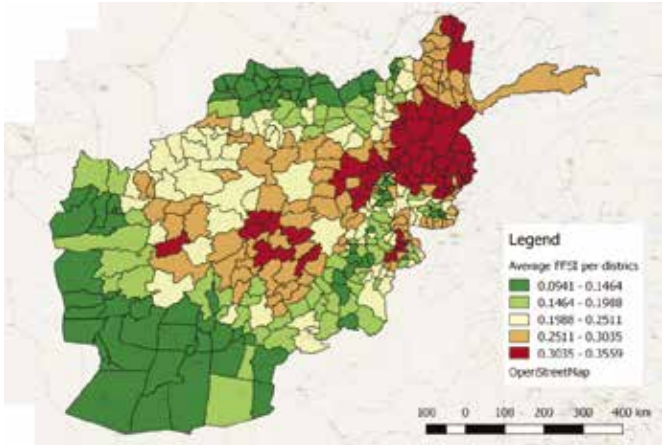

Figure 1-6

FFSI average per administrative unit (districts).

Note: The values shown are median values per area. The color coding is not the same as the high resolution maps.

1.5 Flood risk analysis

1.5.1 Objectives of the analysis

The goal of the flood risk analysis is to assess the impacts of the inundation scenarios on exposed assets and people. The resulting risk analysis indicates which regions and locations within Afghanistan currently suffer the highest (potential) impacts. Also, the quantified monetary damages and risk estimates can be used to support decisions on measures to reduce flood risks and appropriate levels of such investments.

The objectives of the analysis are to assess the following impact types for the riverine flood hazard:

- Quantify the monetary damages;
- Quantify the number of people affected;
- Quantify the affected transport lines and number of critical infrastructures;
- Assess the impacts of historic flood events in Afghanistan; and
- Simulate the impacts for selected historic flood events.

To this end, we use the data to analyze the exposed assets and population. We assess the flood impacts with the Delft-FIAT (Flood Impact Assessment Tool) software, which has been applied in various flood risk studies around the world.

The results from the flood damage analysis using Delft-FIAT includes the assessment of monetary damages for buildings using a standard flood damage model that includes stage damage functions and maximum damages. Results are available as damage estimates per flood return period, and also as expected average annual damage. In addition, estimates are made of people affected and critical infrastructure, by overlaying inundation maps for different return periods with the exposed population maps and critical infrastructure locations. In the following sections the main results from the flood impact analysis are discussed.

1.5.2 Flood damages

Flood damages have been calculated for the following flood impact categories:

- Residential buildings;
- Non-residential buildings (including schools and hospitals); and
- Roads.

The economic exposure layers are turned into flood damage maps by creating an overlay with the hazard maps and the use of vulnerability functions. Vulnerability functions describe a relationship between the flood water depth and the percentage of maximum damages that will occur at that depth. Figure 1-7 gives a schematic overview of the damage calculation.

1.5.2.1 Estimated flood damages at the national level

The flood damage estimates for the national level in Afghanistan are indicated in Table 1-2. Commercial and residential categories make up the majority of expected flood damages, 40 percent and 33 percent, respectively (see Figure 1-8).

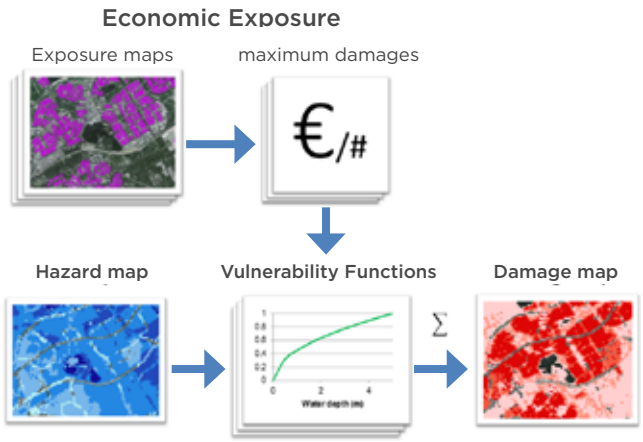

Figure 1-7

Overview of damage calculations in Delft-FIAT.

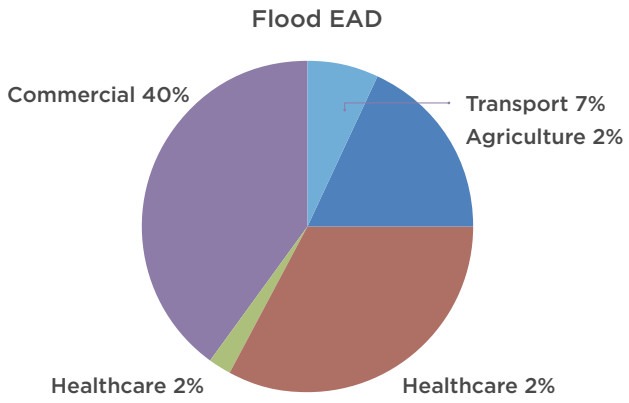

Figure 1-8

Relative share of expected flood damages in Afghanistan.

Table 1-2

Annual expected flood loss per damage category.

Main category	Damage category	Annual expected loss (US$/y)
Agriculture	Agriculture irrigated	9,567,000
	Agriculture rain fed	202,000
Residential	Residential clay urban	2,263,000
	Residential clay urban content	747,000
	Residential stone urban	3,696,000
	Residential stone urban content	813,000
	Residential clay rural	3,862,000
	Residential clay rural content	1,274,000
	Residential stone rural	3,800,000
	Residential stone rural content	836,000
Health care	Hospital	650,000
	Health center	193,000
Commercial	Commercial population	16,903,000
	Commercial area	4,251,000
Transport	Roads	3,866,000
	Total	**52,924,000**

1.5.3 People affected

The number of people affected nationwide by flood events is estimated using an overlay of the flood inundation maps for different return periods, and the rural and urban population maps for Afghanistan. The number of affected people expected annually is over 100,000 persons (Table 1-3).

Table 1-3

Affected people at different return periods.

Return period (y)	Affected people
5	279,000
10	469,000
20	604,000
50	729,000
100	822,000
250	921,000
500	975,000
1,000	1,032,000
Annual expected	**110,777**

1.5.4 Transport lines and critical infrastructure

The impacts from flooding on the following transport lines and critical infrastructures have been analyzed:

- Roads
- Schools
- Hospitals
- Power plants
- Dams
- Bridges
- Airports

For these categories, the number of impacted objects (or in the case of roads, the number of kilometers) has been estimated. Table 1-4 indicates the number (or length) of critical infrastructure that are exposed to the once in a 100-year flood in Afghanistan. These numbers are indicative only, as there was no complete dataset available for these infrastructure types.

Table 1-4

Number of objects exposed to 1:100 year flood.

Object type	Number affected
Airports	0
Bridges	416
Dams	8
Healthcare facilities	37
Hospitals	3
Schools	111
Industrial area affected [m^2]	6,893,099
People affected	822,000
Power plants	1
Roads affected [km]	2,257
Universities	0
Rural houses	73,190
Urban houses	29,839

1.5.5 Historic flood events and impact records

Data has been collected on historical flood events in order to describe past events and understand the frequency and impacts of flooding in Afghanistan. This supports the risk assessment for Afghanistan in the following instances:

1. To establish the type and frequency of flood events;
2. To establish intensity and size of the events (footprints); and
3. To establish impacts, including loss of life, damages, and people affected for single events.

This information can be used for comparison and calibration of the risk assessment.

1.6 Resulting flood risks on the national and provincial level

Table 1-5 and Figures 1-9 – 1-12 show, at the national and district levels, the economic losses and affected people in absolute numbers, as well as in percentages of the total population and total capital stock.

Table 1-5

Economic losses and affected people due to fluvial floods.

Return period	Economic losses (million USD)	Economic losses as a percentage of total capital stock	Affected people	Affected people as a percentage of total population.
Annual average	54	0.12%	101,000	0.37%
5	118	0.26%	279,000	1.03%
10	228	0.51%	469,000	1.73%
20	328	0.73%	604,000	2.23%
50	444	0.98%	729,000	2.69%
100	541	1.20%	822,000	3.03%
250	653	1.45%	921,000	3.40%
500	728	1.62%	975,000	3.60%
1,000	795	1.76%	1,032,000	3.81%

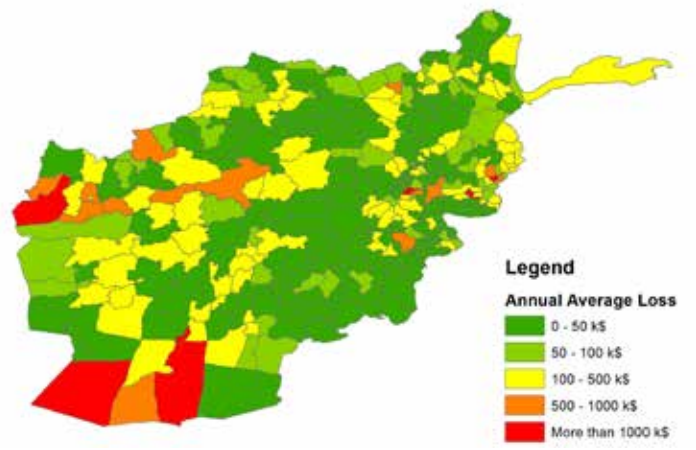

Figure 1-9
Annual average losses.

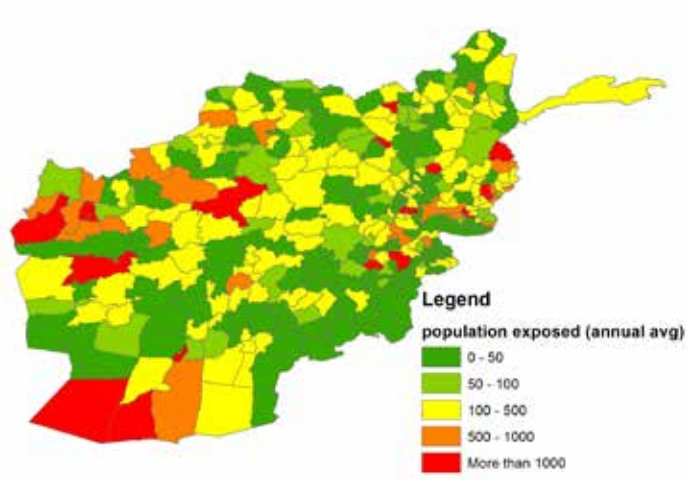

Figure 1-10
Annual average population exposed.

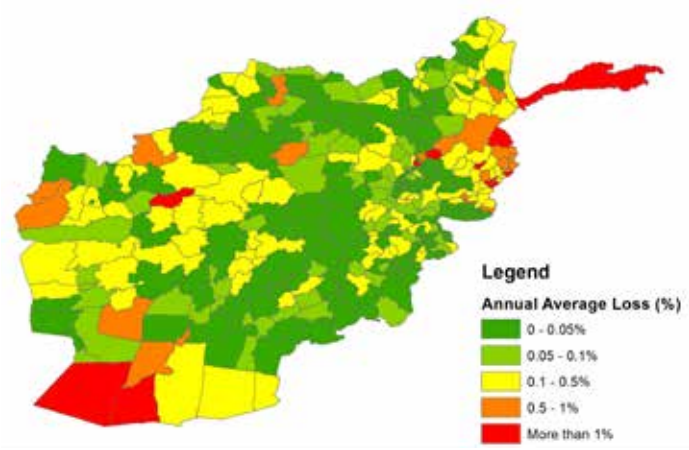

Figure 1-11
Annual average losses as a percentage of total stock.

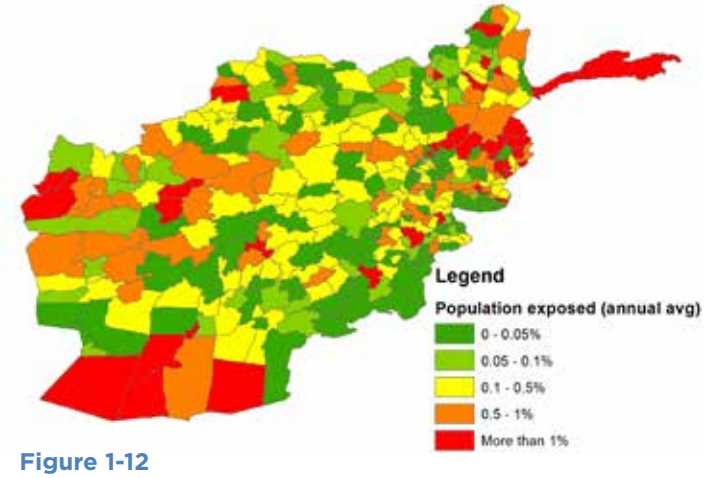

Figure 1-12
Annual average population exposed as a percentage of total population.

1.7 Projection of future flood risk

The information from the SSP (Shared Socio-Economic Pathway) scenarios developed for the Intergovernmental Panel on Climate Change (IPCC) is used to determine the projections of exposed asset values. According to the SSP projections, the flood risk in Afghanistan will increase substantially, as more of the population will be exposed to flooding, and more and more valuable assets are accumulating. In Figures 1-13 and 1-14, the expected annual people affected by flooding, and the expected annual damages from flooding in Afghanistan until the year 2050 are displayed. Note that these figures are based on the future climate scenario simulated by the NorESM GCM (as described in section 1.3.3).

1.8 Measures for resilient reconstruction and risk reduction

1.8.1 Introduction

If the level of flood risk is not acceptable, flood risk reduction is necessary. Several measures can be taken to reduce flood risks, from measures that focus on load reduction (e.g., upstream measures), prevention with dikes, reduction of consequences, or compensation through insurance; see Figure 1-15 for an overview.

Following the definition of risk as a function of probabilities and consequences of a set of scenarios, two types of interventions can be distinguished: those that reduce the probability of flooding (prevention) or those that reduce the consequences (mitigation).

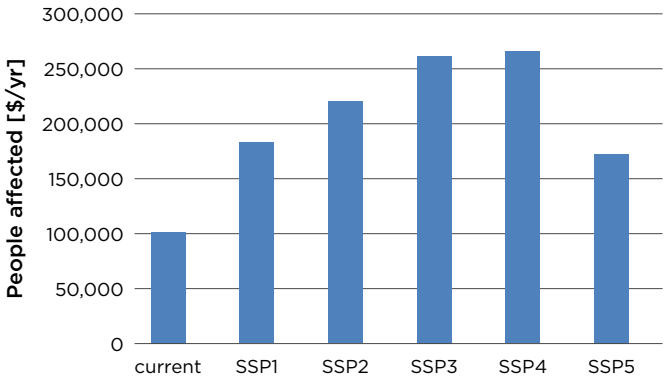

Figure 1-13

SSP projections for the expected number of people affected per year by flooding in Afghanistan in the year 2050.

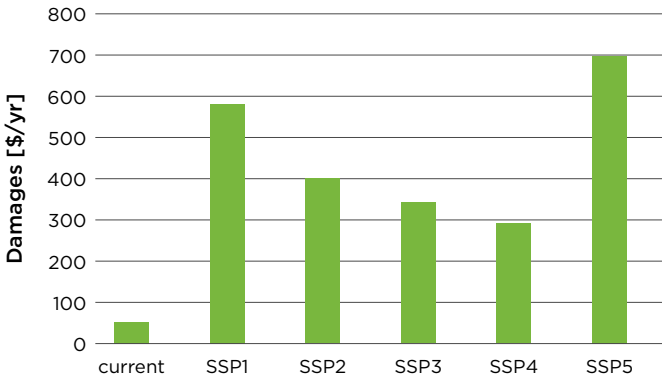

Figure 1-14

SSP projections for the expected annual damages from flooding in Afghanistan in the year 2050.

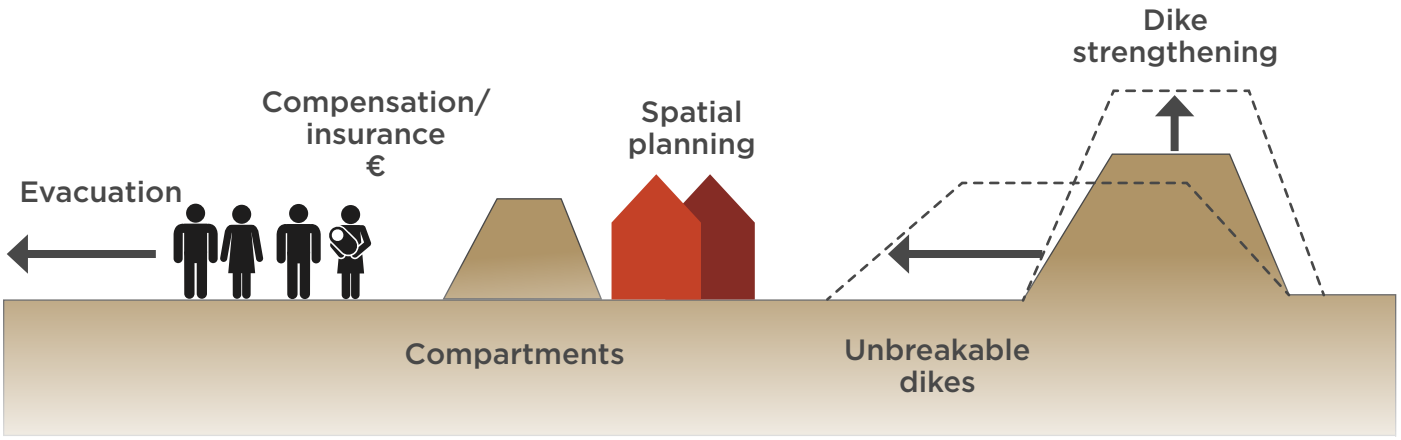

Figure 1-15

Schematic overview of several measures to reduce flood risks. Source: Jonkman and Schweckendiek (2015).

- **Prevention measures** reduce the probability of flooding. They include reducing the loads on a flood defense (e.g., room for rivers or foreshores for wave reduction) or increasing the strength of the flood defense (dike reinforcement).
- **Mitigation measures** reduce the consequences of failure of a flood defense. Examples of mitigation measures include: adaptation of existing or new buildings, the construction of internal compartment dikes to limit the flooded area, and emergency and evacuation plans. A special category of measures concerns insurance or government compensation as it will not reduce the damage from flooding, but instead leads to compensation or redistribution after damage has occurred.
- Several frameworks have been developed for managing flood risks and evaluating portfolios of flood risk reduction measures. Many of these frameworks attempt to combine the different risk reduction measures and the various actors involved. Eventually, all the different interventions can also be expressed by means of their contributions to the reduction of flooding probability or flooding consequences, and thus be evaluated for risk reduction and cost-effectiveness.
- For example, the "multilayer safety" approach (depicted in Figure 1-16) distinguishes **prevention** as a first layer, **land use planning** as a second layer, and **emergency management** as a third layer.

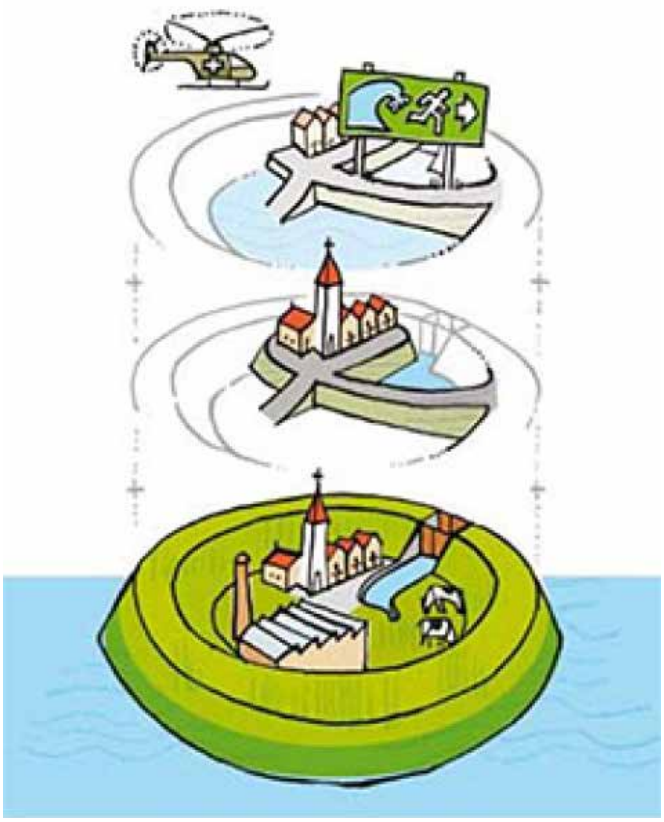

Figure 1-16

The multilayer safety (meerlaagsveiligheid) concept used by the Dutch government.

1.8.2 Types of flood prevention measures

Flood defenses are generally a useful measure to prevent flooding of low-lying areas. A flood defense is a hydraulic structure with the primary objective to provide protection against flooding along the coast, rivers, lakes, and other waterways. Different types of flood defenses exist. The most important ones are:

- A **dike** (levee) is a water retaining structure consisting of soil, with a sufficient elevation and strength to be able to retain the water under extreme circumstances.
- A **dam** is another type of water retaining structure which separates two water bodies.
- A **flood wall** is a water retaining structure which generally consists of concrete, and sometimes steel. Due to the high horizontal forces on the flood wall, a solid foundation is necessary.
- **Temporary flood defenses** are used during periods of high water levels to strengthen dikes or other vulnerable objects. Examples of temporary flood defenses are sandbags, synthetic-bellow barriers, or box barriers that are filled with water for the purpose of stability, and various types of beams and stop logs.
- **Hydraulic structures,** such as sluices, siphons, and pumping stations are structures that can also be a part of a flood defense system.

1.9 Flood risk, erosion, and cost-benefit analysis for focus areas

1.9.1 Introduction on Cost-Benefit Analysis

A Cost-Benefit Analysis (CBA) on flood risk reduction measures is conducted to select the most economically feasible measures. In a CBA the costs, i.e., the investments of a set of measures, is compared with the reduction in flood damages from the proposed measures. When benefits outweigh the costs, a flood risk reduction measure is deemed economically viable. For the examples that are described in this report, we have chosen measures that are effective for frequent flood events (i.e., those with a relative short return period of 1 in 20 years), which are associated with less extensive

flooding in order to limit complexity of the designs of the flood risk reduction measures.

The CBA is based on an analysis over a period of 20 years, and assumes an average economic growth of 7 percent,[1] which is the average economic growth over the past 10 years in Afghanistan, as calculated from the world development index database from the World Bank.[2] The result of the cost benefit analysis is presented as the internal rate of return[3] (IRR) on investments in flood risk reduction, based on initial investments (costs) and avoided damages (benefits). Normally a project is considered economically viable when the IRR is equal or higher to the market interest rate.

In order to conduct a CBA for flood risk reduction measures, vulnerability, or potential damages from flood events with specific return periods, need to be determined. In the design for flood risk reduction measures, the new protection level and resulting reduction in potential flood risk is calculated. Estimates of reductions in flood damages are based on the developed hydrological and hydraulic flood hazard estimates (see sections 1.3 and 1.4), and the results from the flood damage FIAT model (section 1.5) that have been developed within the project. The risk reduction and the investment costs and service life of the risk reduction measures are subsequently compared in the CBA. The annual reduction in flood risk is discounted over the timeframe of the project in order to determine the IRR (see above). When IRR reaches a predetermined value a project is deemed economically viable.

1.9.2 Unit costs

Unit costs for specific flood protection designs are commonly calculated on the basis of total direct construction costs based on material cost and labor and adding surcharges for specific activities, such as planning, detailed designs, supervision, implementation risks, and so on.

For this study the distinction is made between simple and complex construction based on the following characteristics:

- Simple constructions (small earthworks, small masonry structures, mass concrete, rural environment)
- Complex constructions (gabion structures, reinforced concrete structures, large earthworks, urban environment)

Besides flood protection measures such as dams and dikes, the potential reduction of flood damages through adjustments in buildings is assessed. The flood proofing of residential buildings is assumed to be done by either:

- Cement plaster of unfired brick houses; or
- Construction of a concrete protection wall around the dwellings.

The cost-benefit analysis and economic rationale for risk reduction measures is illustrated in two study areas:

1. Kabul city flood risk.
2. Amu Darya (Panj Aumur) flood risk.

For these case studies, typical risk reduction measures are proposed based on a cost calculation.

1.9.3 Kabul city case study

1.9.3.1 Model runs for stochastic events

A hydrodynamic model was set up to simulate flooding in the Kabul area. Stochastic events were simulated for the Kabul and Paghman rivers for return periods of 5, 10, 20, 50, 100, 250, 500 and 1,000 years.

The maximum water depth for a 10-year event resulting from the model is shown in Figure 1-17. First flooding occurs near the confluence of Kabul and Paghman rivers and in the old town located in District 1.

Figure 1-18 displays the maximum water depth modelled for a 1,000-year event. The flood plain extent is much wider compared to the 10-year event; especially the area near the confluence of Kabul and Paghman rivers is heavily flooded.

The modelled maximum water depths are input for the flood risk analysis for Kabul city.

1.9.3.2 Impact and flood risk assessment for Kabul

Two options for flood risk management in the Kabul city center are evaluated: (i) flood wall strengthening and

[1] This means that benefits are assumed to increase by 7 percent annually, in pace with economic growth.
[2] http://databank.worldbank.org/data/reports.aspx?source=world-development-indicators
[3] The IRR on an investment or project is the "annualized effective compounded return rate" or rate of return that makes the net present value (NPV) of all cash flows (both positive and negative) from a particular investment equal to zero. Equivalently, the IRR of an investment is the discount rate at which the net present value of costs (negative cash flows) of the investment equals the NPV of the benefits (positive cash flows) of the investment.

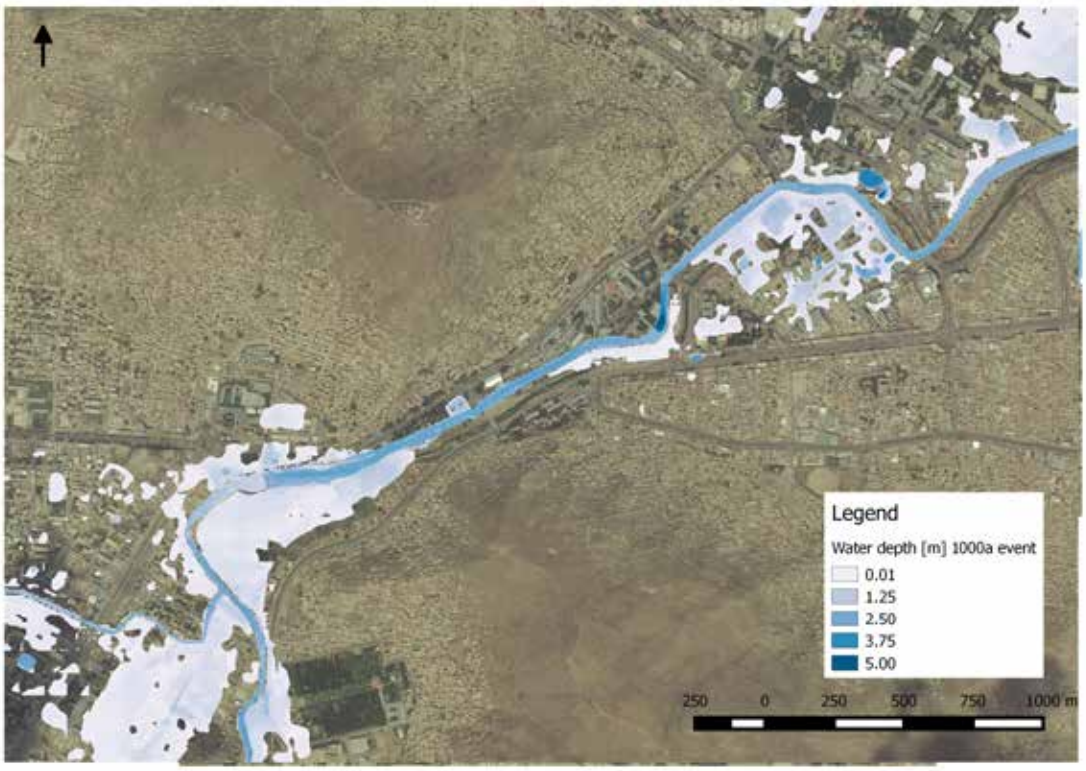

Figure 1-17
Maximum water depth for a 10-year event (1 m grid).

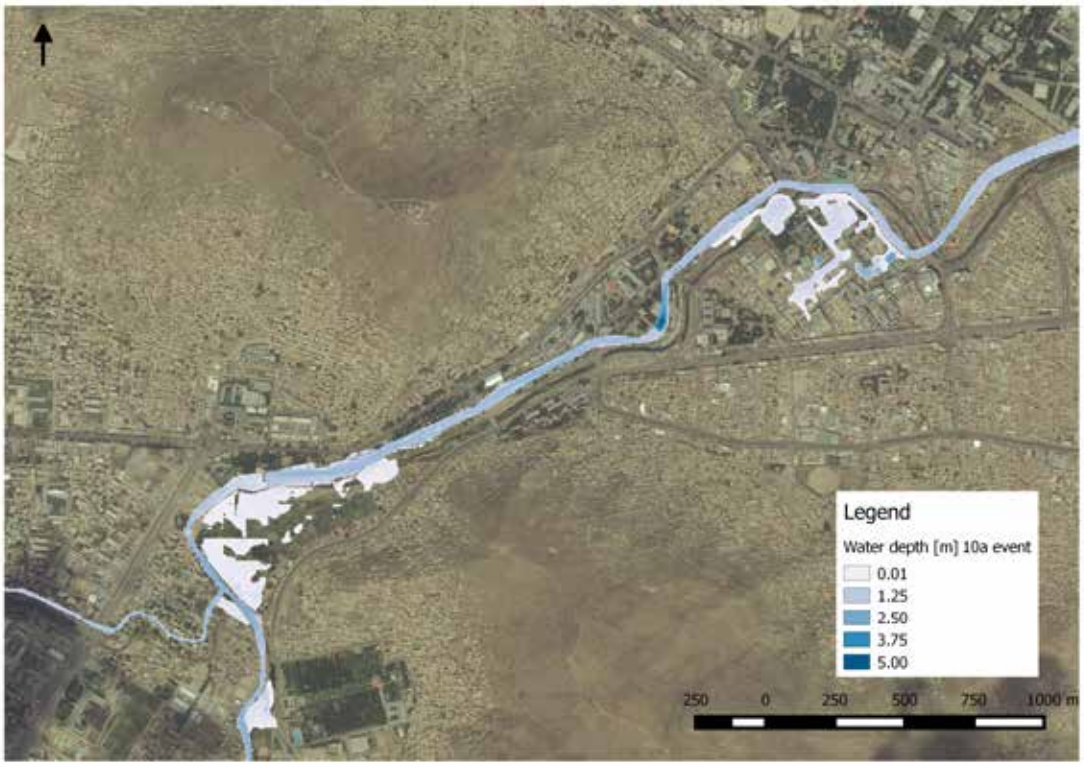

Figure 1-18
Maximum water depth for a 1,000-year event (1 m grid).

(ii) retrofitting of residential buildings through flood proofing. The reconstruction cost for buildings was estimated to be $160/m^2. The maximum damage for commercial property was set to $133/m^2.

The analysis was carried out for three different situations:

- S1: Baseline scenario—situation as currently implemented
- S2: Dike strengthening—increasing the bank level by 1 meter
- S3: Retrofitting—Dry-proofing of residential buildings in the most affected part of District 1, North of Maiwand Street.

1.9.3.3 Risk reduction measures

Dike strengthening

The embankment level is set at 1,800.5 meters, which is an average of 1 meter above the current level of the river bank protection. The model simulations indicate a flood defense with that level prevents flooding of the old town area up to and including a 50-year event. Figure 1-19 and Figure 1-20 show the resulting maximum water depth for a 10-year event and a 1,000-year event. Dike strengthening prevents flooding of the old town for the 10-year event (compare Figure 1-19 with Figure 1-17), but has a minor effect for the 1,000-year event (compare Figure 1-20 with Figure 1-18).

Table 1-6 shows the results of the baseline situation (no measures) S1, compared to the outcomes of measures for S2 and S3. It can be seen that strategy S2 can lead to a significant decrease of flood damages for both residential and commercial buildings. For flood events less frequent than 1 in 100 years, the effect of the embankment is limited.

Retrofitting buildings

The reduction in flood losses after retrofitting residential buildings is less significant for events up to 1 in 100 years, but still has an effect for floods with lower return periods.

1.9.3.4 Cost estimate for risk reduction measures

Flood wall strengthening

Increasing the flood retaining wall within Kabul by 0.5–1 meter over a length of about 600 meters in order to avoid a flood event with a 1 in 50 frequency results in a total cost including flood wall, concrete, and road work of US$398,549. The resulting IRR would be 138 percent, indicating a very positive economic return for investments for flood prevention in Kabul city at this particular location.

Retrofitting buildings

Flood proofing can be achieved by construction of a small concrete/stone wall around a housing compound, or plastering of the lower part of residential buildings (especially mud brick houses) with water proofed cement plaster. Both measures are assumed to have similar costs per protected house.

The cost-benefit analysis is conducted for all houses in Kabul that are exposed to a 1 in 50 years flooding area (with a combined surface of 94,234 m^2 residential houses). Total costs for flood proofing of the residential houses are based on the surface of the exposed residential housing to flooding.

Implementation of flood proofing results in avoided annual damages of US$341,000. This gives an IRR of 10 percent. The construction of a flood wall, with an IRR of 138 percent, indicates the latter is a far better flood risk reduction measure.

Table 1-6

Results of the flood damages for commercial and residential buildings for situations S1, S2, and S3 (all values in $1,000).

	S1			S2			S3		
RP	Commercial buildings	Residential buildings	Total	Commercial buildings	Residential buildings	Total	Commercial buildings	Residential buildings	Total
5	43	198	241	43	198	241	43	166	209
10	947	3,061	4,008	62	274	336	947	783	1,730
20	1,190	3,816	5,006	109	415	524	1,190	941	2,131
50	1,671	5,172	6,843	379	1,100	1,479	1,671	1,619	3,290
100	2,955	9,685	12,640	1,828	6,146	7,974	2,955	5,750	8,705
250	4,482	14,217	18,699	4,045	12,846	16,891	4,482	9,585	14,967
500	5,679	18,017	23,696	5,304	16,775	22,079	5,679	12,692	18,371
1,000	6,907	21,458	28,365	6,651	20,808	27,459	6,907	15,539	22,446

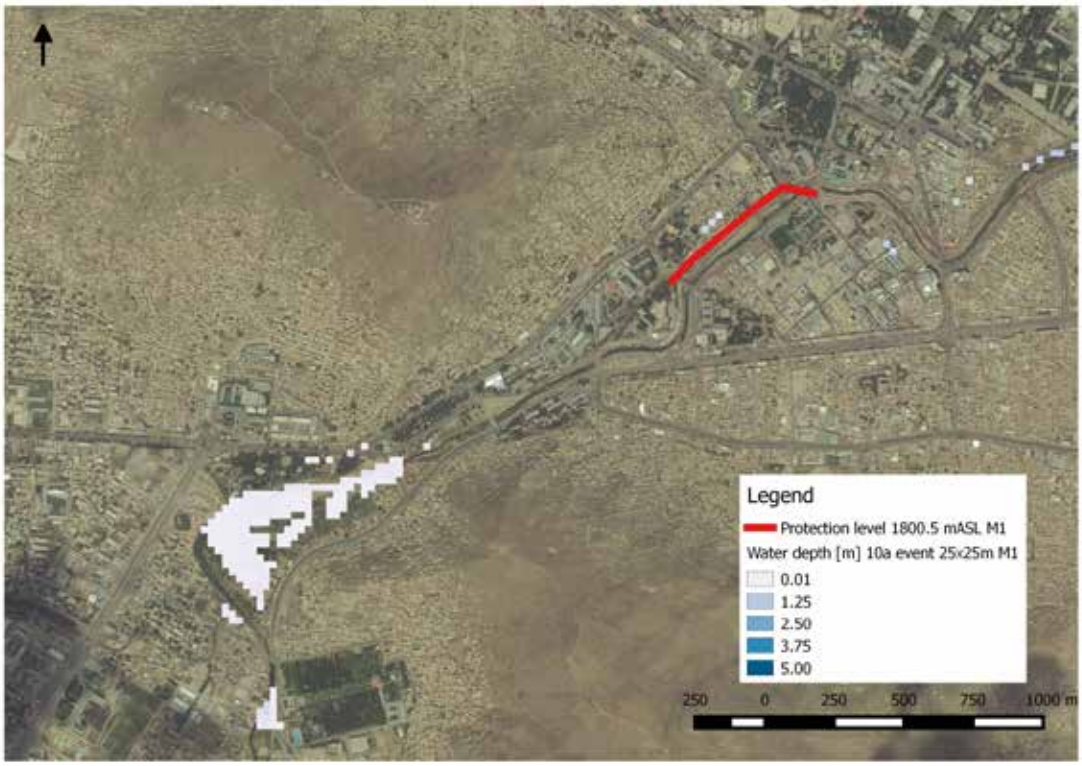

Figure 1-19

New protection level and maximum water depth for a 10-year event (25 m grid) for measure 1 (M1).

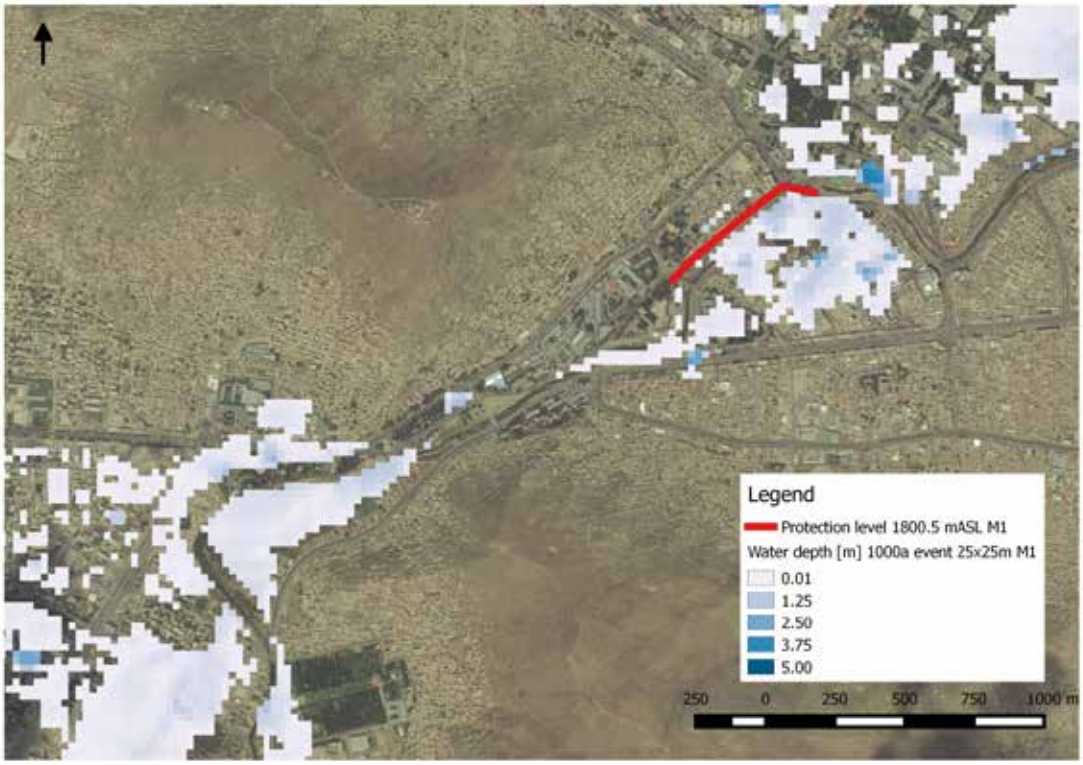

Figure 1-20

New protection level and maximum water depth for a 1,000-year event (25 m grid) for measure 1 (M1).

1.9.4 Panj Amur case study

1.9.4.1 Introduction

In order to gain insight into the possibility and economic rationale for the construction of flood risk prevention, a case study was conducted in the Panj Amur catchment area. Based on the risk maps, several areas with significant damages were selected. The areas and the geographic representation of the damages are presented in Figure 1-21, Figure 1-22, and Figure 1-23. The estimated actual damages for different return periods and consequential values of the expected annual damages (EAD) are presented in Table 1-7.

Table 1-7

Damages and expected annual damages for different return periods in different case study areas.

Areas	Damages per event ($) RP=5	RP=10	RP=20	RP=50	RP=100	EAD [$/y] RP=5-100	EAD [$/y] RP=5-50	EAD [$/y] RP=5-20
Agriculture area Kunduz	1,028,850	1,686,963	2,236,118	2,862,879	3,284,077	341,087	310,353	300,951
Puli Khumri	-	647,116	3,168,274	5,306,463	6,578,321	314,286	254,862	222,789
Fayzabad	61,868	620,992	1,142,947	1,602,845	1,929,526	137,090	119,428	112,530
Kabul Flood wall		3,679,495	4,489,711	5,374,769		563,046	536,172	522,896
Kabul Flood proofing	31,547	2,278,480	2,875,115	3,552,912		358,526	340,762	330,595

1.9.4.2 Cost benefit of risk reduction measures

Kunduz agricultural area

From the flood hazard maps it has been estimated that for the protection of the agricultural lands in Kunduz (Figure 1-21) approximately 35 km of dike are required. Construction of a simple earth dike would cost about US$3.2 million. This measure, assuming a protection level up to and including the 1 in 20 years flood level, would result in benefits of annual reduced damages of about US$301,000. The IRR of the reduction in annual damages, assuming a lifespan of 20 years of the investment and economic growth of 7 percent, would be 14 percent, showing a significant return of the investment in flood reduction measures.

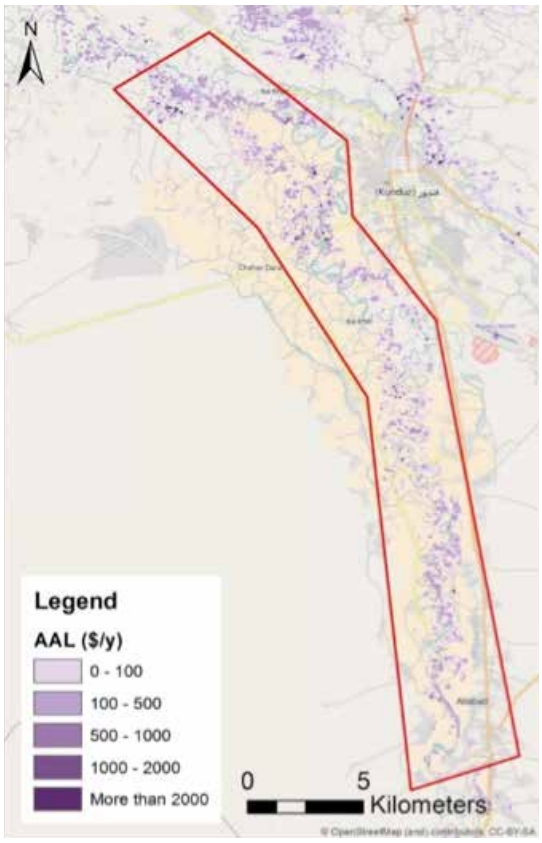

Figure 1-21

Study area—Kunduz agricultural area.

Puli Khumri

From the map of the Puli Khumri area (Figure 1-22) it can be estimated that a protective embankment of 22 km (2 sides of 11 km each) would be required. Assuming that the embankment will require a stone protection, the construction costs would be US$990,000.

Assuming a protection level up to and including the 1 in 20 years flood level, benefits would result in annual reduced damages of US$223,000. The IRR of the reduction in annual damages, assuming a lifespan of 20 years of the investment and economic growth of 7 percent, would be 29 percent.

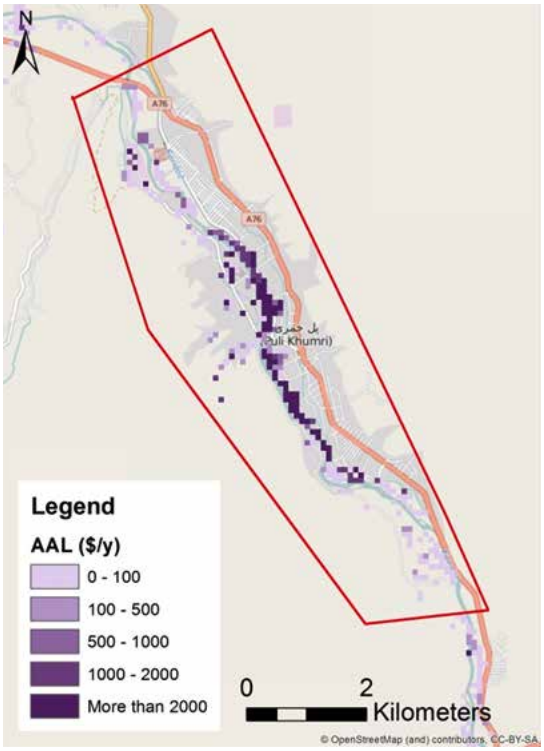

Figure 1-22

Study area—Puli Khumri.

Fayzabad

From the map of the Fayazabad area, (Figure 1-23) it can be estimated that a protective embankment of 6 km (2 sides of 3 km each) would be required. As the proposed embankment is in an urban environment, it is assumed that a more complex construction[4] in reinforced concrete would be required. Construction costs would be US$1.3 million.

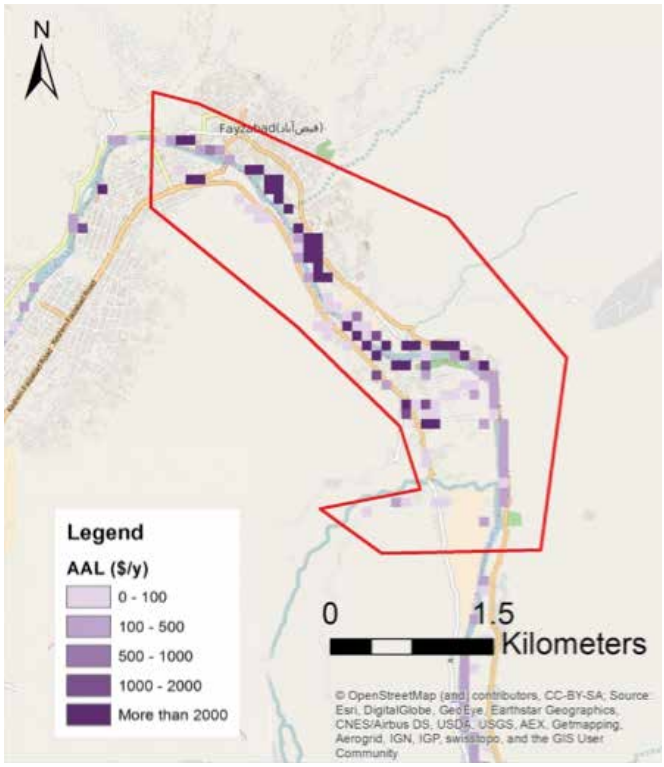

Figure 1-23

Study area—Fayzabad.

Assuming a protection level up to and including the 1 in 20 years flood level, benefits would result in annual reduced damages of US$112,500. The IRR of the reduction in annual damages, assuming a lifespan of 20 years of the investment and economic growth of 7 percent, would be 12 percent.

1.9.5 Conclusions from Kabul and Panj Amur case studies

From the calculated flood damages and possible solutions for flood prevention measures, it is clear that urban environments have much higher flood damages. Therefore, as a risk reduction option flood prevention measures have much higher benefits (through avoided damages) in urban areas than in rural areas, including a higher internal rate of return (IRR). The case study of Kabul indicates that there are substantial damages (US$14 million) in a relatively small area (600 m long wall flood). Although the total damages in the rural Panj Amur cases are similar (around US$9 million) the stretches of dike that need reinforcement are longer (up to 35 km length). Nevertheless, flood risk reductions seem economically feasible in all case studies.

[4] With a larger surcharge factor.

The study from Kabul shows that prevention measures are not required along the full length of the proposed embankments, and that flood proofing of houses has a much lower IRR than construction of a flood retaining wall.

Further recommendations include the following:

- For any flood prevention projects, detailed information on local costs (including transport, labor, etc.) is essential to inform the level of protection and type of implementation that would be economically justified.
- More information on topography, hydraulic characteristics, subsoil, etc. would better determine the required design of the local flood prevention measures, improving the estimates for costs of construction and materials.

The results presented above provide an initial basis for informed decision making on planning and implementing flood protection measures in Afghanistan, based on a financial cost-benefit analysis. A more extended analysis, including indirect costs because of business interruption and other co-benefits of flood projection, such as prevention of injury, ecological impacts, and so on, could allow a social cost benefit analysis.

References

Chapter 1

De Grave, P., and Baarse, G. 2011. Kosten van maatregelen. Retrieved from http://www.deltaportaal.nl/programfiles/13/programfiles/Kosten_-_De_Grave_en_Baarse_2011.pdf

FFEM. 2004. Energy efficiency and passive solar architecture in the construction sector, http://www.ffem.fr/jahia/webdav/site/ffem/shared/ELEMENTS_COMMUNS/U_ADMINISTRATEUR/5-PUBLICATIONS/Changement_climatique/Brochure_FFEM_Afghanistan_sept04_ang.pdf

Hempel, S., Frieler, K., Warszawski, L., Schewe, J., and Piontek, F. 2013. A trend-preserving bias correction – the ISI-MIP approach, Earth Syst. Dynam., 4, 219-236, https://doi.org/10.5194/esd-4-219-2013.

Jacinto, R., Grosso, N., Reis, E., Dias, L., Santos, F. D., and Garrett, P. 2015. Continental Portuguese Territory Flood Susceptibility Index–contribution to a vulnerability index. Nat. Hazards Earth Syst. Sci 15, 1907–1919.

Jaiswal, K. S., and D. J. Wald. 2008. "Developing a global building inventory for earthquake loss assessment and risk management." In Proceedings of 14th World Conference on Earthquake Engineering.

Jonkman, S.N. and Schweckendiek, T. 2015. Flood Defences, Lecture notes CIE5314. Delft University of Technology, 2015

Lindström, G., Johansson, B., Persson, M., Gardelin, M. and Bergström, S. 1997. Development and test of the distributed HBV-96 hydrological model. Journal of Hydrology. 201. 272-288. 10.1016/S0022-1694(97)00041-3.

Meinen, G., Verbiest, P., and de Wolf, P. P. 1998. Perpetual inventory method. Service lives, discard patterns, and depreciation methods. Heerlen-Voorburg: Statistics Netherlands.

Nobre, A. D., Cuartas, L. A., Momo, M. R., Severo, D. L., Pinheiro, A., and Nobre, C. A. 2016. HAND contour: a new proxy predictor of inundation extent. Hydrol. Process. 30, 320–333. doi:10.1002/hyp.10581

Shebalin et al. 1978. Kondorskaya N. V. and Shebalin N. V. (eds). 1982. New Catalogue of strong earthquakes in the USSR from Ancient Times through 1975. 2nd edition, Boulder, Colorado, 608 pp. (1st edition, 1977, Moscow, 536 pp., in Russian).

Smith, Greg. 2003. Flash Flood Potential: Determining the Hydrologic Response of FFMP Basins to Heavy Rain by Analyzing Their Physiographic Characteristics. A white paper available from the NWS Colorado Basin River Forecast Center web site at http://www.cbrfc.noaa.gov/papers/ffp_wpap.pdf, 11 pp.

Stewart, B. 2007. Implementation of a flash flood guidance system with global coverage, A joint proposal by WMO Commission for Hydrology and WMO Commission for Basic Systems, April 2007, http://www.hrc-lab.org/giving/giving-pdfs/WMOProspectus_April-2007.pdf

Stiedl, D. 1998. Productivity Norms for labour based construction. Retrieved from http://www.ilo.org/dyn/asist/docs/F170469982/Techinical Brief No.2 - Productivity Norms for la.pdf

Strahler, A. N. 1964. Handbook of Applied Hydrology, edited by V. T. Chow, pp. 4–39 4–76, McGraw-Hill, New York.

Szabo, A. and Barfield, T. J. 1991. Afghanistan: an atlas of indigenous domestic architecture. Thomas Barfield.

Uppala, S. M., Kallberg, P. W., Simmons, A. J., Andrae, U., Bechtold, V. da C., Fiorino, M., Gibson, J. K., Haseler, J., Hernandez, A., Kelly, G. A., Li, X., Onogi, K., Saarinen, S., Sokka, N., Allan, R. P., Andersson, E., Arpe, K., Balmaseda, M. A., Beljaars, A. C. M., Berg, L. van de, Bidlot, J., Bormann, N., Caires, S., Chevallier, F., Dethof, A., Dragosavac, M., Fisher, M., Fuentes, M., Hagemann, S., Holm, E., Hoskins, B. J., Isaksen, L., Janssen, P. A. E. M., Jenne, R., McNally, A. P., Mahfouf, J.-F., Morcrette, J.-J., Rayner, N. A., Saunders, R. W., Simon, P., Sterl, A., Trenberth, K. E., Untch, A., Vasiljevic, D., Viterbo, P., and Woollen, J. 2005. The ERA-40 re-analysis, Quart. J. Roy. Meteor. Soc., 131, 2961–3012, doi:10.1256/qj.04.176.

USACE. 2011. Amu Darya River, Afghanistan Critical Sites Bank Stabilization Concepts Design Analysis, September 2011.

USAE. 2011. Amu Darya River, Afghanistan Critical Sites Bank Stabilization Concepts; Design Analysis, US Army Corps of Engineers, September 2011

Veldkamp, T. I. E., Wada, Y., Aerts, J. C. J. H. and Ward, P. J. 2016. Towards a global water scarcity risk assessment framework: incorporation of probability distributions and hydro-climatic variability, Environ. Res. Lett. 11 (2016) 024006.

Weedon, G. P., Balsamo, G., Bellouin, N., Gomes, S., Best, M. J., and Viterbo, P. 2014. The WFDEI meteorological forcing data set: WATCH Forcing Data methodology applied to ERA-Interim reanalysis data. Water Resources Research, 50, doi:10.1002/2014WR015638

Software in the 21st Century. pp. 247–261. Springer Berlin Heidelberg, Berlin, Heidelberg (2012).

Photo: manxman.

CHAPTER 2

Drought

2.1 Approach

2.1.1 Overview

Drought is a sustained and regionally extensive occurrence of below average natural water availability. Afghanistan suffered a severe drought from 1998–2006 and another from 2008–2009 and is battling yet another dry spell with serious consequences for food security. We made an overview of reported historical drought losses, based on public domain data such as the EM-DAT disaster database.

Drought can be classified into three categories or any combination of the three:

- Meteorological (lack of precipitation);
- Hydrological (reduced stream flow);
- Agricultural (low soil moisture).

Identification of drought is not trivial. A lack of precipitation (meteorological drought) may not directly result in hydrological drought because of a buffer capacity in the system (storage of water in the subsoil, groundwater zone). Likewise, hydrological drought may not directly result in water shortage because of the buffer capacity of reservoirs. A socioeconomic drought impact occurs when the available water is not sufficient to meet the demand for water supply (domestic, municipal, and industrial), agriculture, hydropower, and environmental flows.

The drought risk analysis is based on two models: the distributed rainfall-runoff model WFLOW and the water balance model RIBASIM. WFLOW provides the necessary input flow series for RIBASIM, which assesses the impacts of meteorological and hydrological droughts on water users. We distinguish three main user categories: agriculture (crop production), hydropower production, and Domestic, Municipal, and Industrial (DMI). Impacts are expressed in terms of annual losses relative to average or potential conditions:

Agriculture	Water shortage for irrigation (%)	Calculated as the relative difference between the volume of water shortage and the volume of water demand.
Hydropower	Hydropower production losses (%)	Calculated as the relative difference between actual hydropower production and median production.
DMI	Water shortage for public water supply (%)	Calculated as the relative difference between the volume of water shortage and the volume of water demand.

2.1.2 Water balance model RIBASIM

The RIBASIM water balance model has been designed and set up for all of Afghanistan. The model covers all known and potential water users and infrastructures. Afghanistan is sub-divided into five major river basins (Figure 2-1):

1. Endorheic Aral Sea basin, including the Panj and Amu Darya rivers;
2. Endorheic Karakum Desert with Harirud and Murghab rivers;
3. Endorheic Sistan basin with Harut, Farah, Helmand, and Ghazni rivers;
4. Indus River basin flowing into the Arabian Sea with the Kabul river; and
5. Endorheic Northern basin with Shirin Tagab, Sare Pul, Balkh, and Khulm rivers.

Figure 2-1
The five major river basins in Afghanistan.

For the purpose of the drought risk analysis, we further divided these five basins into 105 subbasins or catchments based on the location of infrastructures like rivers, dams, recording stations, and water user intakes. For each subbasin we collected data on irrigated areas and population. Subsequently, a node-link network schematization was designed covering all existing known and potential infrastructures and users. The water balance was computed for each subbasin over time on a half-monthly basis.

2.1.3 Drought hazard analysis

The meteorological and hydrological analyses (drought hazard) are based on the same WFLOW model simulation results as in Chapter 1.

Multiple year historical meteorological (rainfall and snowmelt) and hydrological (discharge) time series per subbasin were generated. Those series were used for the computation of drought hazard indicators and as input for RIBASIM. The length of the simulated time period is 44 years (1958–2001).

As an indicator for meteorological drought, we used a derivative of the Standardized Precipitation Index (SPI) (McKee et al. 1993).

The agricultural water shortages were translated into economic damages as follows:

- In case of a water shortage in percentage of the total demand, crop losses were assumed to be the same percentage for each crop type. In other words, it was assumed a drought event does not result in a change in percentages of crop types planted.
- For each crop a market price was established using local expertise and FAOSTAT 2016.

Furthermore, hydropower losses were computed with the RIBASIM model and translated to economic losses assuming a market price of US$50 per MWh.

2.1.4 Future conditions

The meteorological forcing for future climates as carried out in Chapter 1 resulted in new meteorological and hydrological time series, which were used to analyze the climate in 2050. Finally, the 2050 climate projection was combined with the population growth scenario SSP4.

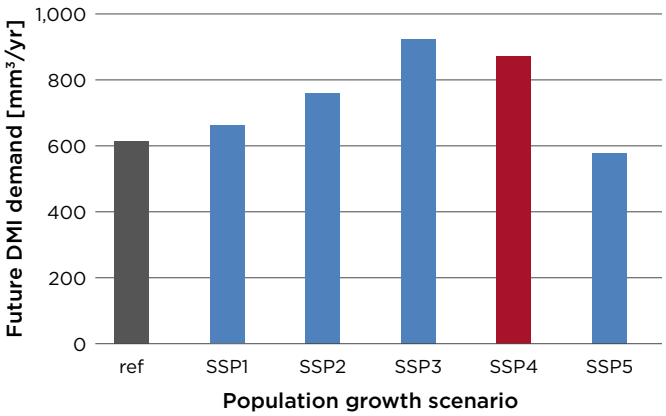

Figure 2-2
Projected DMI surface water demand for 2050 as follows from the five population growth scenarios.

The SSP4 scenario provides a growth factor for urban population and rural population. In the reference situation we estimated for each subbasin the urban and

rural population that is connected to public water supply from surface water. Applying the growth factors results in an increase of the total population that requires a water supply from surface water: from 12,191,434 to 26,410,673 persons. Figure 2-2 shows how the different scenarios translate into different total annual demands for public water supply (DMI). The SSP4 scenario results in the second largest DMI water demand.

2.2 Data gathering and analysis

Data required for the drought analysis consists of meteorological and hydrological time series of catchment runoff, monitored river flow, rainfall, open water evaporation and reference crop evapotranspiration, data on historical drought losses, water supply infrastructure (dams), and water use, especially agriculture and DMI water use and hydropower.

2.3 Results

2.3.1 Historical drought losses

Drought in Afghanistan is caused by below normal precipitation in the winter and early spring season, which results in insufficient water stored for use throughout the summer season. A dry winter may translate into a small snowpack, low reservoir levels, streams that run dry, and low water levels in wells. This could cause a shortage of safe potable water, shortage of irrigation water, diminished quality of rangelands, diminished forests, loss of crop diversity and productivity, and reduction in livestock. In turn, this may result in food shortage, loss of jobs, migration, and other socioeconomic problems (IWMI, 2004).

Because drought is a slow onset phenomenon with long duration and diverse impacts, it is difficult to know whether observed losses can be directly assigned to the drought. Table 2-1 gives an overview of drought losses in Afghanistan from various data sources. A well-known drought that affected the whole of Afghanistan occurred from 1998–2002. The EM-DAT database only reports losses from 2000–2002, but other sources mention 1998 as the start of a multiyear drought (UNEP, 2009).

2.3.2 Drought hazards (meteorological)

2.3.2.1 National scale

Figure 2-3 shows a time series of annual precipitation for Afghanistan. It also shows the moving average (window of two years) and the average over the entire period. It follows from this figure that over a period of 40 years (1959–1998) three nationwide meteorological droughts occurred: 1969–1970, 1982–1985 and 1996–1998.

Table 2-1

Overview of reported droughts and losses in Afghanistan.

Year	Provinces affected	Number of people affected	Economic impact (1,000 US dollar)	Source
1969		48,000	200	EM-DAT database
1971–1973	Central, north-west, north-east, west			EM-DAT database
2000–2002	Kandahar, Helmand, Nimroz, Zabul, Uruzgan, Herat, Farah, Badghis, Paktia, Khost, Ghazni, Baghlan, Kunduz, Takhar, Badakhshan	2,580,000	50	EM-DAT database
2006		1,900,000		EM-DAT database
2008	Kunduz, Balkh, Faryab,Badghis	280,000		EM-DAT database
2011	Balkh, Samangan, Takhar, Sraipul, Heart, Badghis, Faryab, Jowzjan, Baghlan, Kunduz, Badakshan, Bamiyan, Daikundi, Ghor	1,750,000	142,000	EM-DAT database
Jan 2012	Ghor	714		RAF
May–Jun 2012	Kandahar	1,512		RAF
Jul 2013	Ghor	104,000		HUMRES 2016
Oct 2013–Jun 2014	Badghis, Ghor, Hirat	7,468		RAF
Nov 2014–Feb 2015	Badghis, Hirat	623		RAF

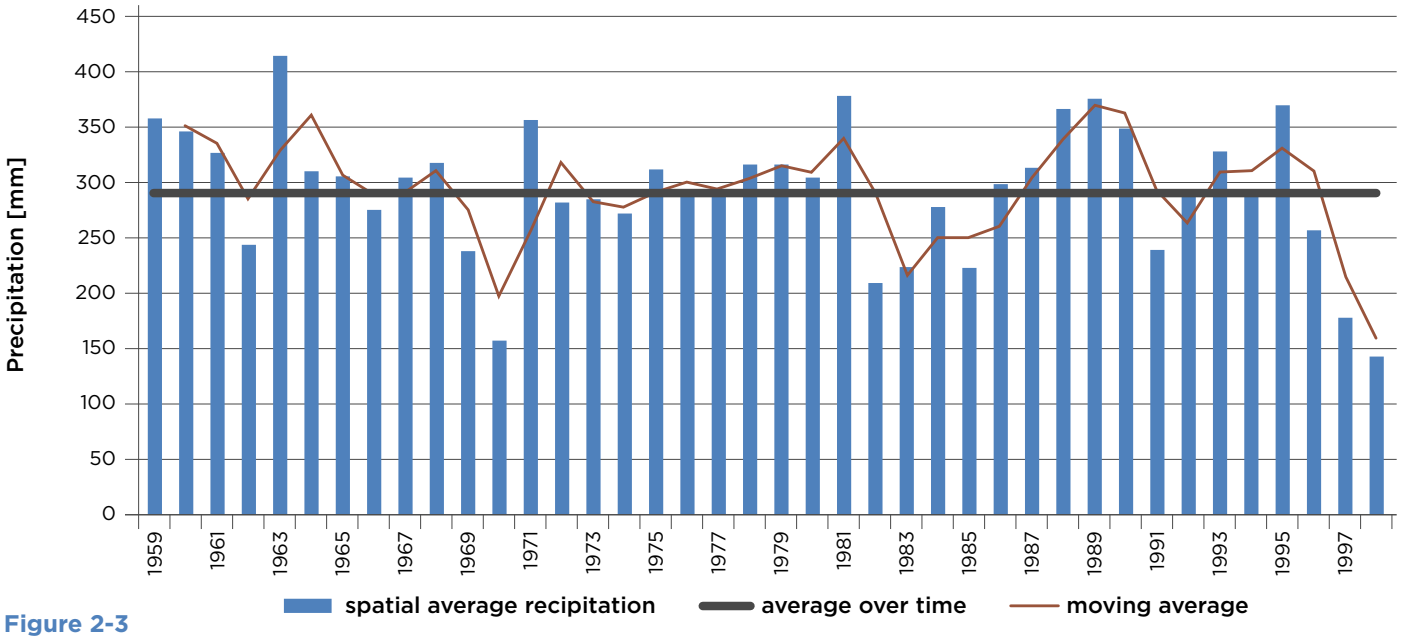

Figure 2-3

Annual and moving average precipitation over all Afghanistan river basins compared to average precipitation over time.

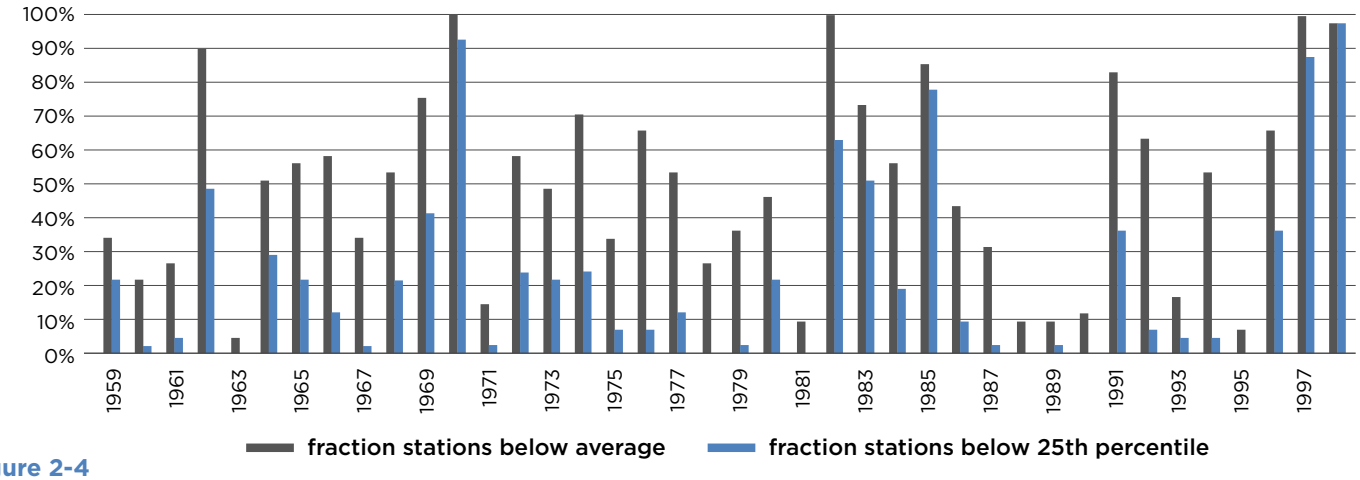

Figure 2-4

Fraction of basins where yearly precipitation sums are below average (grey) and below 25th percentile (blue).

To obtain insight into the spatial extent of meteorological droughts, we calculated for each year how many of the 41 catchments (%) had below-average precipitation and how many had a precipitation total below the 25th percentile (Figure 2-4). The years 1970, 1982, 1985, 1997, and 1998 stand out. This corresponds well with the earlier mentioned identified meteorological droughts.

The Asian Development Bank (cited in IWMI 2004) states that droughts with a nationwide extent occur on average every 20–30 years, local droughts have a re-occurrence period of three to five years and regional droughts recur every nine to eleven years.

Subbasin scale—historical droughts

A comparison with the drought loss years in the previous section shows that there is a time lag between meteorological drought and drought losses. The reported losses in 1971–1973 may have stemmed from the lack of precipitation in 1969–1970. Likewise, the reported losses in 2000–2002 may stem from the lack of precipitation starting in 1996–1998. An explanation for this time-lag may be found in over-year storage capacity in reservoirs. Another explanation could be that some of the reported losses stem from water shortages from groundwater wells, in which water levels drop after a few years of precipitation deficit, and/or that farmers have some financial reserves to survive one or two drought years.

2.3.2.2 Subbasin scale—drought hazard for various return periods

A meteorological drought can be quantified as a percentage deviation from the median annual precipitation. An example map for a return period of 10 years is given in Figure 2-5. It shows that the drought probability is highest in the relatively dry South-Western regions and lowest in the relatively wet Northern regions. The Northern regions receive up to 80 percent of median precipitation with a return period of 10 years, and up to 60 percent of median precipitation with a return period of 100 years. In other words, in these regions precipitation variability relative to the median is small. The dry regions that receive less precipitation on average (South-West) have larger precipitation variability relative to the median and thus a larger probability of meteorological drought. In those regions, precipitation is up to 50 percent of the median once in 10 years, and may reduce to 20 percent of the median once in 100 years.

Exposure to drought is quantified as the population number and percentage of irrigated agriculture on the national scale, the basin scale, and the subbasin scale.

2.3.3 Drought risk

2.3.3.1 Water shortage for DMI for various return periods

The RIBASIM simulation results show that there is only a small risk of water shortage for domestic, municipal, and industrial use. Note that the analysis only takes into account the public water supply from surface water and summarizes water availability and demand for the entire subbasin. Shortages may still occur for people within the basin that are not well connected to the surface water supply. Furthermore, there can still be a shortage of water from other resources such as groundwater.

2.3.3.2 Water shortage for agriculture for various return periods

Water shortage is defined in terms of percentage deviation from the water demand. Water shortage for agriculture in each subbasin was calculated for various return periods T. Figure 2-6 and Figure 2-7 show the resulting maps for T = 10 and T = 1,000. The maps show that agricultural drought risk is highest in the Helmand basin and lowest in the northeast of the country. Missing values in the figures are due to the data containing too many zero values to fit a frequency curve. Note that return periods are calculated for each subbasin individually, which means that the deficits in the subbasins do not necessarily occur simultaneously.

According to the future climate projections obtained using the GCM scenario that was selected for drought risk analysis, precipitation will decrease in most subbasins. This not only decreases the surface water availability, but also increases the agricultural demand for surface water irrigation.

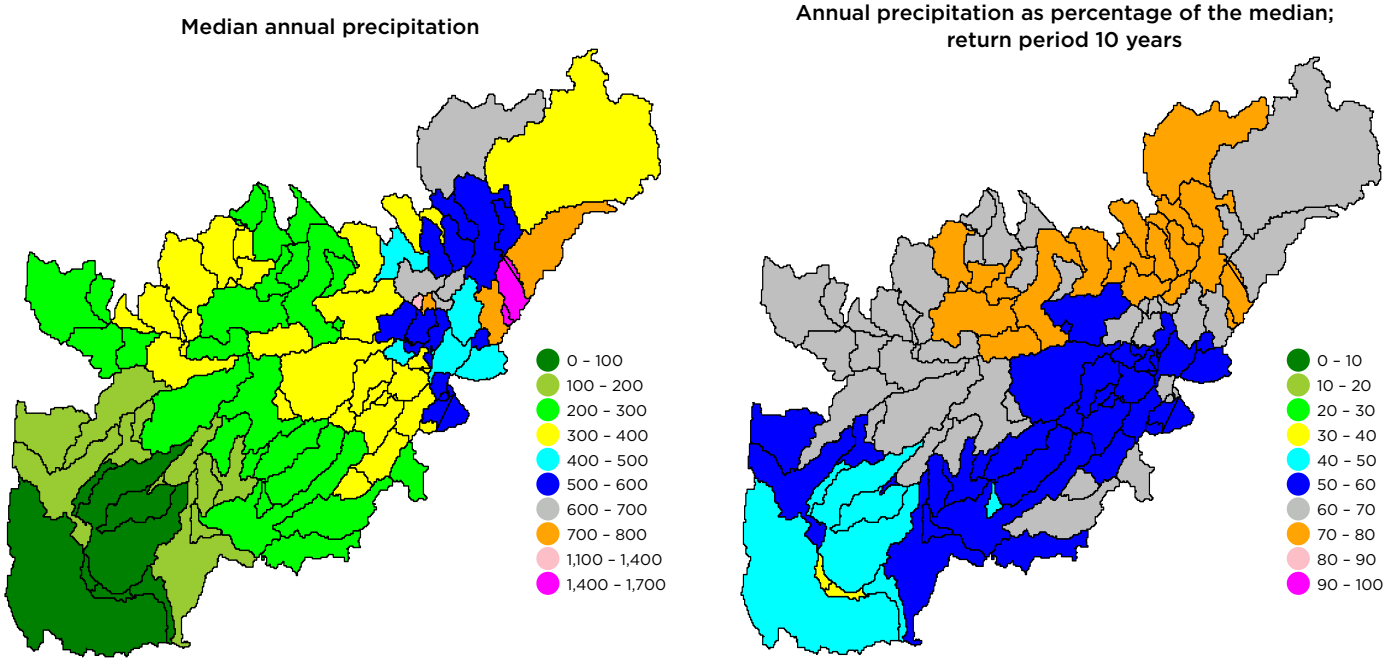

Figure 2-5

Left panel: median annual precipitation map (mm/year). Right panel: T = 10 annual precipitation map as percentage of the median.

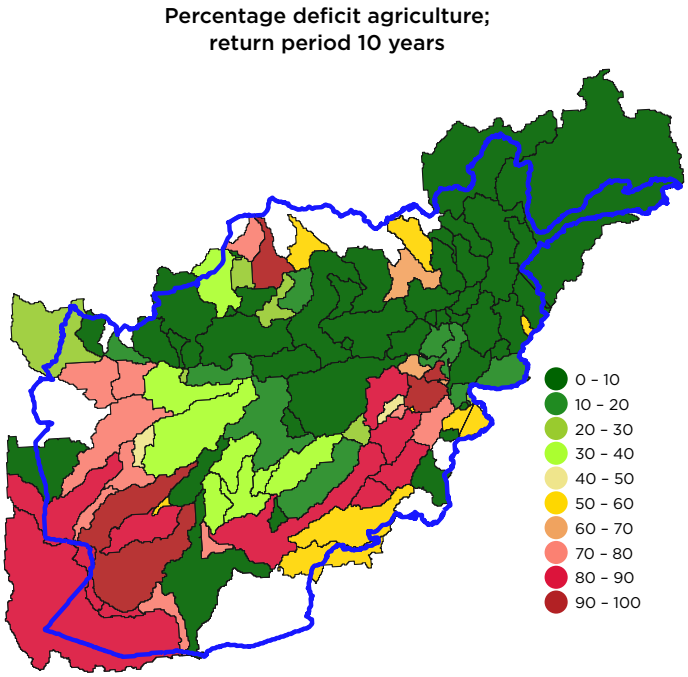

Figure 2-6

Agricultural drought risk map: water shortage in percentage of water demand for T = 10 years.

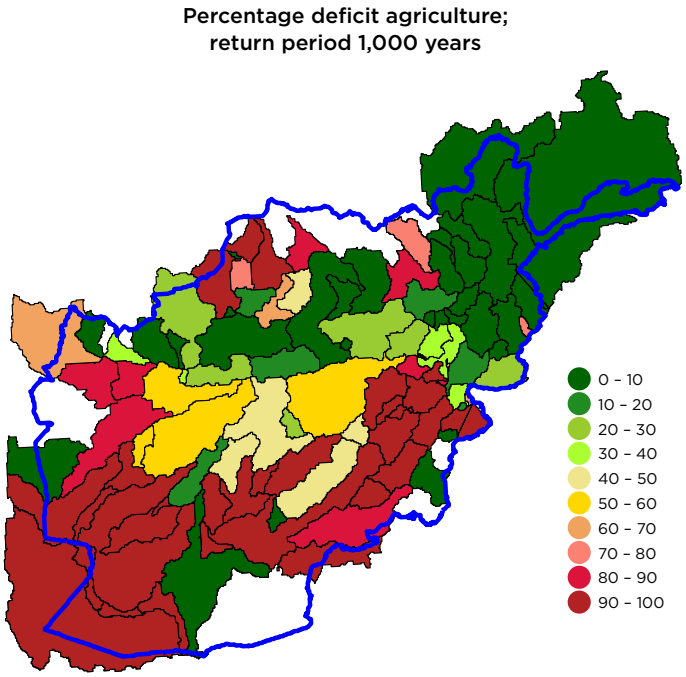

Figure 2-7

Agricultural drought risk map: water shortage in percentage of water demand for T = 1,000 years.

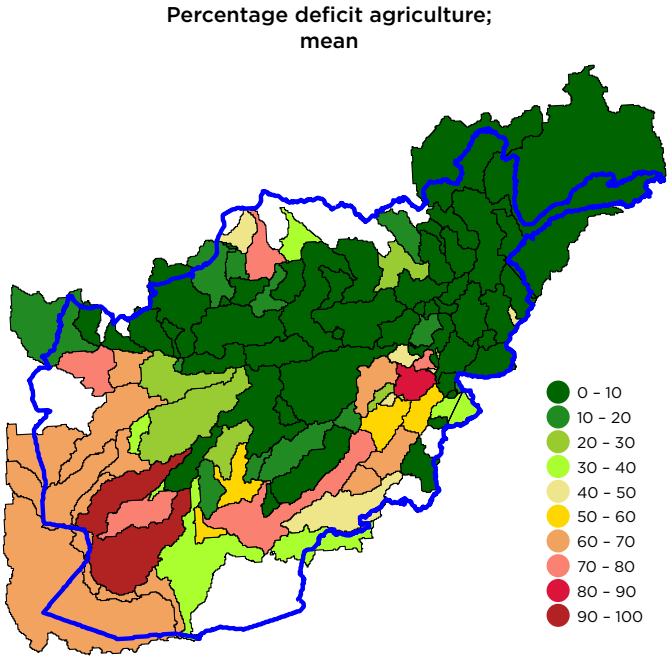

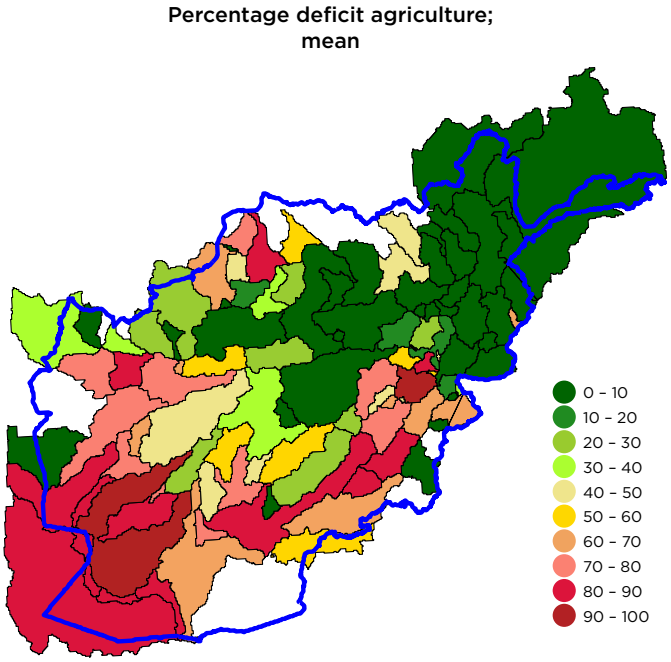

Figure 2-8

Agricultural drought risk map (expected annual water shortage in percent), for current (left) and future (right) conditions.

2.3.3.3 Hydropower production for various return periods

We simulated hydropower production for the reservoirs of Kajaki and Naghlu, and fitted frequency distributions on the annual hydropower production results. Table 2-2 shows the estimated production for various return periods. For example, one in ten years the Kajaki reservoir production is expected to go down to 134 GWh (37 percent of the median), and the Naghlu production to 64 GWh (31 percent of the median).

When future climate follows the dryer (IPSL) scenario and population is increasing, in 2050 the hydropower production is projected to reduce significantly (Table 2-3). Zero production can then be expected once every 10 years at Kajaki and once every 20 years at Naghlu.

Table 2-2

Hydropower production for various return periods for two reservoirs.

	Kajaki		Naghlu	
T	GWh	% median	GWh	% median
10	134	37	64	31
20	43	12	51	25
50	41	11	0	0
100	41	11	0	0
250	41	11	0	0
500	41	11	0	0
1,000	41	11	0	0
Median	**359**		**205**	

Table 2-3

Hydropower production for various return periods for two reservoirs, under the 2050 scenario.

	Kajaki		Naghlu	
T	GWh	% median	GWh	% median
10	0	0	12	12
20	0	0	0	0
50	0	0	0	0
100	0	0	0	0
250	0	0	0	0
500	0	0	0	0
1,000	0	0	0	0
Median	**130**		**98**	

2.3.3.4 Economic losses

Table 2-4 and Figures 2-9 and 2-10 show, on the national and provincial levels, the economic losses in absolute numbers as well as in percentages of the total capital stock.

2.3.3.5 Population affected

Drought impacts on population are more difficult to quantify as a water flow deficit in a given area may be alleviated by a water flow surplus in a nearby area. In other words, human interventions have a major impact on drought risks, and these impacts can only be quantified in a detailed analysis. In order to still have some indication on droughts and affected populations, we applied the following relatively straightforward and large-scale approach:

Figure 2-4

Computed damages per return period and the expected Annual Average Losses (AAL).

	Return period							
	10	20	50	100	250	500	1,000	AAL
Million USD	2,510	2,725	2,974	3,125	3,261	3,352	3,432	279
Percentage of the total capital stock	5.56%	6.04%	6.59%	6.93%	7.23%	7.43%	7.61%	0.62%

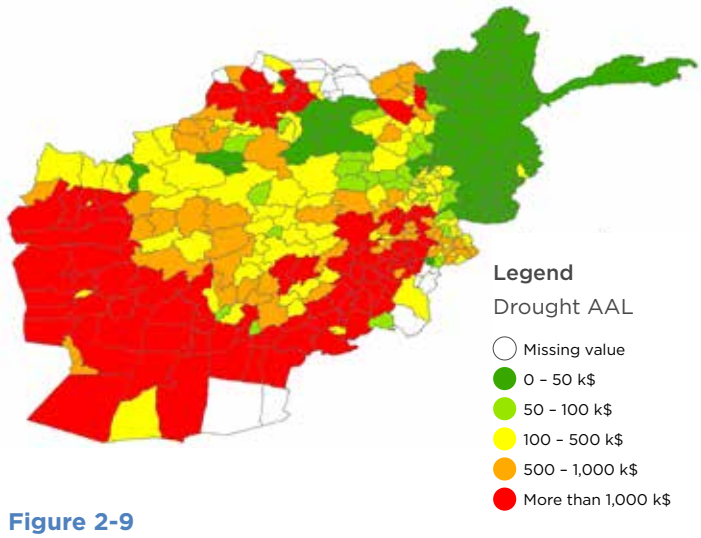

Figure 2-9

Annual average losses for agriculture.

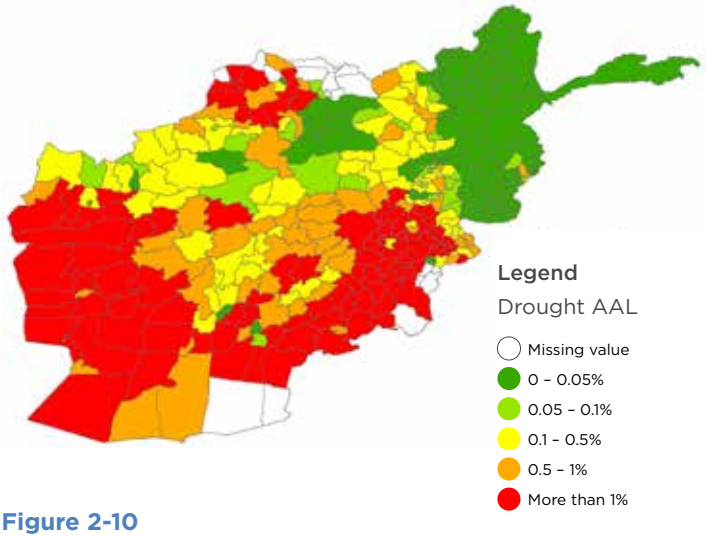

Figure 2-10

Annual average losses for agriculture as a percentage of total stock.

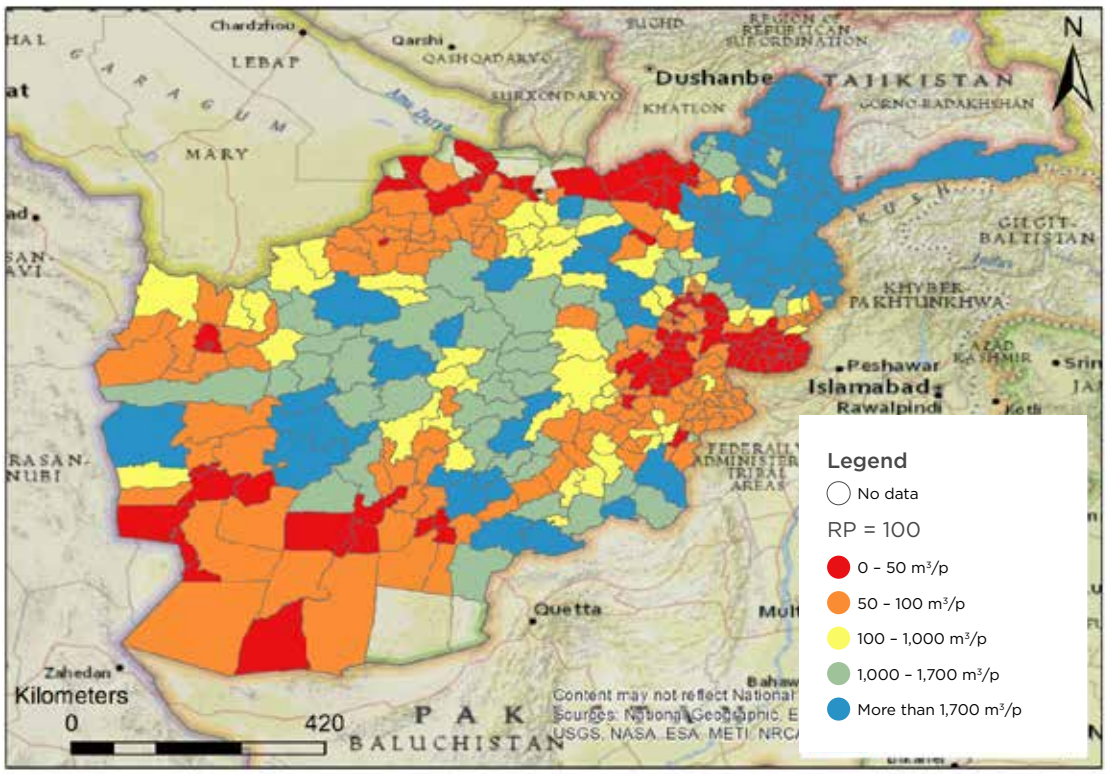

Figure 2-11

Resulting classes for drought affected population for a return period of 10 years.

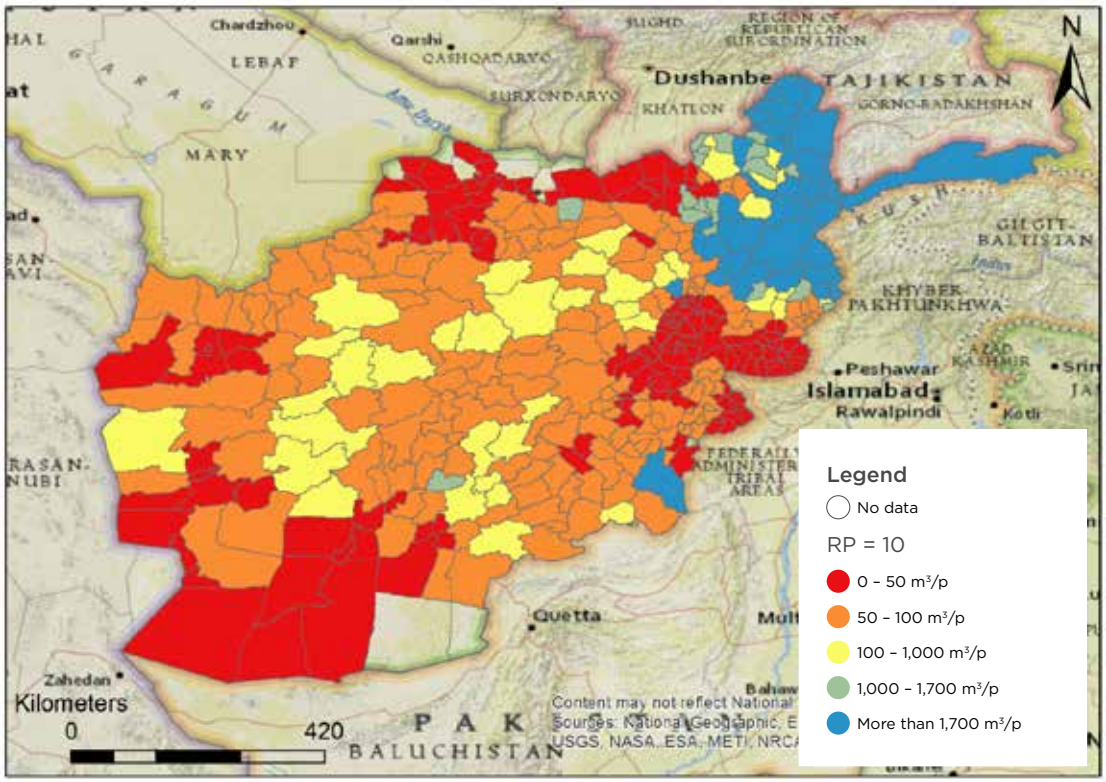

Figure 2-12

Resulting classes for drought affected population for a return period of 100 years.

1. Compute the total annual water flow for each subbasin, not including the flow that is generated in upstream subbasins;
2. Compute the total annual water flow per province and per district by overlaying the subbasins on the provinces and districts; and
3. Compute the total water availability per capita by dividing the total annual flow by the total number of inhabitants.

Results are presented in terms of five classes, varying from severe drought (Class 1) to abundance of water (Class 5); see Table 2-5. The class boundaries were mainly based on Veldkamp et al. (2016). We added an additional class boundary of 50 m³/capita/year, to make a further distinction between the severest of drought conditions.

Table 2.5

Definition of classes to assess drought-affected population.

Class	Lower limit [m³/capita/year]	Upper limit [m³/capita/year]
1	0	50
2	50	500
3	500	1,000
4	1,000	1,700
5	1,700	–

The resulting classes were derived for both historical years (1959–2002) and for various return periods. Figure 2-11 and Figure 2-12 show the results for return periods of 10 years and 100 years.

References

Chapter 2

IWMI working paper 91. 2004. Drought series. Paper 5. Drought impacts and potential for their mitigation in Southern and Western Afghanistan, Kamal Bhattacharyya, Pir Mohammad Azizi, Sayed Sharif Shobair and Mohammad Yasin Mohsini. ISBN 92-9090-589-1.

McKee, T. B., N. J. Doesken, and J. Kleist 1993. The relationship of drought frequency and duration of time scales. Eighth Conference on Applied Climatology, American Meteorological Society, Jan 17–23, 1993, Anaheim CA, pp.179–186.

Veldkamp, T.I.E., Wada, Y., Aerts, J.C.J.H., Ward, P.J. 2016. Towards a global water scarcity risk assessment framework: Incorporation of probability distributions and hydro-climatic variability. Environmental Research Letters. 11. 10.1088/1748-9326/11/2/024006.

FAOSTAT 2016. Database of food and agriculture statistics. http://faostat.fao.org/site/339/default.aspx

HUMRES 2013. Drought in Ghor - statement to press. https://www.humanitarianresponse.info/en/operations/afghanistan/document/drought-ghor-statement-press

Photo: Lukasz Nowak1.

CHAPTER 3

Landslide

3.1 Introduction

The main output of this chapter is the estimation of landslide susceptibility of source areas, namely the likelihood of a landslide originating from an area, for the entire country. A more detailed analysis has been conducted for two focus areas: the Kabul district and the Salang Pass. For the focus areas landslide susceptibility was estimated for source, transit, and accumulation areas; the landslide expected runout was calculated; and the risk associated with each landslide was assessed considering the impacts on structures and infrastructures, the locations of assets and their vulnerability and socioeconomic value.

The methodology pursued, the data exploited, the accuracy level of the assessment (depending on the availability of suitable data), and the results produced are described in the following sections.

3.2 Approach

The assessment consists of several phases, described below.

Phase 1
Compile a landslides inventory according to the following classifications:

1. **Bedrock landslides in slow evolution,** including rotational slides, translational slides, earth flows, and lateral spreading;
2. **Bedrock landslides in rapid evolution,** including falls and toppling—this type of landslide is often induced by earthquakes; and
3. **Cover material landslides in rapid evolution,** including debris-mud flows.

Each class has different physical characteristics, and as a consequence, a different degree of susceptibility, hazard, and risk.

The inventory of historical events has been compiled analyzing first available data and maps of Afghanistan, and then data extracted from remote sensing imageries and gathered from web searches.

Phase 2
Evaluate the causes of landslides by GIS procedures, based on the spatial overlay of existing/surveyed landslides extracted from the available data.

Phase 3
Identify through statistical analysis two different sets of triggering variables:

- Discriminating parameters; and
- Predisposing factors.

Discriminating parameters are necessary but not sufficient conditions for the occurrence of a given type of landslide. They include:

- Slope angle in the niche zone before the event; and
- Bedrock lithology where the rupture surface is imposed.

Predisposing factors are geomorphological, morphometric, geological, geotechnical, hydrogeological and land use factors, which determine the level of susceptibility of each slope.

Phase 4
Through the GIS overlay of discriminating parameters, map and classify the territory into areas (units) characterized by the presence of both discriminating parameters.

Phase 5
Identify through GIS processing the areas characterized by a specific combination of discriminating and predisposing factors in order to quantify the source areas susceptibility.

Phase 6
Compose a susceptibility function.

Phase 7
Produce susceptibility, hazard, and risk maps.

The approach was applied at two different levels of detail (Figure 3-1): nationwide (regional scale) and local scale (focus study areas).

At the national scale (the entire territory of Afghanistan) it is possible to evaluate only the location and susceptibility of all source areas, i.e., the areas where a land-

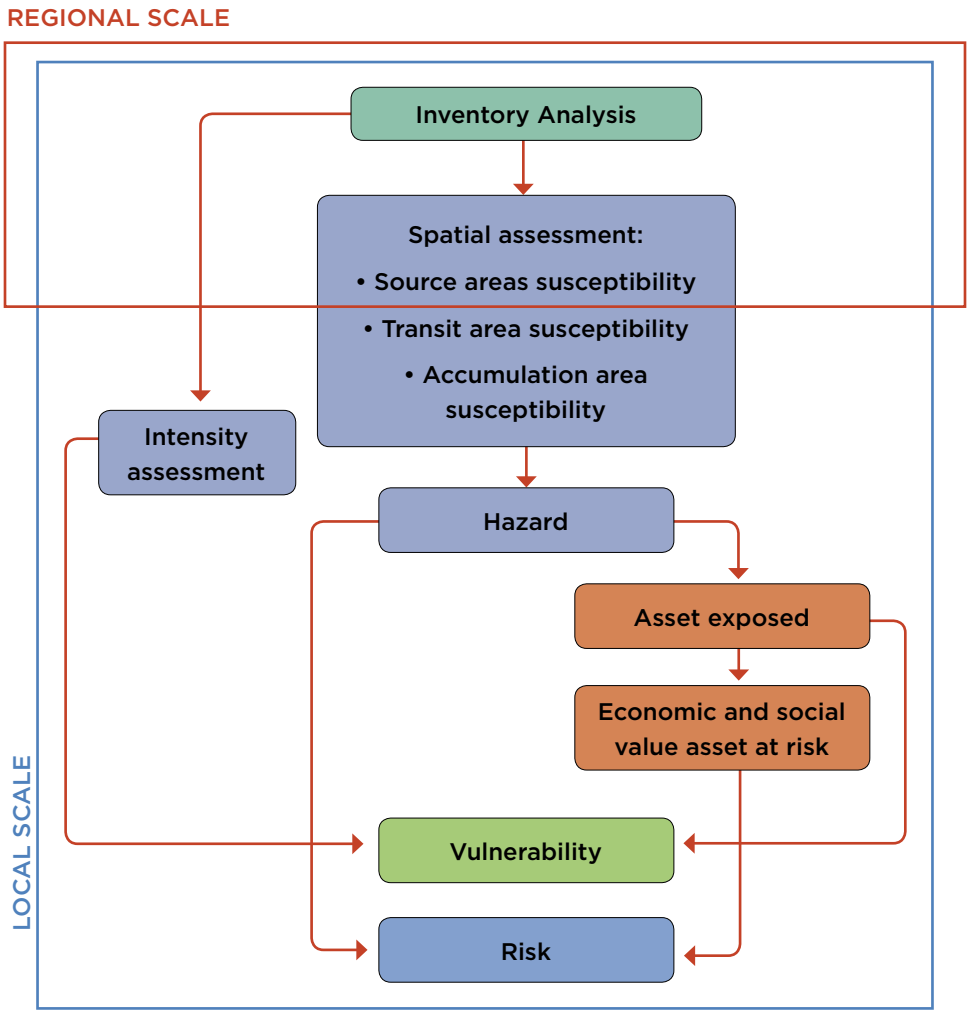

Figure 3-1
Flow diagram for the susceptibility/exposure/risk assessment.

slide can potentially start. A more detailed local-scale approach was adopted to investigate two specific focus areas identified as hotspots: the Kabul District and the Salang Pass (Figure 31). Risk assessment at the local scale accounts for specific geomorphological characteristics, which makes it possible to evaluate transit area susceptibility, accumulation area susceptibility, hazard, runout, intensity, and risk. Vulnerability and socioeconomic value of exposed assets are also assessed at the local scale.

3.3 Data inventory

In order to conduct the analysis,[1] the following data have been used:

- Landslide inventory;
- Digital Terrain Models (DTMs);
- Slope maps;
- Slope and curvature profile maps;
- Geological, lithological, and tectonic maps;
- Geological faults; and
- Land cover maps.

3.3.1 Landslide inventory

The landslide inventory is a collection of landslide events in Afghanistan including event date, location, characteristics, damages, etc. Since no proper inventories were available, it was compiled based on web-search procedures and visual interpretation of remote sensing imagery.

3.3.2 Data analysis

A list of 68 events including damage, possible casualties, and areas affected was retrieved from the United Nations Office for the Coordination of Humanitarian Affairs (OCHA).[2] Since the coordinates of each point are not representative of the precise location of the event, the areas around the points were analyzed in order to identify the starting/triggering sites of landslide events. This analysis has led to the identification of 323 trigger points subdivided as follows: 2 bedrock landslides in slow evolution, 216 cover material landslides, and 105 bedrock landslides in rapid evolution.

Bedrock landslides in slow evolution have lower impacts on structures and infrastructures than rapid landslides because they allow adaptation to the phenomenon. Therefore, in many cases they are not recorded, and only two slow evolution landslide events were identified.

3.4 Source area susceptibility assessment

For each landslide type, discriminant parameters and predisposing factors have been defined. The procedure involves a heuristic approach based on previous experience, literature, similarity, etc., to set the initial values of weights/indexes for the various classes of predisposing factors (lithology, slope, and land use), and a refinement stage where statistical correlations are established between the past events in the landslide repository and the predisposing factors.

For the local scale analysis (Kabul District and Salang Pass), a more detailed assessment of susceptibility was carried out by using a higher resolution (5 x 5 m) DTM and relying on an improved version of the inventory of landslide events.

3.5 Transit and accumulation areas susceptibility assessment (focus areas)

The first step of the local scale analysis was the spatial assessment of source areas and transit area susceptibility for each typology of landslide. To this end, two zones were selected as study areas:

- Kabul District
- Salang Pass

To perform the susceptibility assessment, different approaches were pursued for each type of landslide because the physics of each landslide typology is substantially different.

[1] The methodology used to assess the landslide hazard was developed by ENEA and was tested, during the last decade, in about 20 sites at different scales in several countries.

[2] Source: The Humanitarian Data Exchange (HDX): https://data.humdata.org/organization/ocha-afghanistan? The United Nations Office for the Coordination of Humanitarian Affairs (OCHA, http://www.unocha.org/) manages HDX. OCHA is part of the United Nations Secretariat.

3.6 Results

3.6.1 Susceptibility Maps

Susceptibility maps have been produced for each landslide type:

1. Maps of bedrock landslides in slow evolution are presented at the national level in Figure 3-2, for the Kabul District in Figure 3-5, and for the Salang Pass in Figure 3-8;
2. Maps of bedrock landslides in rapid evolution are presented at the national level in Figure 3-3, for the Kabul District in Figure 3-6, and for the Salang Pass in Figure 3-9; and
3. Maps of cover material landslides in rapid evolution are presented at the national level in Figure 3-4, for the Kabul District in Figure 3-7, and for the Salang Pass in Figure 3-10.

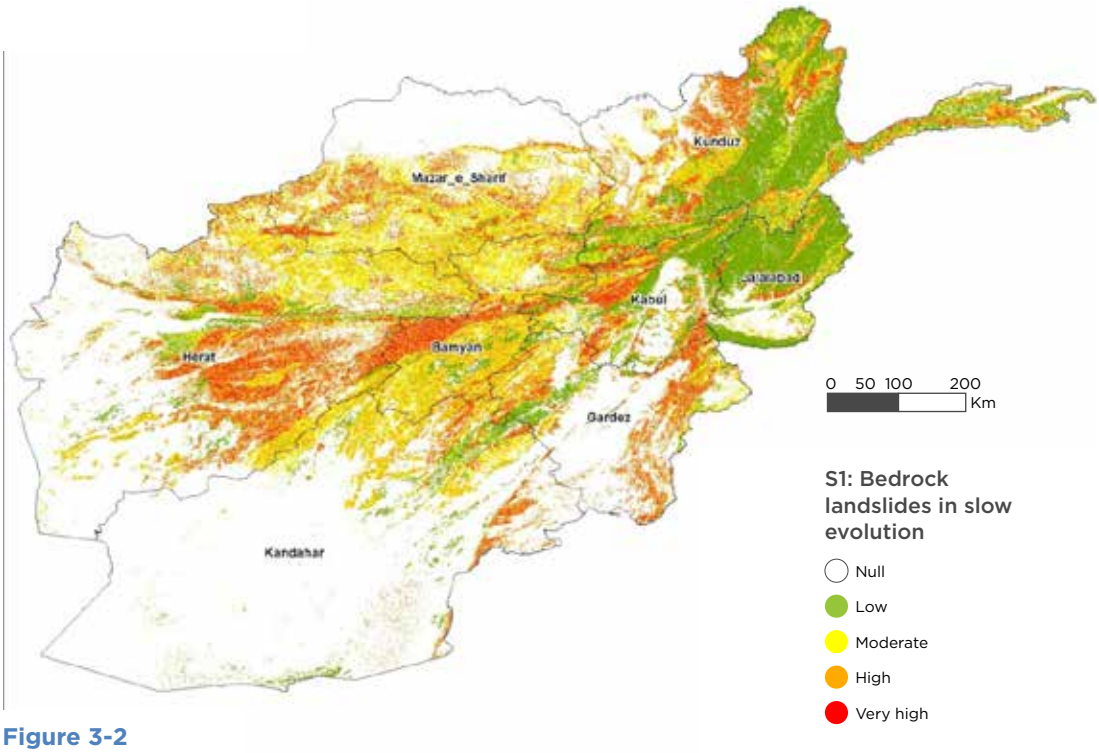

Figure 3-2

Susceptibility map for bedrock landslides in slow evolution (nationwide).

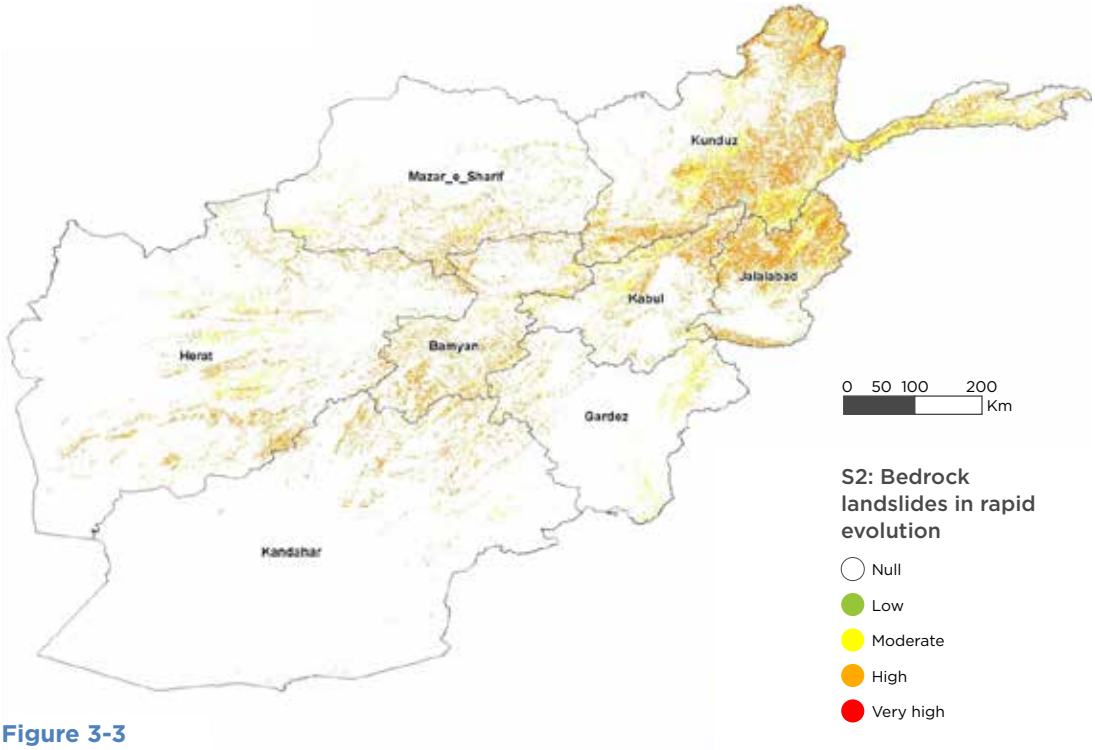

Figure 3-3

Susceptibility map for bedrock landslides in rapid evolution (nationwide).

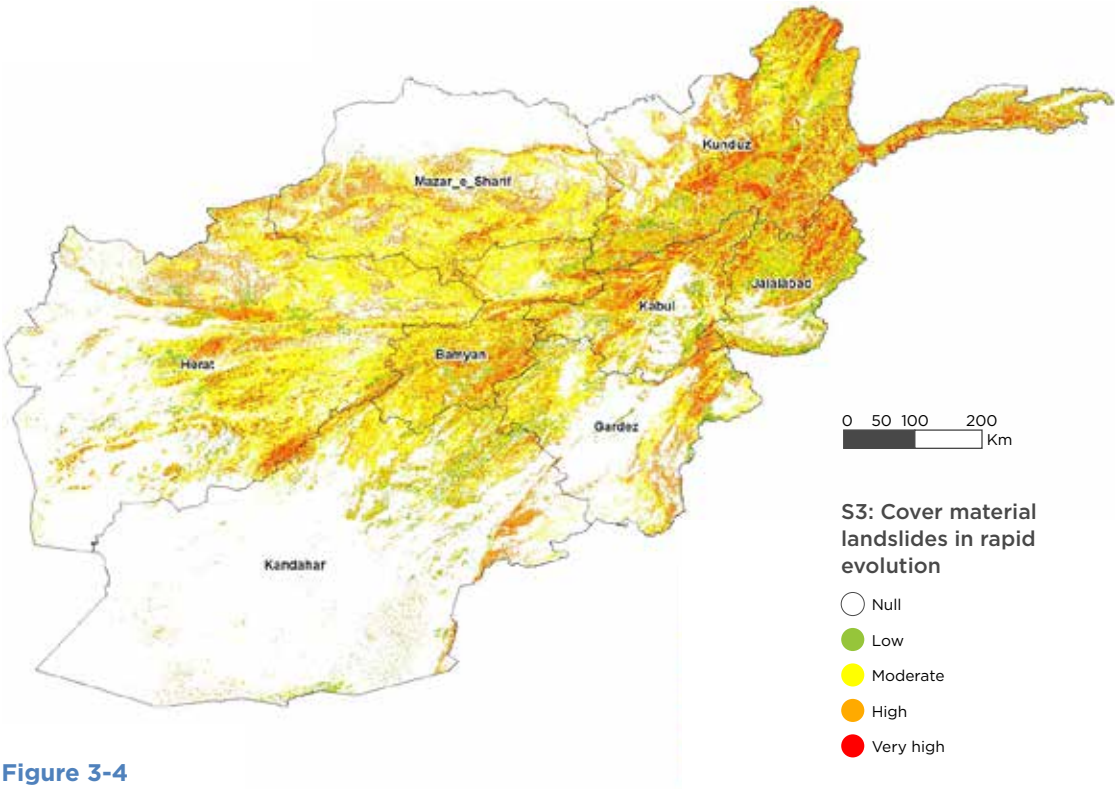

Figure 3-4

Susceptibility map for cover material landslides in rapid evolution (nationwide).

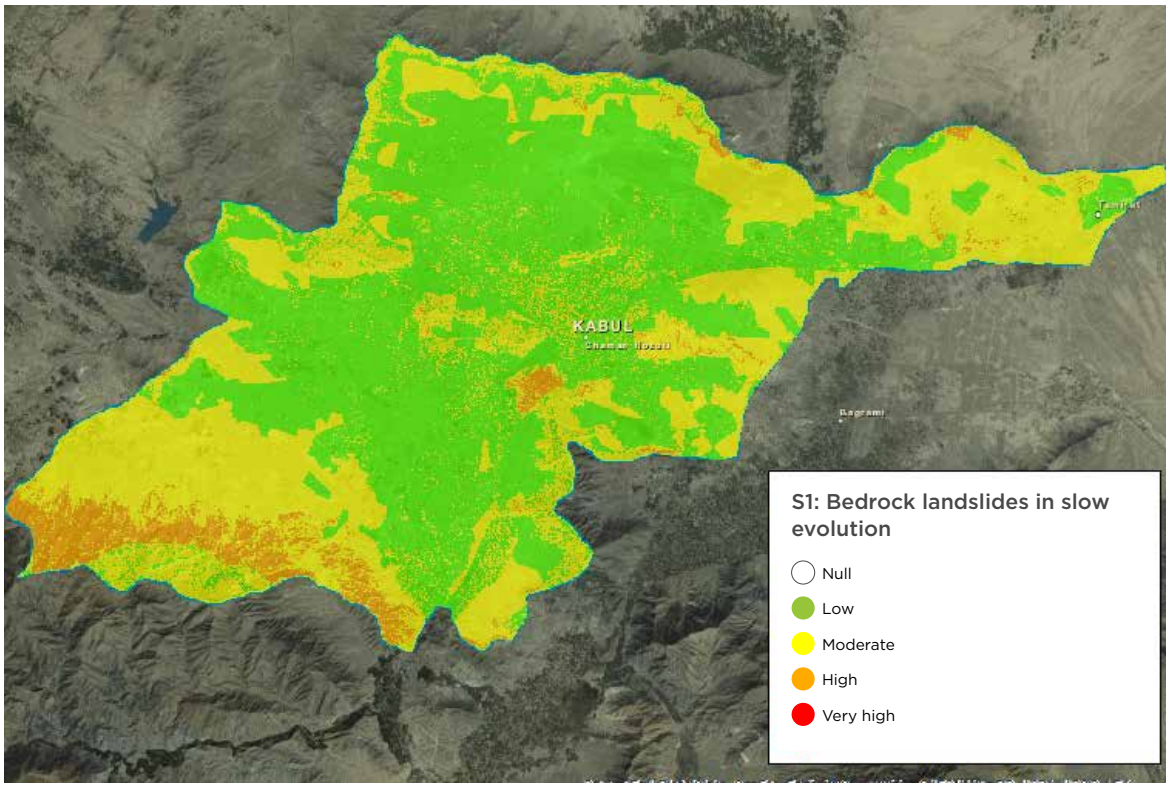

Figure 3-5

Susceptibility map for bedrock landslides in slow evolution (Kabul District).

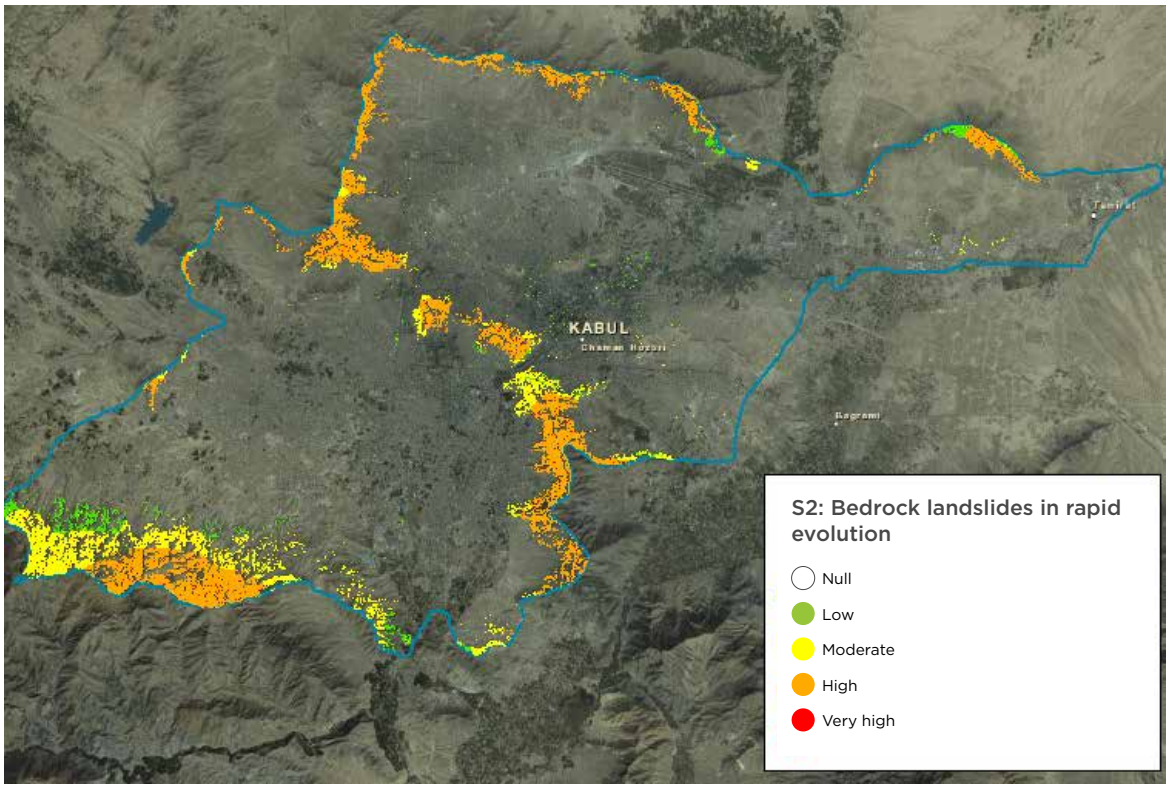

Figure 3-6

Susceptibility map for bedrock landslides in rapid evolution (Kabul District).

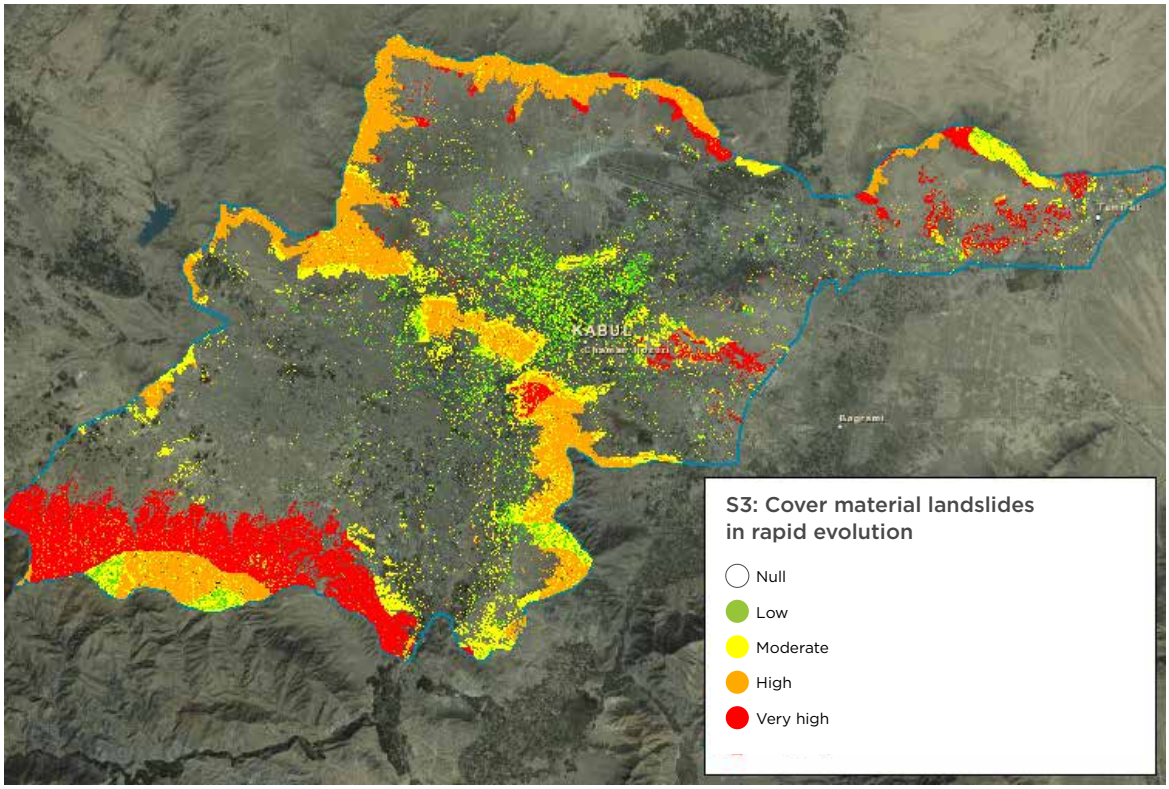

Figure 3-7

Susceptibility map for cover material landslides in rapid evolution (Kabul District).

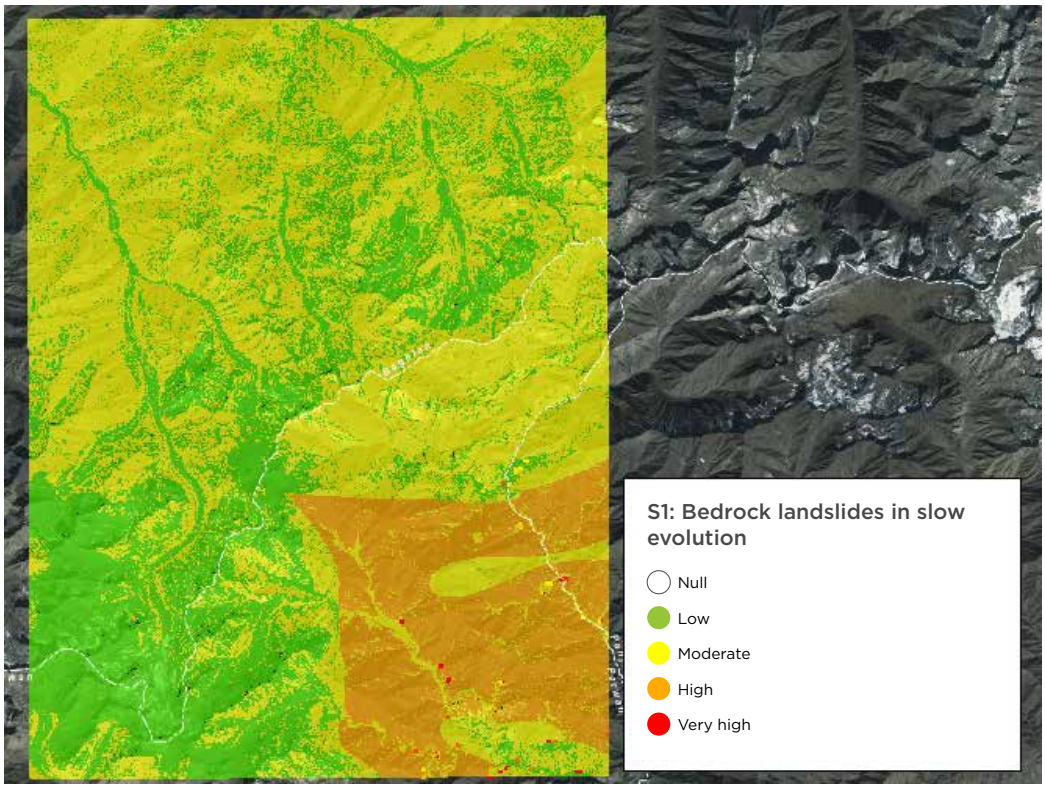

Figure 3-8

Susceptibility map for bedrock landslides in slow evolution (Salang Pass).

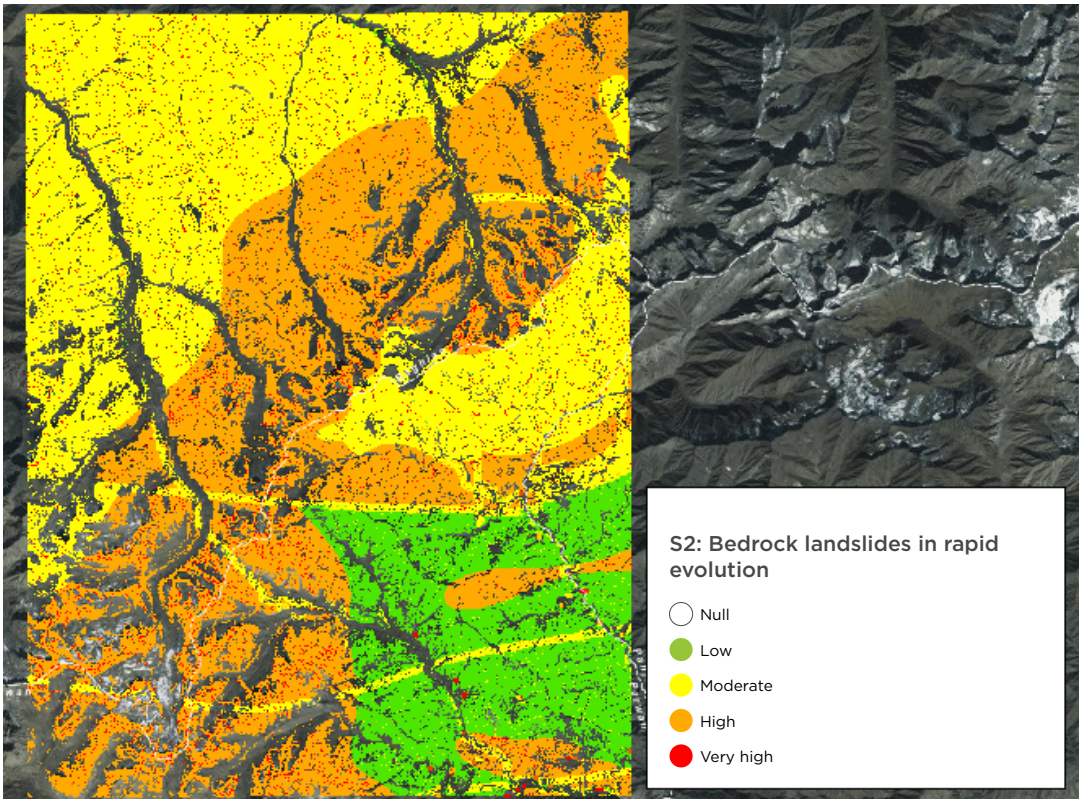

Figure 3-9

Susceptibility map for bedrock landslides in rapid evolution (Salang Pass).

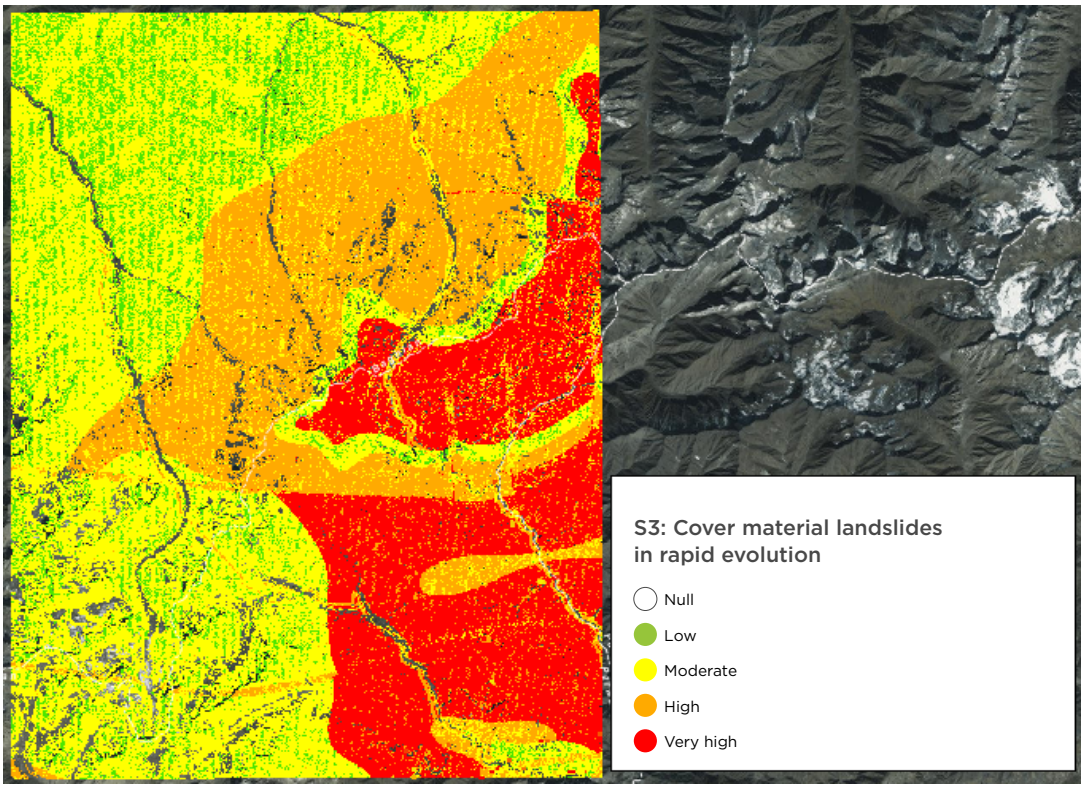

Figure 3-10

Susceptibility map for cover material landslides in rapid evolution (Salang Pass).

3.6.2 Exposure maps: nationwide

At the national level it was not possible to produce landslide risk maps for lack of geomorphological information to determine transit and accumulation areas, runout, intensity, and mass of the landslide, which are needed to determine the impacts and damage to population and infrastructure. Instead, a more qualitative analysis was conducted to provide hazard exposure information, by overlaying the footprint of the landslides with population and assets layers.

In order to evaluate the level of exposure, different assets (population, infrastructures, schools, health facilities, roads, etc.) were considered according to their relevance and socioeconomic value. Such an approach provides a comprehensive overview of the general exposure at the national level. The available exposure data layer for each sector (population, government buildings, commercial and residential buildings, agricultural, infrastructure, and GDP) are as follows:

- Agriculture irrigated (extension in m^2 and value in USD)
- Agriculture rainfed (extension in m^2 and value in USD)
- Clay rural structures (extension in m^2 and value in USD)
- Clay urban structures (extension in m^2 and value in USD)
- Industrial areas (extension in m^2 and value in USD)
- Residential areas (extension in m^2)
- Nonresidential areas (value in USD)
- Roads (length in m and value in USD)
- Roads (classified in four classes according to typology)
- Airports (count)
- Bridges (count)
- Dams (count)
- Health centers and hospitals (count)
- Power plants (count)
- Schools and universities (count)
- Education (classified in four classes by number of students)
- Urban buildings (count)
- Rural buildings (count)
- Population (count)
- Population (classified in four classes by number of people)

As an example, the results for two categories of assets exposed to landslide hazard, population, and GDP, are reported here. The intersection of hazard and exposed datasets has been carried out by using the three landslide susceptibility maps produced at the national level. The datasets of rural, urban, and total population were used. Table 3-1 and Table 3-2 provide overviews of the total population exposed to landslides at the national and provincial levels, respectively. In total, about 8.0 percent of the Afghanistan population are potentially exposed to bedrock landslides in slow evolution events, about 0.1 percent to bedrock landslides in rapid evolution, and about 4.0 percent to cover material landslides in rapid evolution.

Table 3-1

Population and relative percentage to the total population exposed to landslide hazard nationwide, for the three landslide types.

	Bedrock landslides in slow evolution	Bedrock landslides in rapid evolution	Cover material landslides in rapid evolution
Population exposed	2,125,103	26,259	965,778
Percentage of total population	8.0%	0.1%	4.0%

Table 3-2

Population exposed to landslide hazard by province, for the three landslide types.

Province	Number of people exposed to bedrock landslides in slow evolution	Number of people exposed to bedrock landslides in rapid evolution	Number of people exposed to cover material landslides in rapid evolution
Badakhshan	167,525	4,441	109,589
Badghis	66,263	573	29,609
Baghlan	104,631	16	81,861
Balkh	51,587	58	17,642
Bamyan	154,532	416	42,132
Daykundi	223,134	59	35,358
Farah	21,121	0	228
Faryab	100,666	681	58,641
Ghazni	48,003	7	10,648
Ghor	203,946	49	42,961
Hilmand	6,634	0	641
Hirat	37,027	0	17,104
Jawzjan	21,572	0	5,589
Kabul	112,067	6,909	51,295
Kandahar	8,752	0	1,629
Kapisa	14,765	0	10,839
Khost	48,398	0	38,074
Kunar	50,808	387	34,787
Kunduz	9,280	2	6,238
Laghman	24,994	583	21,854
Logar	10,768	0	6,345
Nangarhar	61,765	148	32,693
Nimroz	1	0	0
Nuristan	22,960	7,222	23,136
Paktika	15,272	0	10,257
Paktya	74,434	295	53,655
Panjsher	19,113	429	7,473
Parwan	99,831	2,821	45,516
Samangan	58,089	34	29,914
Sar-e-Pul	94,079	1,120	50,652
Takhar	98,104	9	59,122
Uruzgan	18,876	0	6,942
Wardak	70,538	0	22,324
Zabul	5,568	0	1,030

Figure 3-11 and Figure 3-12 present overview maps of population exposed to landslide hazards. It should be emphasized that these results are merely qualitative and do not give a specific indication of the location where a landslide event could occur. These maps should be considered as a guide to identify administrative areas (provinces or districts) potentially, severely affected considering their population.

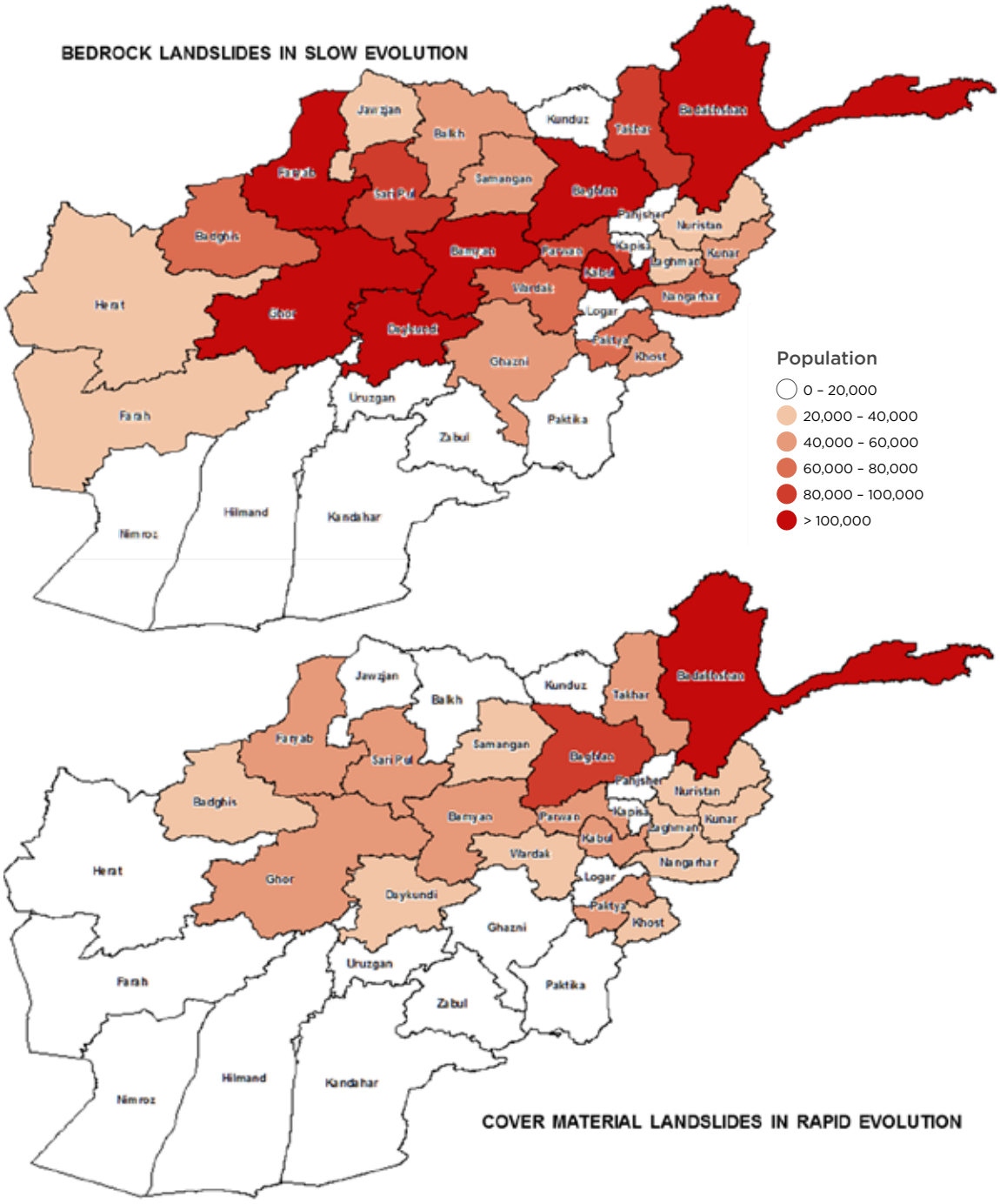

Figure 3-11

Overview maps, depicting population exposed to landslide hazard (bedrock landslides in slow evolution [top] and cover material landslides in rapid evolution [bottom]) by province.

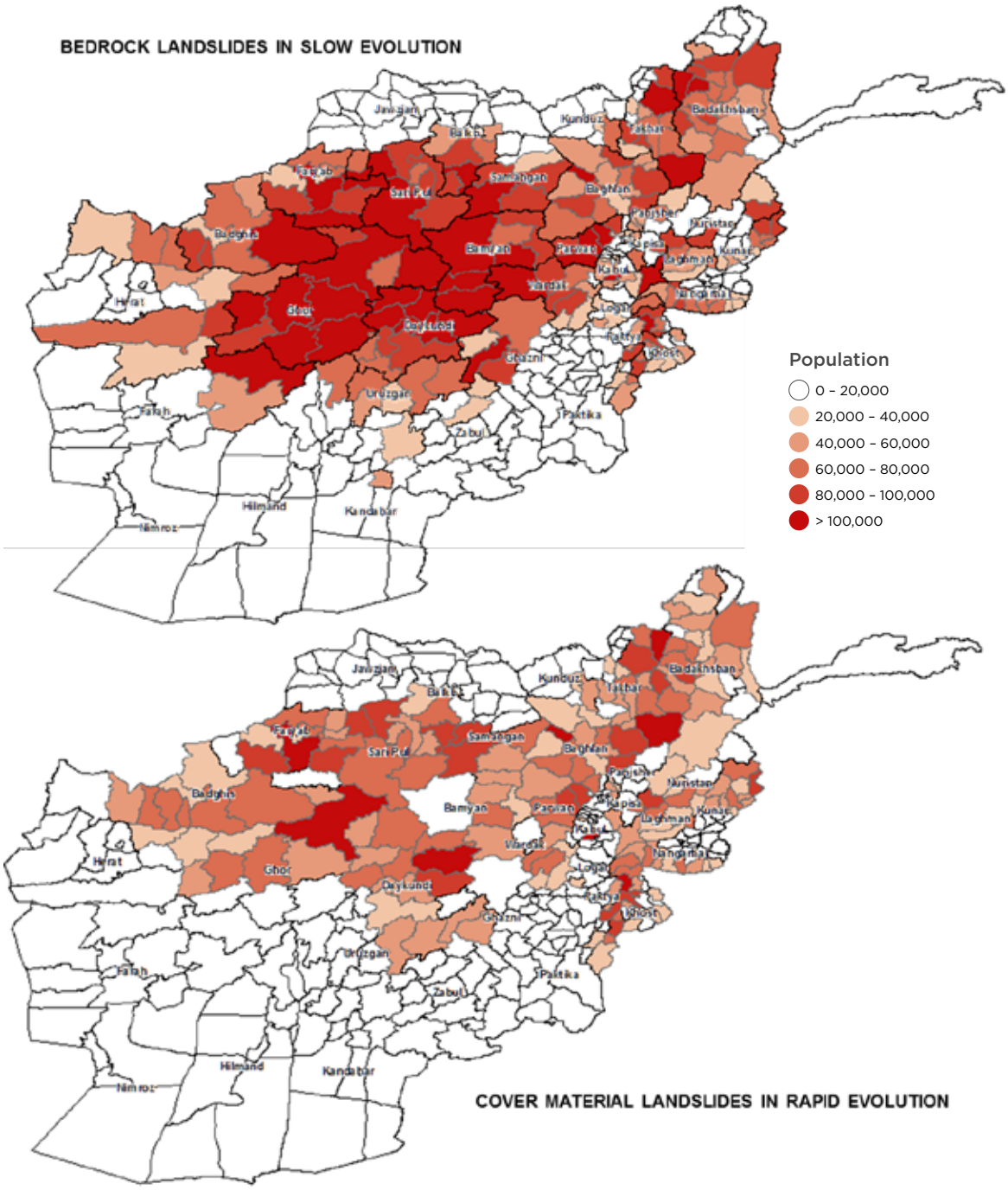

Figure 3-12

Overview maps, depicting population exposed to landslide hazard (bedrock landslides in slow evolution [top] and cover material landslides in rapid evolution [bottom]) by district.

The landslide exposure of assets can be viewed also in terms of GDP (US$). It should be noted that there is no distinction between assets that are destroyed or damaged within this summary—it is assumed that if there is an intersection of the given asset with the assigned landslide susceptibility, then the asset requires replacement. Table 3-3 and Table 3-4 provide an overview of the total GDP exposed to landslides nationwide, and at the province level. Moreover, Figure 3-13 shows the total exposed GDP (US$) for each district.

Table 3.3

Total GDP exposed (assets) nationwide.

Bedrock landslides in slow evolution	Bedrock landslides in rapid evolution	Cover material landslides in rapid evolution
$4,232,212,323	$125,705,141	$2,072,731,037

Table 3.4

Total GDP exposed (assets) by province.

Province	Bedrock landslides in slow evolution (total GDP US$)	Bedrock landslides in rapid evolution (total GDP US$)	Cover material landslides in rapid evolution (total GDP US$)
Badakhshan		$43,820,653.00	$326,232,038.00
Badghis	$172,003,761.00	$3,755,269.00	$87,107,187.00
Baghlan	$201,372,436.00	$3,059,763.00	$148,682,313.00
Balkh	$102,276,908.00	$1,543,359.00	$41,055,048.00
Bamyan	$281,836,574.00	$5,493,782.00	$80,728,076.00
Daykundi	$333,278,933.00	$2,683,418.00	$62,043,911.00
Farah	$44,207,913.00	$47,047.00	$3,470,926.00
Faryab	$219,177,207.00	$6,366,330.00	$118,439,347.00
Ghazni	$66,220,706.00	$714,075.00	$15,873,438.00
Ghor	$327,678,143.00	$3,190,022.00	$71,551,880.00
Hilmand	$20,567,047.00	$25,530.00	$4,565,559.00
Hirat	$94,361,232.00	$536,008.00	$57,941,635.00
Jawzjan	$41,737,123.00	$360,302.00	$15,267,709.00
Kabul	$240,878,510.00	$8,141,415.00	$114,486,930.00
Kandahar	$28,079,397.00	$138,328.00	$9,080,667.00
Kapisa	$24,169,980.00	$600,391.00	$16,780,495.00
Khost	$79,454,047.00	$38,257.00	$56,531,385.00
Kunar	$78,183,875.00	$1,439,973.00	$55,868,210.00
Kunduz	$59,216,152.00	$331,272.00	$32,392,634.00
Laghman	$34,581,852.00	$2,226,951.00	$30,378,873.00
Logar	$25,486,156.00	$764,410.00	$17,310,858.00
Nangarhar	$120,549,449.00	$3,259,726.00	$72,919,456.00
Nimroz	$514,828.00	—	$414,387.00
Nuristan	$28,874,207.00	$15,858,663.00	$39,954,804.00
Paktika	$34,880,849.00	$59,059.00	$19,245,544.00
Paktya	$105,301,318.00	$711,683.00	$73,391,091.00
Panjsher	$34 170 265.00	$5 996 142.00	$21 488 648.00
Parwan	$140 516 148.00	$3 857 310.00	$65 976 174.00
Samangan	$139 751 028.00	$3 285 646.00	$65 363 231.00
Sar-e-Pul	$210 616 760.00	$4 630 102.00	$103 508 714.00
Takhar	$335 540 589.00	$1 553 091.00	$185 112 301.00
Uruzgan	$34 391 964.00	$335 663.00	$9 450 861.00
Wardak	$114 166 850.00	$829 118.00	$45 042 325.00
Zabul	$15 646 957.00	$52 383.00	$5 074 382.00

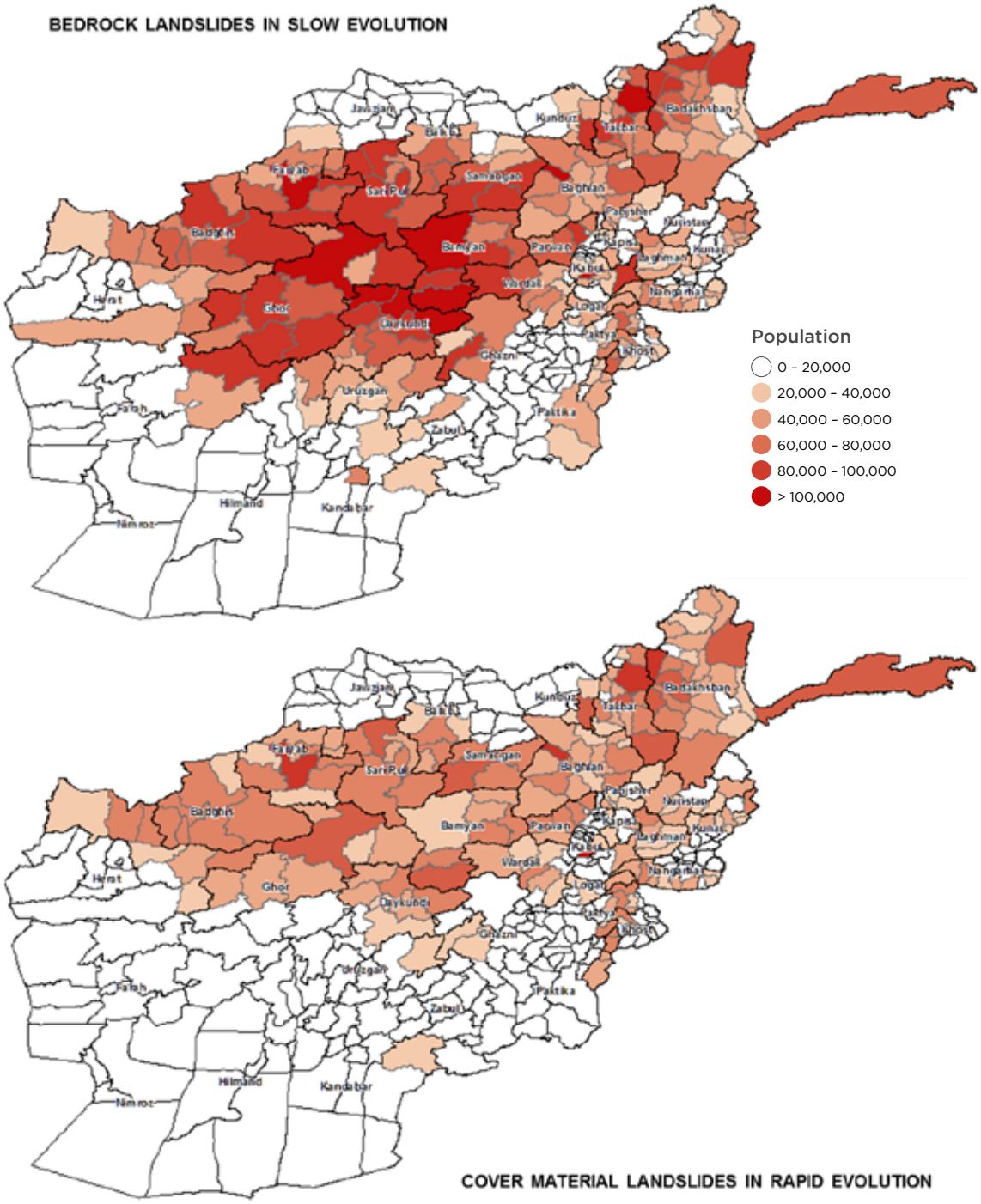

Figure 3-13

Overview maps depicting GDP exposed (total assets) to landslide hazard (bedrock landslides in slow evolution [top] and cover material landslides in rapid evolution [bottom]) by district.

Projections to 2050 for landslide risk have been produced, based on population and GDP growth. Table 3-5 presents the projected exposed rural, urban, and total population, as well as total damage (GDP affected in US$) in 2050.

Projections to 2050 were produced under the assumption that landslide hazard does not change with time; the only varying parameters were population and GDP, according to the Shared Socio-Economic Pathway SSP4.

Table 3-5

Projected exposed rural population, urban population, total population and total damage (GDP affected in US$) in 2050

	Bedrock landslides in slow evolution	Bedrock landslides in rapid evolution	Cover material landslides in rapid evolution
Rural population exposed in 2050	2,278,775	28,157	1,035,616
Urban population exposed in 2050	2,949,113	36,442	1,340,261
Total population exposed in 2050	5,227,888	64,599	2,375,877
GDP exposed in 2050	$10,834,463,547	$321,805,161	$5,306,191,455

3.6.3 Risk analysis (focus areas)

Since the damage is often localized in the areas where the material transits to or accumulates, risk assessment applied to the focus areas includes a geomorphological analysis to evaluate susceptibility to transit and accumulation areas, runout, and intensity. Subsequently, vulnerability and socioeconomic value of the exposed assets has been assessed.

The risk associated with each landslide type was assessed by crossing the calculated impact data with the locations of assets and their vulnerability and socioeconomic value. The risk was classified according to four different levels:[3]

- R1: Low risk
- R2: Moderate risk
- R3: High risk
- R4: Very high risk

Risk maps were produced for each focus area, representing the hazard exposure and the loss of footprint layers for each typology of landslide and related to each asset considered (those listed in the previous section). Figure 3-14 shows risk levels for infrastructures (roads and bridges) and facilities (schools, hospitals, etc.) for the Kabul District focus area, for cover material landslides in rapid evolution. Figure 3-15 shows risk levels for the population for the Kabul District focus area for cover material landslides in rapid evolution. Figure. 3-16 shows risk levels for infrastructures (roads and bridges) for the Salang Pass focus area for cover material landslides in rapid evolution.

[3] The four levels of risk correspond to the classification used by the Italian Department of Civil Protection (I-DPC).

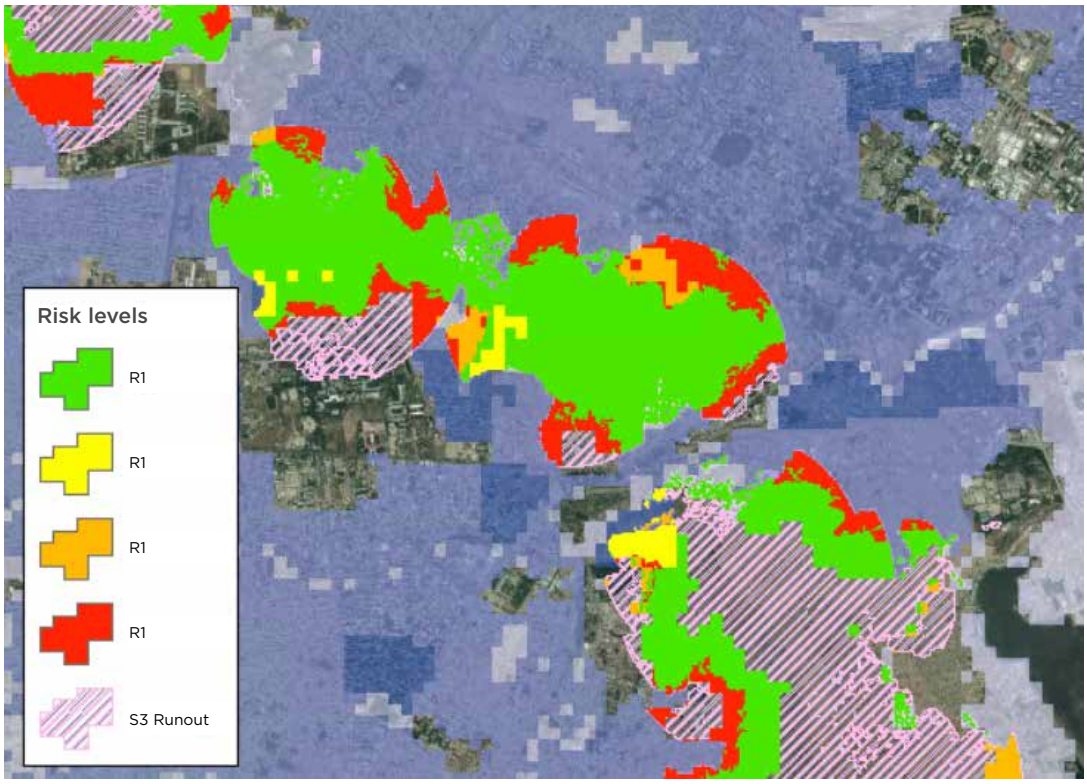

Figure 3-14

Risk levels for infrastructures (roads and bridges) and facilities (schools, hospitals, etc.) for the Kabul District focus area (landslide typology: cover material landslides in rapid evolution).

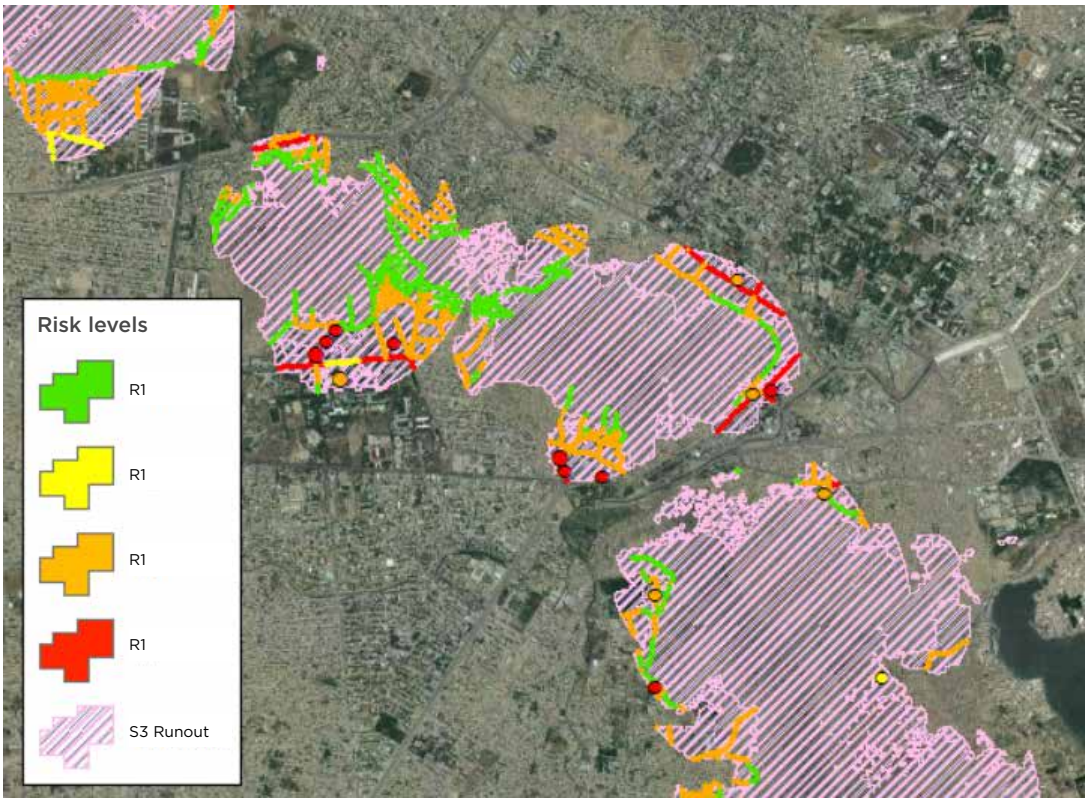

Figure 3-15

Risk levels for the population for the Kabul District focus area (landslide typology: cover material landslides in rapid evolution).

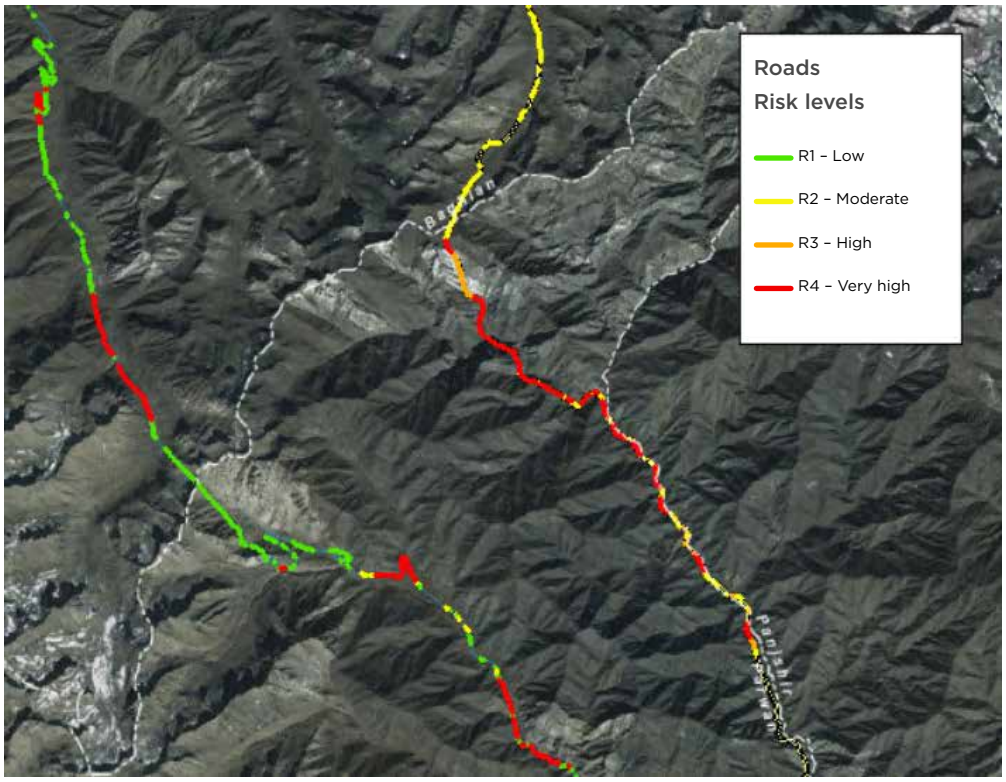

Figure. 3-16

Risk levels for infrastructures (roads and bridges) for the Salang Pass focus area (landslide typology: cover material landslides in rapid evolution).

References

Chapter 3

Casagli, N., Catani, F., Puglisi, C., Delmonaco, G., Ermini, L., and Margottini, C. 2004. An Inventory-Based Approach to Landslide Susceptibility Assessment and its Application to the Virginio River Basin," Italy. Environmental and Engineering Geoscience 2004 10: 203–216.

Carrara, A., Cardinali, M., Guzzetti, F., and Reichenbach, P. 1995. GIS Techniques in Mapping Landslide Hazard. In: "Geographical Information Systems in Assessing Natural Hazards," A. Carrara and F. Guzzetti (eds.), Kluwer Academic Publishers, Netherlands, 135–175.

Crosta, G. B., Dal Negro, P., and Frattini, P. 2003. Soil slips and debris flows on terraced slopes. Natural Hazards and Earth System Sciences 3: 31–42.

Falconi, L., Campolo, D., Leoni, G., Lumaca, S., and Puglisi, C. 2011. Geomorphology hazard assessment of Giampilieri and Briga river basins after the rainfall event on October 1, 2009 (Sicily, Italy). Proceedings of the Second World Landslide Forum—3–7 October 2011, Rome.

García-Ruiz, J. M., Beguería, S., Lorente, A., and Martí, C. 2002. Comparing debris flow relationships in the Alps and in the Pyrenees. Instituto Pirenaico de Ecología, Zaragoza, Spain.

Gunasekera, R., Ishizawa, O., Aubrecht, C., Blankespoor, B., Murray, S., Pomonis, A., and Daniell, J. 2015. Developing an adaptive global exposure model to support the generation of country disaster risk profiles. Earth-Science Reviews, 150, 594–608.

Guzzetti, F., Carrara, A., Cardinali, M., and Reichenbach, P. 1999. Landslide hazard evaluation: a review of current techniques and their application in a multi-scale study, Central Italy. Geomorphology, 31(1–4): 181–216.

Leoni, G., Barchiesi, F., Catallo, F., Dramis, F., Fubelli, G., Lucifora, S., Mattei, M., Pezzo, G., and Puglisi, C. 2009. GIS Methodology to Assess Landslide Susceptibility: Application to a River Catchment of Central Italy. Journal of Maps, 2009, 87–93.

Puglisi, C., Falconi, L., Gioè, C., and Leoni, G. 2015. Contribution to the Runout Evaluation of Potential Debris Flows in Peloritani Mountains (Messina, Italy). Engineering Geology for Society and Territory—Volume 2: Landslide Processes, Springer International Publishing, pp. 509–513.

Rickenmann, D. 1999. Empirical Relationships for Debris Flows. Natural Hazards, 19: 47–77.

Photo: sArhangel.

CHAPTER 4

Snow Avalanche

In the high Hindu Kush mountain range of Afghanistan, leading into both the Parmir and Himalayas, the threat of snow avalanches, as shown in Figure 4-1 of the Salang Pass, affects people, settlements, and infrastructure. To gain an overview of the avalanche hazards and risks that Afghanistan faces, we performed a detailed avalanche study gathering historic avalanche data and performing numerical modeling of the avalanche runout potential and dynamics nationwide. In this chapter, the methodology and data collection techniques applied to perform the avalanche hazard and risk assessment, and the results are presented.

4.1 Snow avalanches and general data requirements for avalanche modeling

Snow avalanche modeling is performed to produce avalanche hazard maps which identify the likely starting and transition zones of avalanches, in particular the runout areas of avalanche deposits. In addition, dynamic avalanche modelling provides the flow properties during runout, such as flow and deposition heights, avalanche velocities, and impact pressures on objects (buildings, infrastructures, etc.). The task involves the analysis of meteorological data and snow properties to determine model input parameters. Also involved is the calibration of the dynamic avalanche model and the necessary boundary conditions that best describe the physical runout behavior of avalanches, based on the analysis of recent snow avalanche events in the region. Snow avalanche hazard and risk modeling is used to assist with planning land-use, transport routes, electricity transmission lines, and other critical infrastructure. It also provides the necessary input data for the effective designing of buildings, infrastructure, and protection measures.

Defining avalanche model parameters is challenging because the flow mechanics of avalanches is governed by release volume, topography, terrain morphology, and the snow properties, each of which may change with location and time. In principle, three different types of avalanches occur:

1. Dry snow dense flow avalanches;
2. Wet snow plug flow avalanches; and
3. Powder snow avalanches.

Their occurrence depends on the snow cover characteristics, topography, and morphology of the terrain. The focus of this analysis, as in most large-scale avalanche analysis, is on dry snow avalanches, which nominally reach velocities up to 30 meters per second.

Figure 4-1

Salang Pass avalanches of 2010 resulted in 165 fatalities amid much destruction of vehicles and infrastructure.

Several approaches are available to avalanche modeling, each of which requires calibration using past avalanche events with a greater or lesser degree of detail. The model's purpose is to link the avalanche starting conditions in the release zone to the runout dynamics in the transition zone and the stopping conditions in the deposition zone (Figure 4-2). In this study the RAMMS::AVAL model was used (Christen et al., 2012 and 2013). The a-b model (McClung and Lied, 1987) is used to a lesser degree for the hazard analysis and to cross-validate the input parameters used in the RAMMS::AVAL model, based on past recorded avalanche events.

4.2 Data inventory and applied data

4.2.1 Required and available data for avalanche modeling

Snow avalanche hazard modeling requires several different data, such as:

1. Snow properties and local weather conditions;
2. Avalanche release area (geometry, morphology, etc.);
3. Avalanche transition and runout geometry (historical or recent avalanche events);
4. Topography data set; and
5. Avalanche cadaster.

Snow properties and local weather conditions provide information on the amount of snow to be released in the avalanche starting zone. Of major importance are the following:

- Snow height (total);
- Freshly fallen snow height (in 24 and 72 hours);
- Snow profiles; and
- Wind speed and direction (wind transports snow from luv (windward) to lee (leeward) over large distances and causes additional snow accumulation in lee slopes).

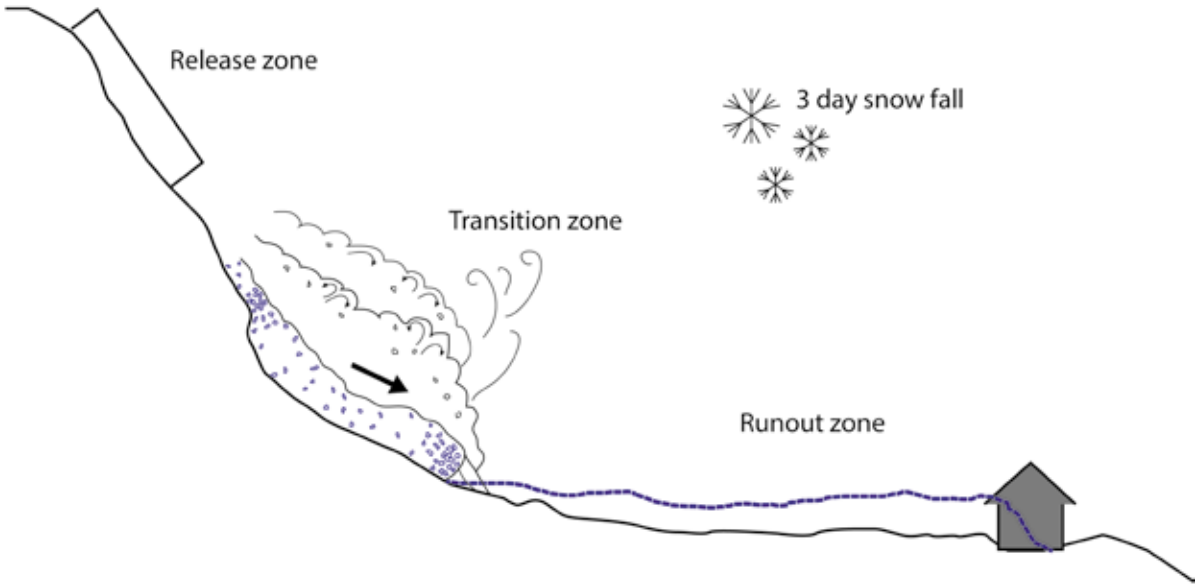

Figure 4-2

Modeling snow avalanches links together: (i) the release conditions in the release zone such as potential snow slabs (upper left rectangle); (ii) the flow dynamics in the transition zone such as avalanche velocity, flow depth, and pressure; and (iii) the runout distance or path of the avalanche runout zone and the nature of the avalanche deposits (e.g., the blue dashed line) which can impact buildings and infrastructure.

Of some minor importance are the following:

- Snow density ρ (kg m^{-3});
- Snow water content;
- Snow temperature; and
- Air temperature.

Commonly these data are taken from direct field measurements or automatic weather stations providing continuous time series measurements. These measurements should be taken daily over at least a year because snow accumulations that result in avalanches are closely coupled with weather and climate. Therefore, only daily measurements of the prevailing snow properties on an annual basis will give sufficient insight into the characteristic avalanche situation for a given location.

Vulnerability and avalanche pressure

An avalanche hazard analysis produces maps delineating the runout areas of avalanches. The results include avalanche pressure. A list of known damages to structures due to avalanches, and the corresponding pressure in kilo Pascal (kPa) are given in Table 4-1. The impact pressure is perpendicular to the flow direction.

Table 4-1

Avalanche impact pressures perpendicular to flow direction and respective damages to structures (L. Stoffel and S. Margreth, SLF Davos, personal communication 2016).

Impact pressure (kPa)	Potential damage
2–4	Breaks windows
3–6	Pushes in doors, damages roofs and walls
10	Damages wood-framed structures
20	Destroys wooden houses, damages cemented walls
30	Destroys cemented and concrete buildings

The above scale was adapted to fit the construction standards and methods of Afghanistan.

4.3 Results, deliverables, and data products

4.3.1 Avalanche hazard mapping

The nationwide avalanche hazard mapping was conducted for a 100-year avalanche return period scenario. Figure 4-3 shows the nationwide map of avalanche pressures in kilo Pascal (kPa) for Afghanistan.

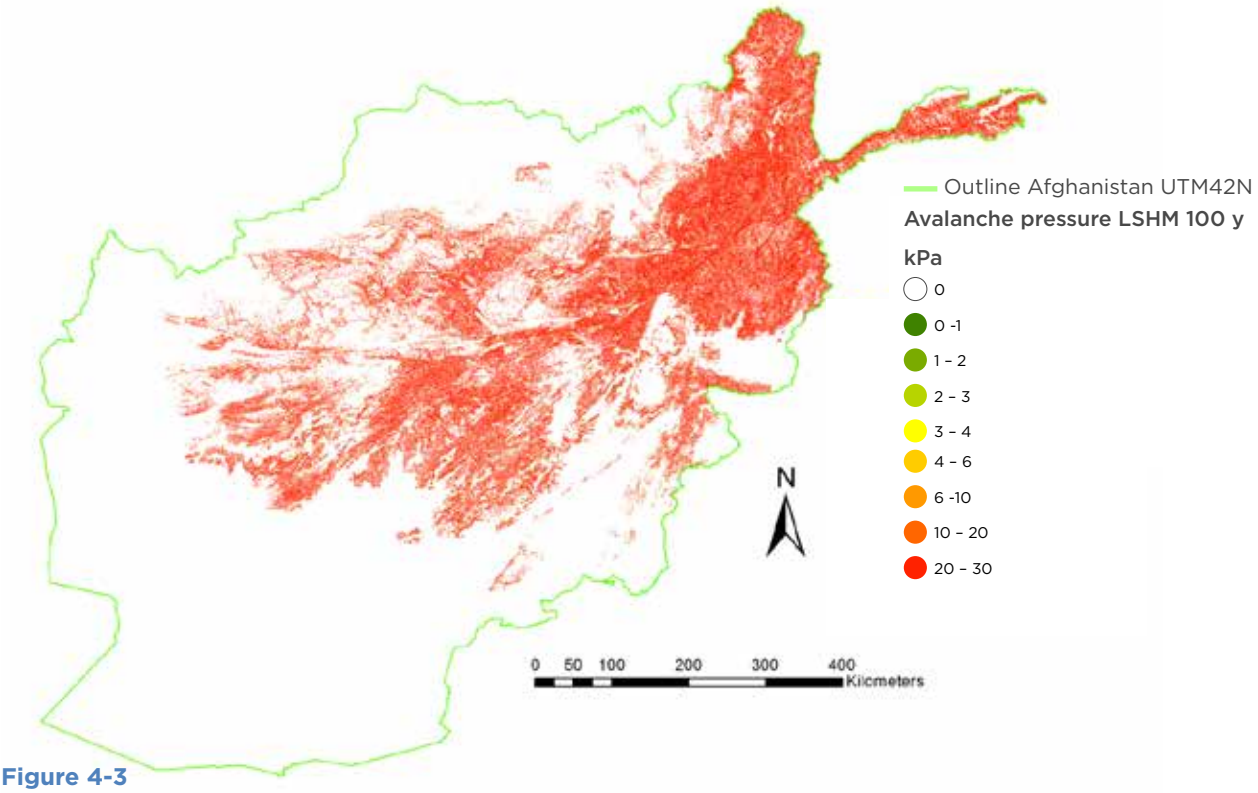

Figure 4-3

Avalanche pressure map for Afghanistan.

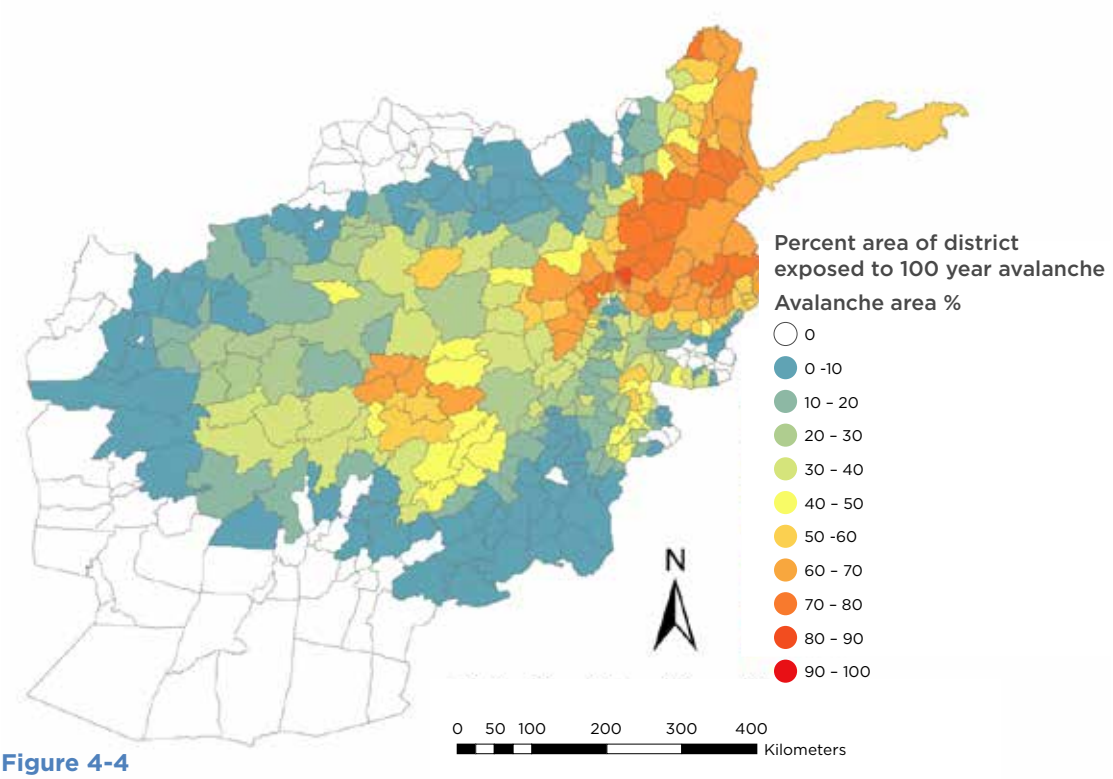

Figure 4-4

Proportion of the district area that is exposed to the 100-year avalanche return period hazard scenario.

As expected, much of the avalanche danger resides in high altitude areas. The ratio of avalanche footprint area exerting pressures in exceedance of 1 kPa to the district area is displayed in Figure 4-4.

The districts that have more than 60 percent of their area exposed to a 100-year avalanche return period are in the following provinces:

- Badakhshan
- Baghlan
- Daykundi
- Kapisa
- Kunar
- Laghman
- Nuristan
- Panjsher
- Parwan
- Takhar
- Wardak

4.3.2 Tabulated record of historical losses

This section presents some of the available avalanche historical data recorded in Afghanistan. Figure 4-5 and Figure 4-6 are based on the dataset of tabulated avalanche records of historical losses.

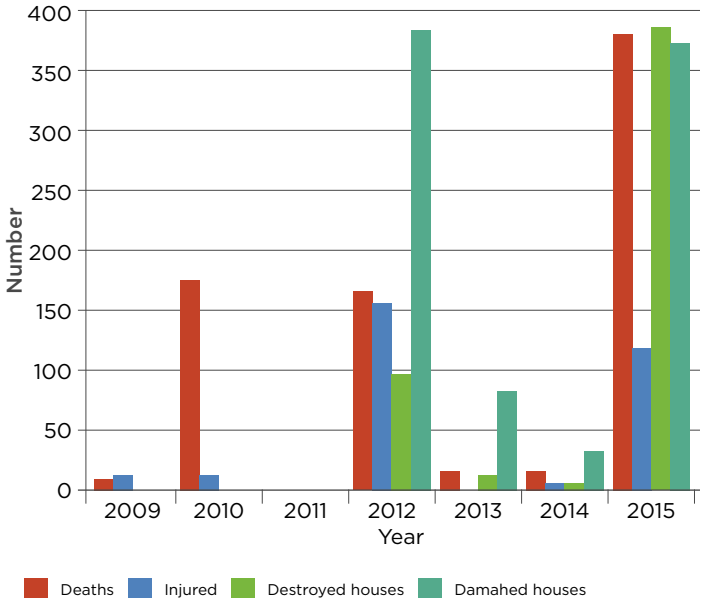

Figure 4-5

Record of deaths, injured people, destroyed houses, and damaged houses due to reported snow avalanches in Afghanistan from 2009–June 2015.

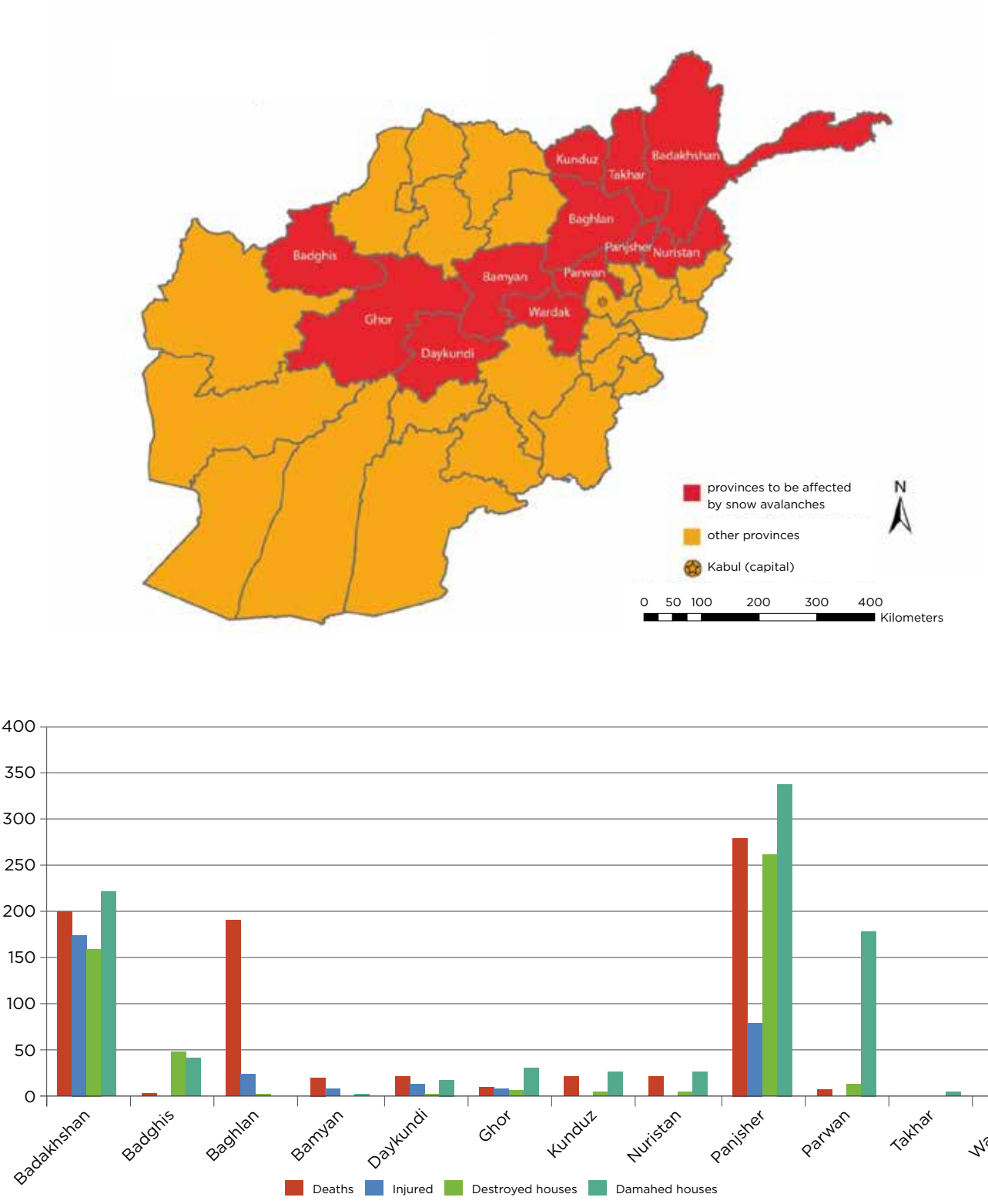

Figure 4-6

Overview of Afghan provinces reported to be affected, including a record of death and injured individuals for provinces caused by snow avalanches (2009–2015).

4.3.3 Hazard, exposure, and risk analyses

The base risk analysis estimates hazard exposure from hazard maps, assuming that all snow-covered areas pose an avalanche threat. A refined, but less conservative analysis can be conducted, excluding the areas that receive insufficient snowfall to generate a 100-year snow avalanche event.

The base analysis defines potential avalanche release areas, flow depth, and volume, along with the avalanche flow parameters that fit the Afghanistan 100-year avalanche event scenario. A refined risk analysis uses snow water equivalent (SWE) data derived from a general circulation model, and based on the EU-WATCH ensemble, as an additional parameter to determine the trigger points of avalanches. In the following sections, we present the results of risk analysis for avalanche hazard exposed assets, divided into four categories:

- Population
- Buildings and residential areas
- Infrastructure and industry
- GDP and replacement costs

4.3.3.1 Population

The datasets of total population, urban population, and rural population are considered. Since personal injuries and death are commonly a secondary consequence of damages to surrounding buildings and infrastructure, the minimum impact pressure to represent a potential for injury or death was assumed to be 1 kPa for a 100-year return period.

An overview of the total population exposed to a 100-year avalanche scenario in Afghanistan is presented in Table 4-2. About 8 percent of the population is exposed, not accounting for snow depth and the exact location of the area footprint of avalanches within each district.

Avalanches affect more of the rural population, both proportionally and in absolute terms, with 9.60 percent of the rural population exposed, compared to 3.17 percent of the urban population.

Figure 4-7 shows the frequency of occurrence of the minimum snowfall required to generate a 100-year avalanche, which can be used to prioritize the areas more likely to be impacted. The frequency of occurrence every 100 years was calculated from the SWE values, which were obtained modelling a period of 44 years.

Risk of human loss

Avalanche risk of injury and death is closely coupled with building and infrastructure (especially transport infrastructure) damage statistics.

4.3.3.2 Buildings and residential areas

The number of buildings exposed to avalanches can be obtained by coupling the population census with the building stock data sets. However, it is not possible with a large-scale approach to delineate local hazard zones and distinguish between partially damaged and completely destroyed buildings. In this regard, the figures presented here are an indication of the number of buildings exposed, not an assessment of which individual buildings are exposed. Figure 4-8 maps the number of rural buildings exposed per district.

Table 4-2

Overview of total population figures and those exposed to the threat of avalanche nationwide.

Item	Value	Unit
Total population	27,092,862	Number. of people
Urban population	6,417,209	Number. of people
Rural population	20,678,653	Number. of people
Total population avalanche exposure	2,192,384	Number. of people
Total population percent avalanche exposure	8.09%	Percent
Urban population avalanche expos	203,638	Number. of people
Percent of urban population exposed	3.17%	Percent
Rural population avalanche exposure	1,988,846	Number. of people
Percent of rural population exposed	9.62%	Percent
Death due to snow avalanche (based on historiacl data)	2,700 – 3,500	Possible range in number of people
Injury due to snow avalanche (based on historiacl data)	1,100 – 11,200	Possible range in number of people

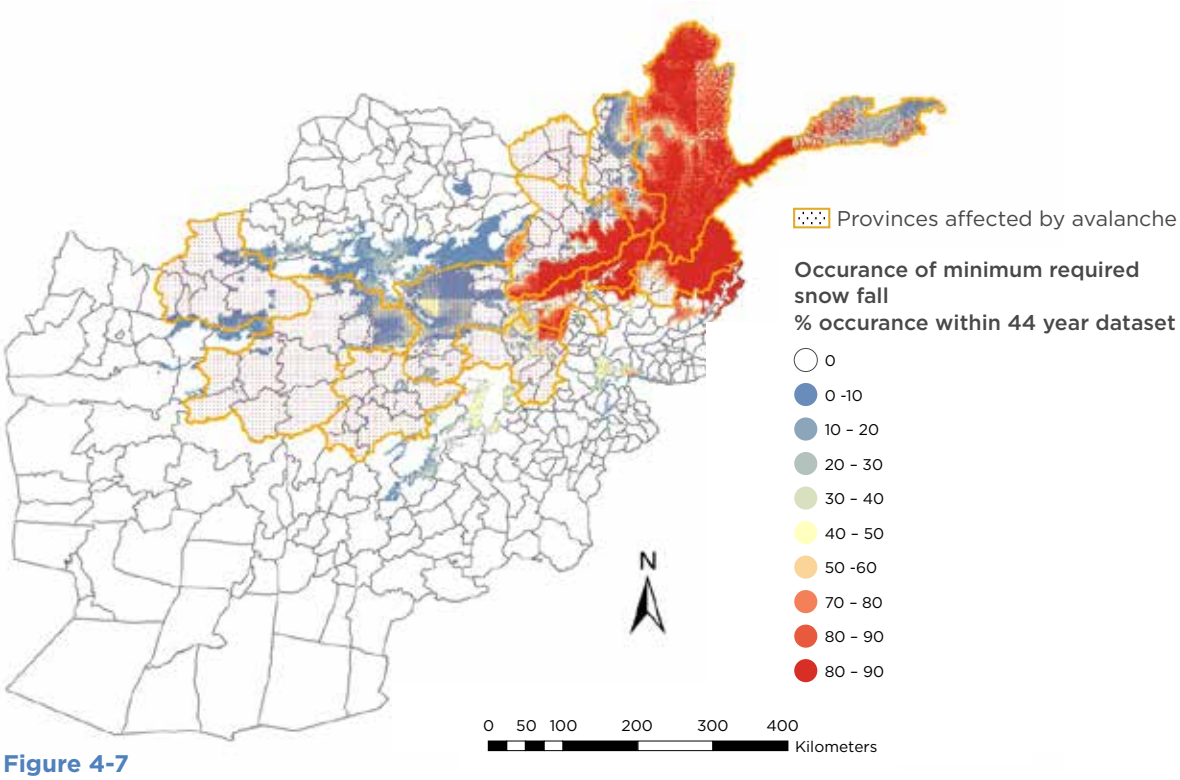

Figure 4-7

Map depicting the provinces that have a record of avalanche events highlighted in orange, and the mapped occurrence of SWE values that deliver sufficient snowfall within a year to fulfil the possibility of the 100-year avalanche scenario.

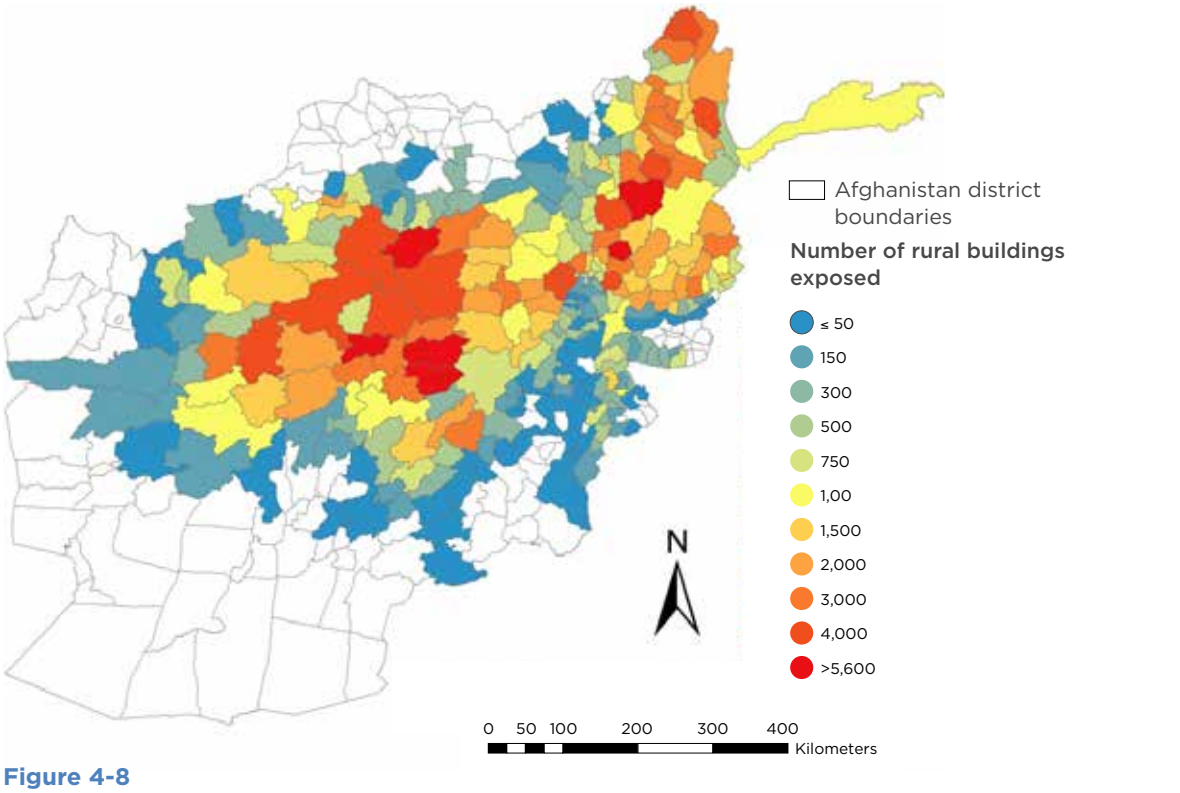

Figure 4-8

Map of the number of rural buildings exposed to the 100-year avalanche hazard scenario footprint per district.

With respect to the number of urban buildings exposed, the distribution of exposure is more scattered and does not show the same regional trends seen in rural building exposure. Figure 4-9 shows the number of urban buildings exposed to the threat of avalanche per district; no discernible trend can be extracted.

Table 4-3 reports the number of buildings exposed and the number of houses destroyed or damaged by avalanches, estimated by applying the same ratio obtained from historical data.

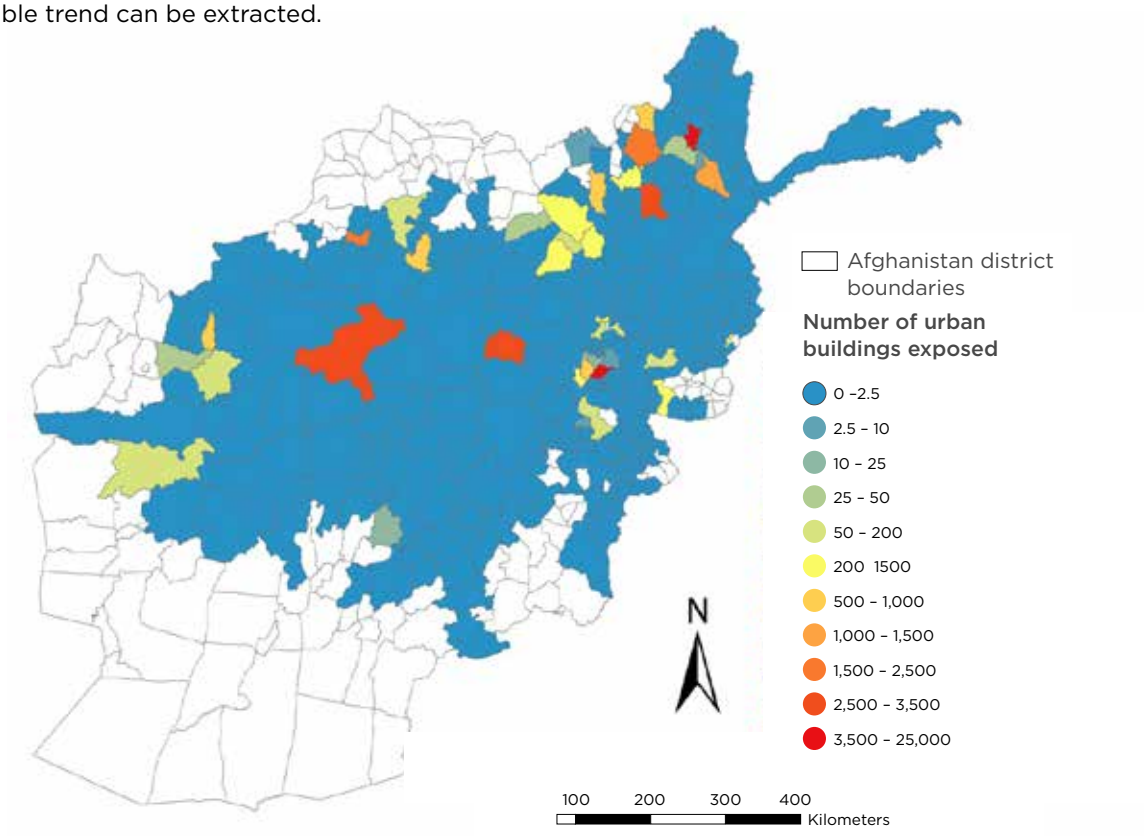

Figure 4-9

Map of the number of urban buildings exposed to the 100-year avalanche hazard scenario footprint per district.

Table 4-3

Statistics summary of residential and urban buildings that are exposed to avalanches in Afghanistan.

Item	Value	Unit
Residential area total	341,747	ha
Rural buildings total	2,698,792	Number of buildings
Urban buildings total	962,839	Number of buildings
Residential area exposed to avalanches	19,374	ha
Residential area exposed to avalanches	5.67%	Percent
Rural building exposed to avalanches	248,460	Number of buildings
Rural building exposed to avalanches	9.21%	Percent
Urban buildings exposed to avalanches	27,592	Number of buildings
Urban buildings exposed to avalanches	2.87%	Percent
Houses destroyed (based on historial data)	61,295	Number of houses
Houses destroyed (based on historial data) % of total exposed	22.89%	Percent
Houses damaged (based on historial data)	77,534	Number of houses
Houses damaged (based on historial data) % of total exposed	28.09%	Percent

4.3.3.3 Infrastructure and industry

The hazard exposure of infrastructure and industry has also been assessed. If an area is exposed to the avalanche hazard, only the portion of the area that intersects with the avalanche footprint is considered, instead of the total area of the asset.

Table 4-4 provides an overview of the number of assets exposed to avalanches nationwide. Industrial areas are commonly located in valley bottoms where the best transport routes are accessible. Therefore, the avalanche hazard exposure for industrial areas is small in comparison to all other exposure layers, with only 0.5 percent of all industrial areas being exposed to avalanche hazard.

Of particular interest is the hazard exposure of the road network, which is given in Figure 4-10 and Figure 4-11.

Considering the total kilometers of roads exposed, a large portion of the exposure resides in the northeast mountain regions; some districts in the lower regions also have high exposure (Figure 4-10).

The exposure of roads with respect to the total road network length of each district is much higher in the mountain regions to the northeast (Figure 4-11).

Table 4-4

Statistics for Afghanistan national admin level 0 for infrastructure and industrial areas exposed to avalanches.

Item	Value	Unit
Roads total	67,397	km
Roads exposed to avalanches	10,017	km
Roads exposed to avalanches (%)	14.86%	Percent
Bridges total	2,180	Number of bridges
Bridges exposed to avalanches	583	Number of bridges
Bridges exposed to avalanches (%)	26.74%	Percent
Industrial area total	27,440.61	ha
Industrial exposed to avalanches (3kpa)	138	ha
Industrial exposed to avalanches (%)	0.50%	Percent
Power plants total	41	Number of power plants
Power plants exposed to avalanches	20	Number of power plants
Power plants exposed to avalanches (%)	48.78%	Percent
Dams total	25	Number of dams
Dams exposed to avalanche	4	Number of dams
Dams exposed to avalanche (%)	16.00%	Percent
Airports total	69	Number of airports
Airports exposed to avalanche	2	Number of airports
Airports exposed to avalanche (%)	2.90%	Percent
Health centers total	1,465	Number of health centers
Health centers exposed to avalanche	322	Number of health centers
Health centers exposed to avalanche (%)	21.98%	Percent
Universities total	19	Number of universities
Universities exposed to avalanche	3	Number of universities
Universities exposed to avalanche (%)	15.79%	Percent
Schools total	3,588	Number of schools
Schools exposed to avalanche	665	Number of schools
Schools exposed to avalanche (%)	18.53%	Percent

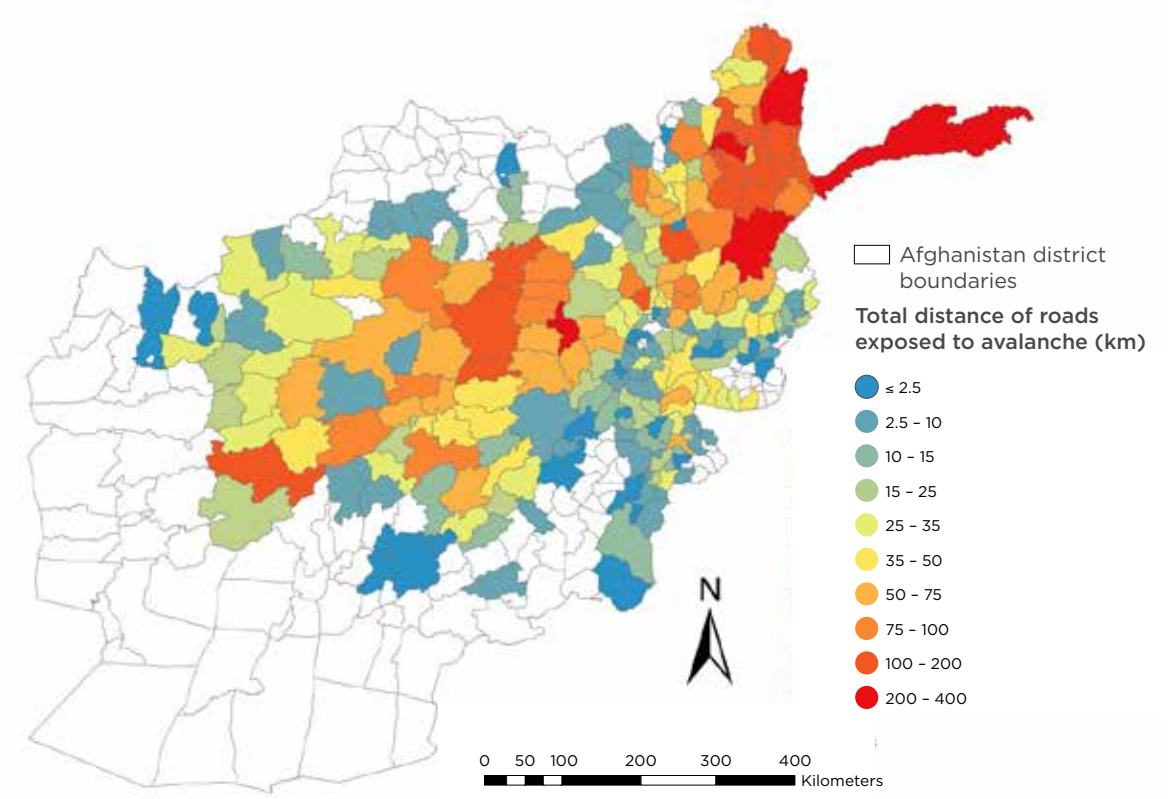

Figure 4-10

Avalanche hazard exposure of the roads in Afghanistan displayed as total kilometers exposed in each district.

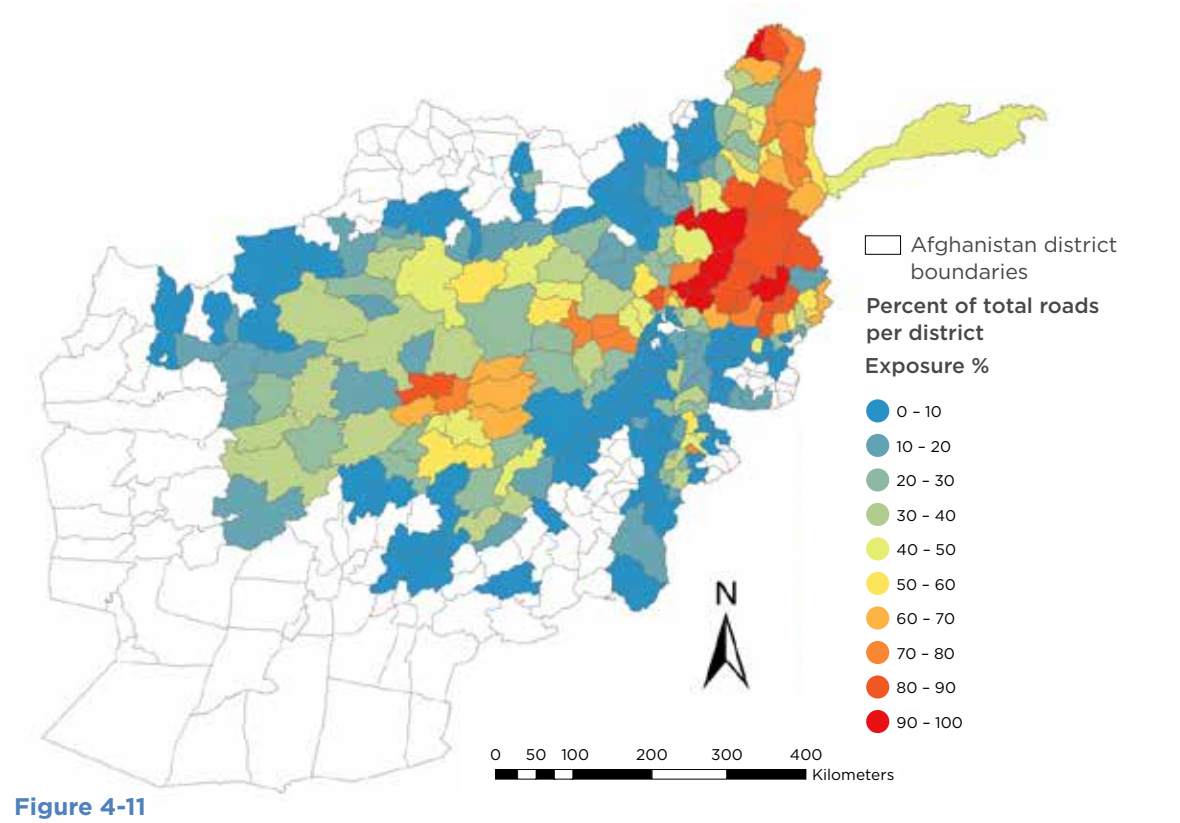

Figure 4-11

Avalanche hazard exposure of all roads in Afghanistan displayed as the percentage of roads exposed, with respect to the total roads of each district.

4.3.3.4 GDP and cost of replacement (USD) exposed to avalanche hazard

The avalanche exposure of assets can be viewed in terms of GDP (USD). In Table 4-5, we present the exposed total GDP and the replacement cost of assets in USD. No distinction is made between assets that are destroyed or damaged; in other words we assume that if a given asset is impacted above the avalanche vulnerability pressure then it needs to be replaced. Table 4-5 provides an overview of all assets exposed to avalanches that have been either destroyed or damaged to the point of requiring replacement.

The avalanche pressure does not usually cause structural damage to the roads, but only to ancillary road assets, such as roadside barriers and traffic signs. Thus, the exposed value for roads does not necessarily reflect the actual costs of any damages to structural elements of the roads.

Table 4-5

GDP (USD $) of assets exposed to avalanche damage vulnerability pressures deemed to cause sufficient damage to warrant replacement.

Item	Value	Unit
Rural clay total	3,339,275,039	USD $
Rural clay exposed to avalanches	261,372,738	USD $
Rural clay exposed to avalanches	7.83%	Percent
Urban clay total	1,862,628,350	USD $
Urban clay exposed to avalanches	58,675,671	USD $
Urban clay exposed to avalanches	3.15%	Percent
Rural stone total	6,317,675,608	USD $
Rural stone exposed to avalanches	562,808,351	USD $
Rural stone exposed to avalanches	8.91%	Percent
Urban stone total	1,294,384,430	USD $
Urban stone exposed to avalanches	31,003,442	USD $
Urban stone exposed to avalanches	2.40%	Percent
Non-residential total	17,292,667,795	USD $
Non-residential exposed to avalanches	1,397,419,167	USD $
Non-residential exposed to avalanches	8.08%	Percent
Industrial area total	8,506.587.743	USD $
Industrial area exposed to avalanches (3kpa)	42,686,590	USD $
Industrial area exposed to avalanches (3kpa)	0.50%	Percent
Roads total	8,263.103.992	USD $
Non-residential exposed to avalanches	1,727,324,885	USD $
Non-residential exposed to avalanches	20.90%	Percent
Health centers total	175,800,000	USD $
Health centersl exposed to avalanches	38,646,000	USD $
Health centers exposed to avalanches	21.98%	Percent
Hospital total	28,500,000	USD $
Hospitals exposed to avalanches	1,800,000	USD $
Hospitals exposed to avalanches	6,32%	Percent
GDP total	20,600,000,000	USD $
GDP exposed to avalanches	1,667,000,000	USD $
GDP exposed to avalanches	8.09%	Percent

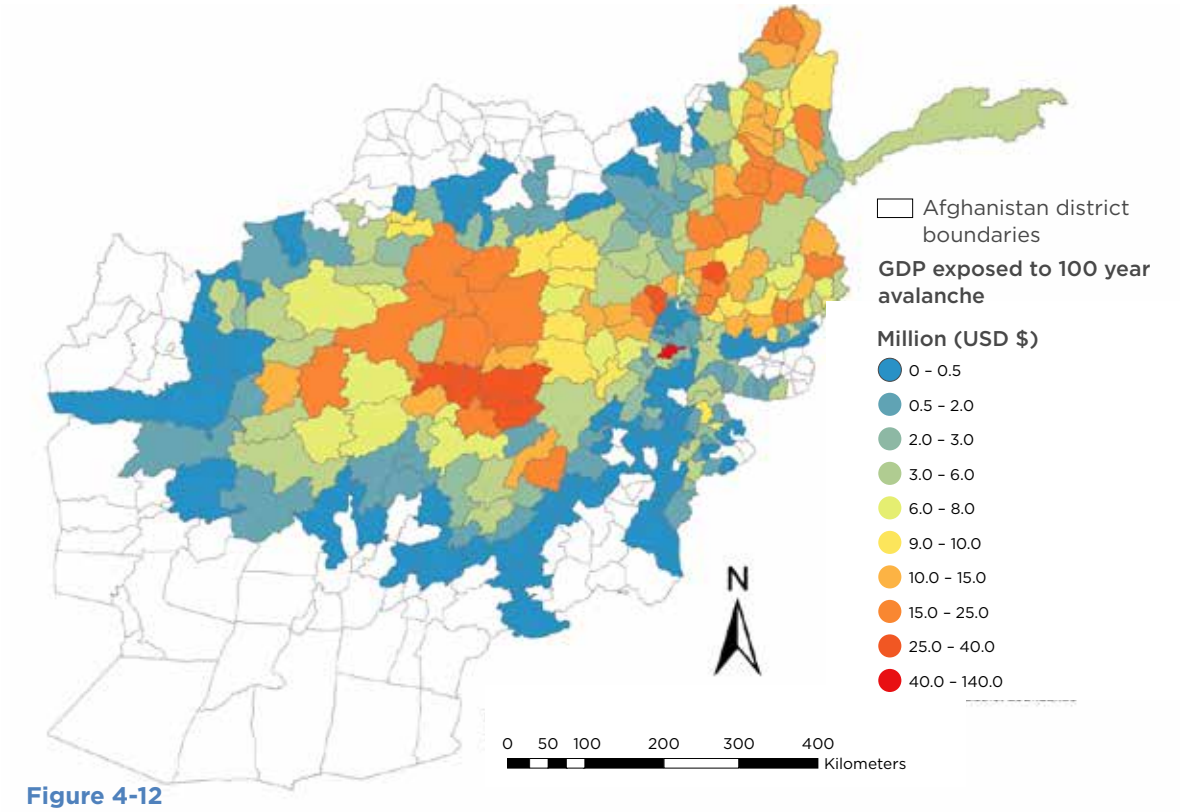

Figure 4-12

Overview map of the avalanche exposure of total GDP (in USD) given in millions for each district of Afghanistan.

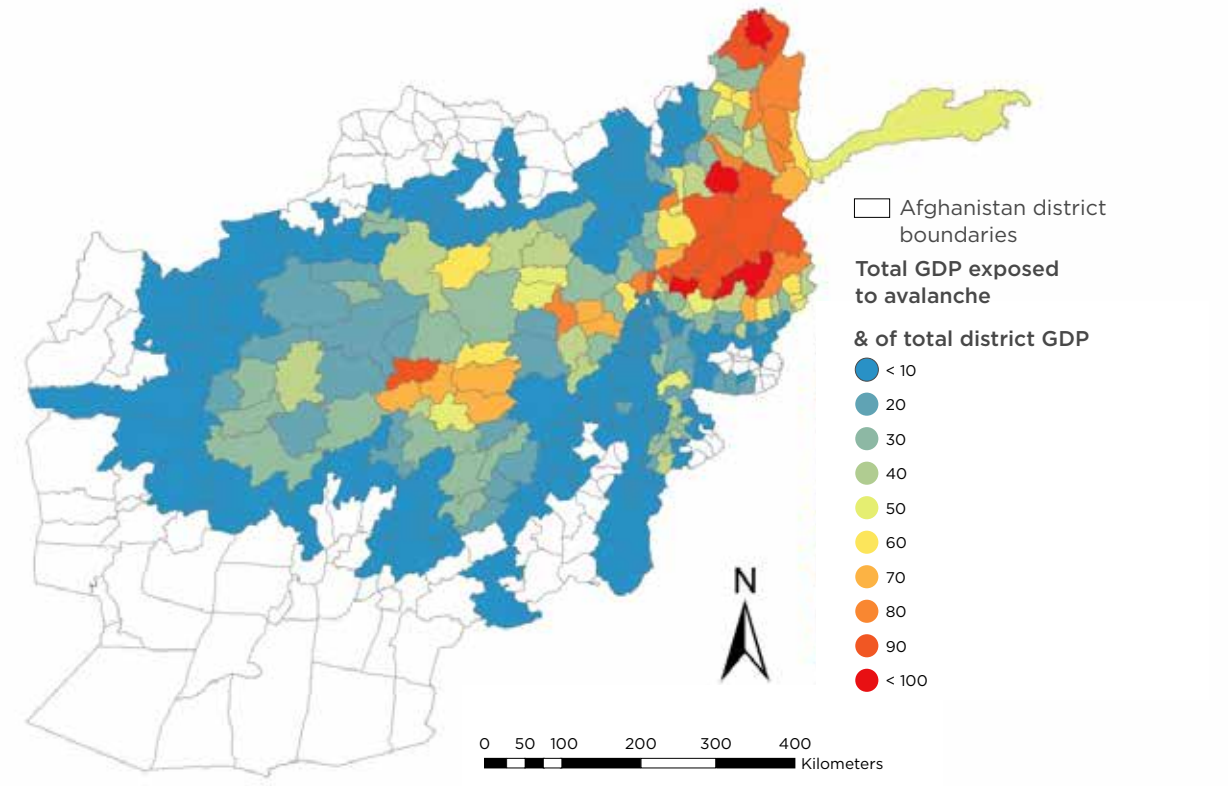

Figure 4-13

Overview map of the percentage of avalanche-exposed GDP with respect to the total GDP for a given district of Afghanistan.

Figure 4-12 shows the total exposed GDP (in USD) in millions for each of the districts in Afghanistan. The highest exposure is to the northeast and to the west. The spike around Kabul is likely the result of the high number of urban buildings in a district with large exposure (within the conservative scenario which does not account for SWE).

The proportion of a district's GDP exposed to avalanches is shown in Figure 4-13. Note that in this case, the trend of higher avalanche exposure for northeastern mountain regions becomes clearer, and the spike of exposure observed for Kabul disappears.

4.3.4 Avalanche protection

Many different types of avalanche protection are available to reduce vulnerability of communities living in mountainous areas. The avalanche protection approaches can be categorized into two types:

Short-term measures deal with an immediate avalanche threat, often relying upon avalanche bulletins and weather forecasts. Such measures can be:

1. Avalanche warning services
2. Evacuation of settlements
3. Road closures
4. Artificial avalanche releases

Long-term measures provide protection on a more permanent basis. The approach can be broken down into:

1. **Preventive measures** designed at preventing avalanche formation:
   - Avalanche barrier construction (snow fences and nets)
   - Wind deflection fences to reduce snow drift and snow accumulation
   - **Reforestation and** civil-cultural measures
2. **Passive measures** such as land use planning based on avalanche hazard mapping
3. **Active measures** designed to stop or deflect the avalanche flow:
   - Earth/concrete dams
   - Concrete galleries to protect roads and tunnel portholes
   - Tunnels

Eight avalanche protection measures, with a brief description of their application, are presented below.

Snow supporting structures

Snow supporting structures are active permanent protection measures designed to prevent the initiation or limit the extent of avalanches by increasing the capability of a slope to hold back snow (Figure 4-14).

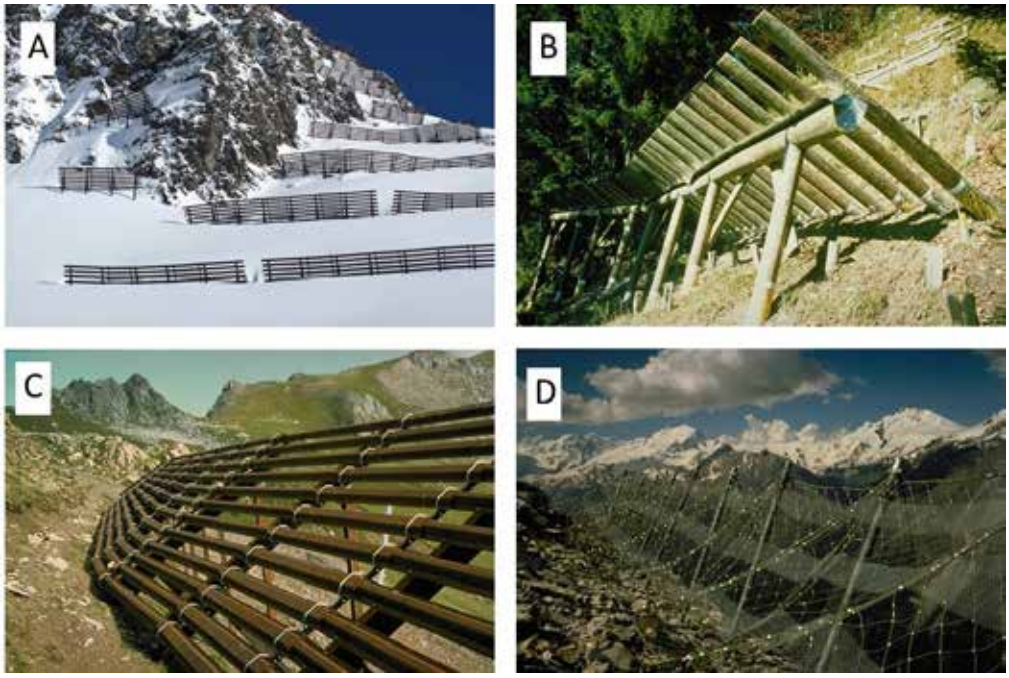

Figure 4-14

Snow supporting structures installed in avalanche-prone areas. The barriers are fixed to the slope and allow collection of snow behind them to prevent avalanche release (A). The structures have many different designs: wooden constructions (B), ridged steel fences (C), and flexible high tensile steel netting (D).

Snow Drift Fences
Snow drift fences exploit the mechanics of wind-driven snow; they prevent deposition on the leeward slope by disrupting the process of snow scouring on the windward side.

Often snowdrift structures on the windward slope are used in conjunction with snow supporting structures on the leeward slope to ensure that the retention capacity of supporting structures is not exceeded (Figure 4-15).

Artificial avalanche release
Avalanches are artificially induced using shock waves to dislodge snow before it accumulates to the point of becoming unmanageable. The required shock waves can be obtained by several methods:

- Explosive thrown into the snow pack and detonated
- Artillery
- Gas pulse
- Detonation from a mast

Building and structural design
Buildings and structures built on avalanche tracks can be protected by defense walls mounded with earth. Building elements can also be reinforced or designed to reduce impacts, such as a dividing wedge to split the avalanche and reduce the active pressure that otherwise would be perpendicular to the wall.

Avalanche dams
Avalanche protection dams break and slow down avalanches, and retain snow mass in the large containment area created by the dam. They are built perpendicular to the avalanche track, and their construction can range from compacted earth mounds, to retention walls of earth and boulder blocks, and to more sophisticated constructions involving geotextiles (Figure 4-16).

Avalanche deflection dams
Avalanche deflection dams consist of large flanking walls constructed to intercept avalanches during their runout and deflect them away from buildings and infrastructure. They are constructed using earth, rubble boulder, and often geotextiles, and are built parallel to the avalanche flow direction (Figure 4-17).

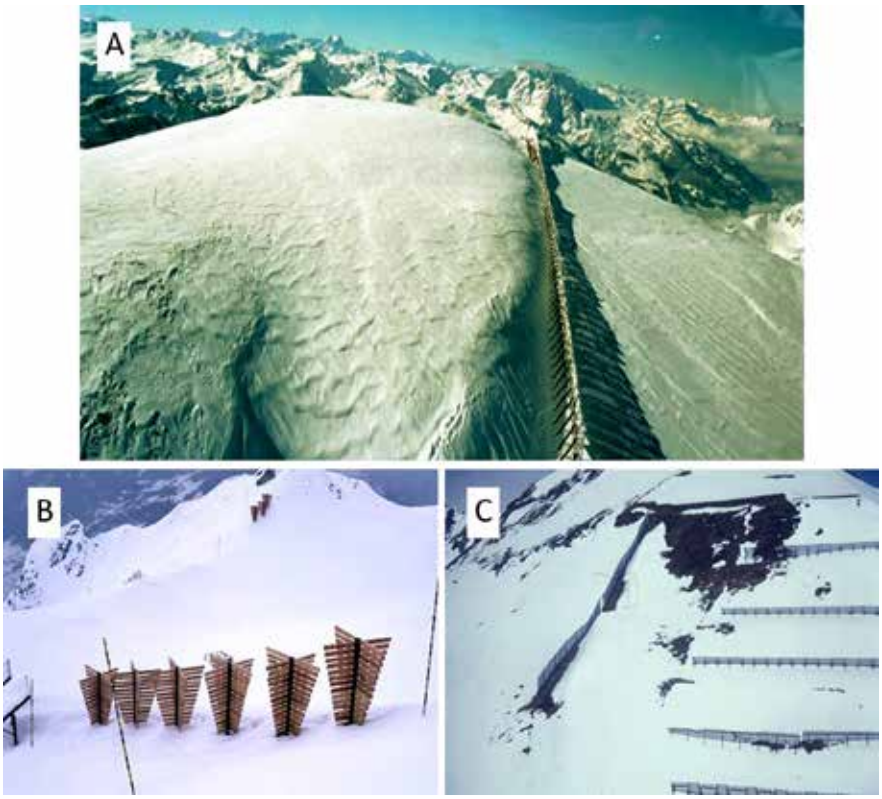

Figure 4-15
Snowdrift fences are designed to stop the wind, increasing snow accumulation on the windward side of the slope and preventing snow accumulation on the leeward slope. Image (A) shows snowdrifts accumulating around the snowdrift fence to the left-hand side; Image (B) shows modern designed snowdrift structures optimized for wind disturbance; image (C) shows a snowdrift fence used to prevent overloading of the snow retention structures.

Figure 4-16

Avalanche protection dams built on a slope perpendicular to the avalanche track, provide a breaking effect and offer retention of snow in the dam.

Figure 4-17

Avalanche deflection dam constructed to protect the village and roadways at the base of the slope. The v-shaped design provides protection from avalanches arriving on both flanks. (Images: www.ismennt.is)

Snowsheds/avalanche galleries
Avalanche galleries, or snowsheds, provide active permanent protection for roadways and transport lines on avalanche endangered routes. Their principal function is to provide a sheltered covering over which the avalanche can flow.

Biological measures—protection forests
It has long been recognized that intact, dense forests can prevent the release of avalanches; numerous very old protection forests are evidence of this (Feistl et al., 2014). However, even a healthy, stable forest cannot stop a moving avalanche if it is released above the forest line. Such avalanches flow through the forest, often leaving considerable damage. The protective capability of the forest therefore consists in preventing the formation of avalanches within the forest area.

4.3.5 Projection to 2050

The remaining analysis discusses the possible avalanche trends for the coming years, based on the Representative Concentration Pathway (RCP) 6.0 climate scenario for projections 2050.

With increasing global temperatures, it is likely that the snow line will shift toward higher altitudes. It is also likely that avalanche activity at higher altitudes will increase due to elevated temperatures, which will also affect the nature of the snowfall (i.e., wetter snowfalls). Because of the snow line shift, risks to populations, buildings, and infrastructure in low altitude areas is expected to decrease.

Exposed population and GDP
Consistent with the changes in snow patterns and avalanche activity, exposure of population and assets will also change. The changes in exposure have been included in the 2050 projection analysis by adjusting the population and GDP datasets according to the Shared Socio-Economic Pathway developed for the Intergovernmental Panel on Climate Change (IPCC). The hazard exposure and risk analysis projection for 2050 was performed for all five SSP scenarios (SSP1, SSP2, SSP3, SSP4, and SSP5). The data are displayed in Figure 4-18, Figure 4-19, and Figure 4-20.

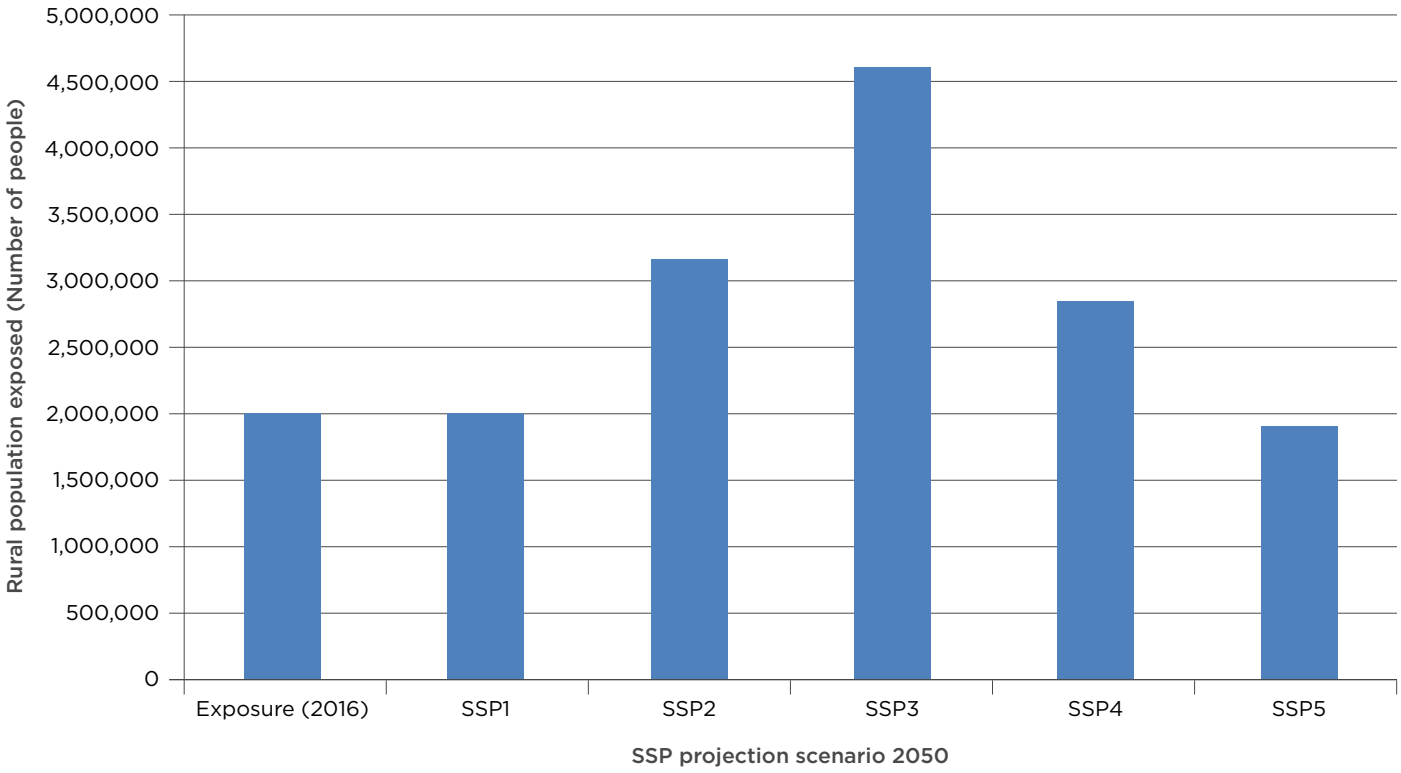

Figure 4-18
Projections for the exposed rural population in 2050, according to the SSP scenarios.

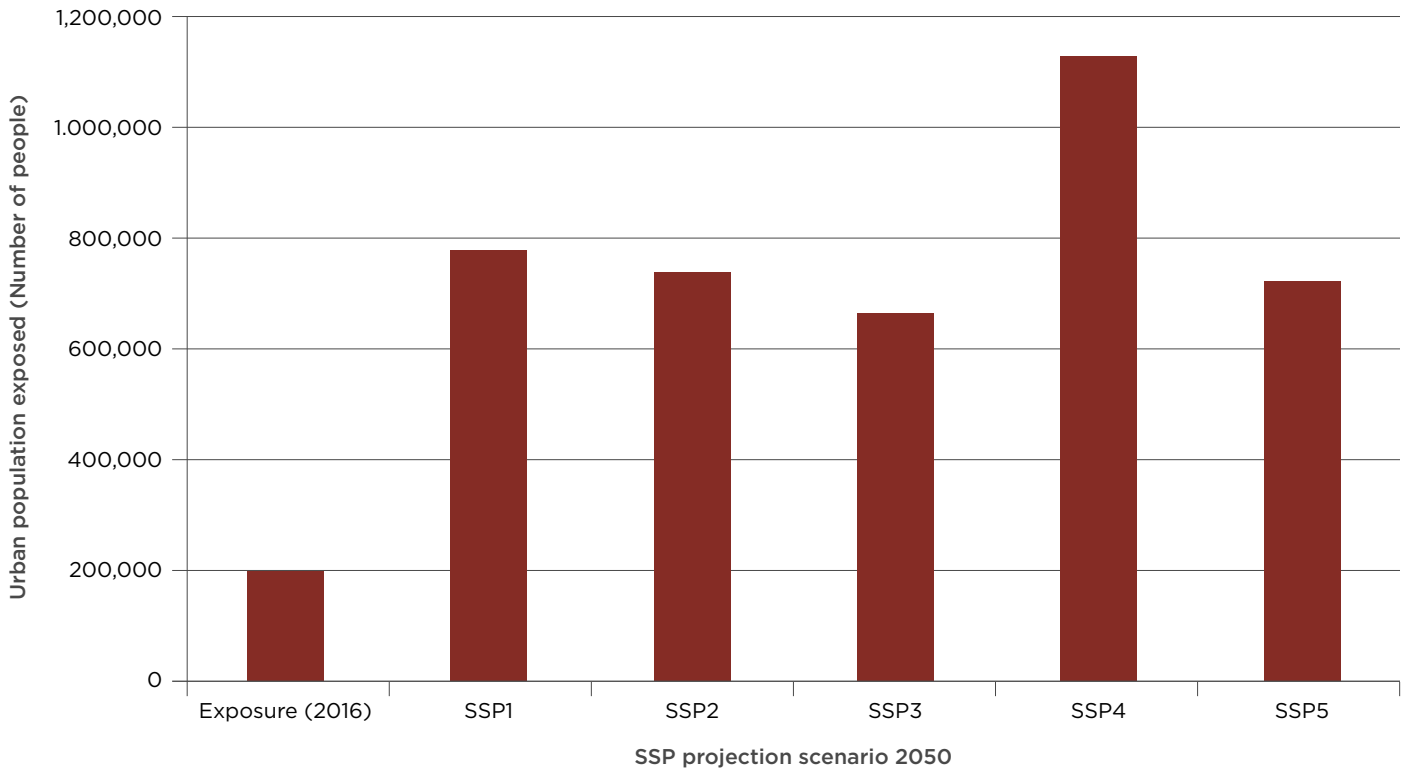

Figure 4-19

Projections for the exposed urban population in 2050, according to the SSP scenarios.

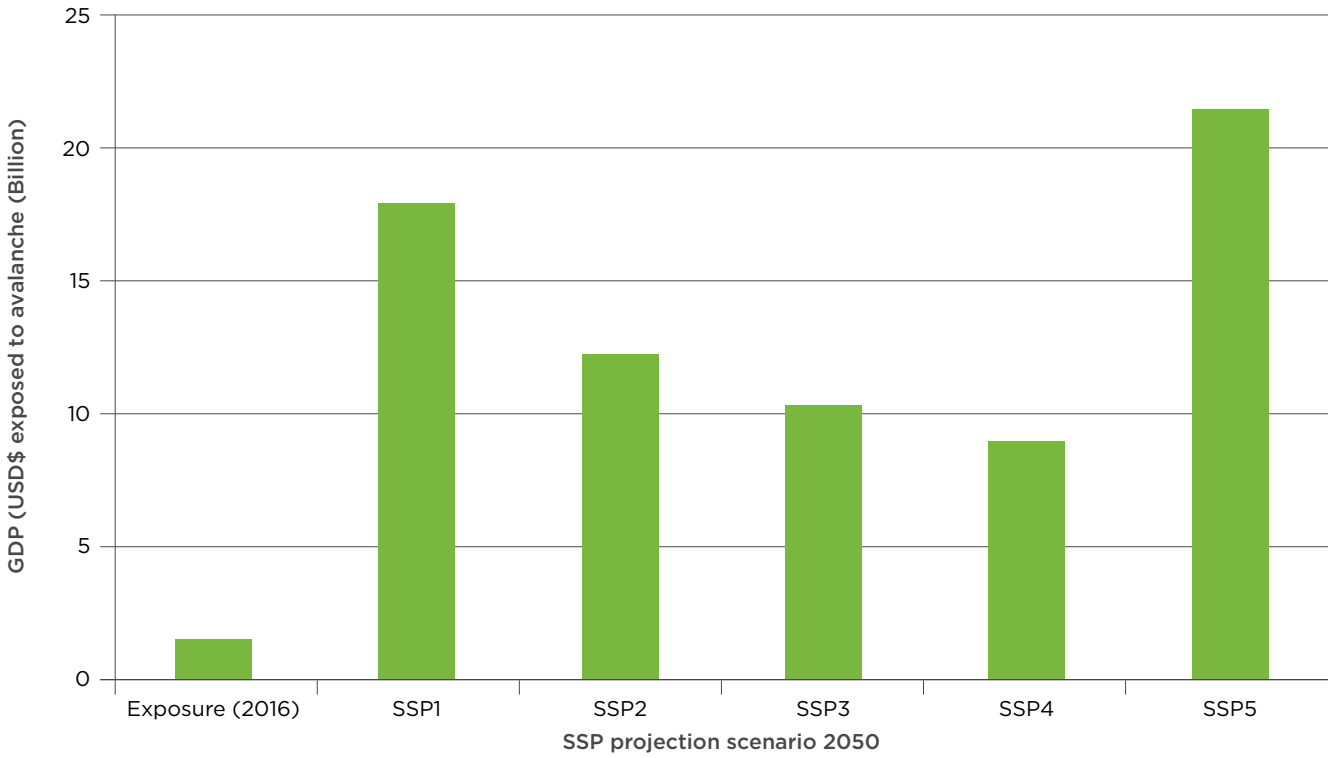

Figure 4-20

Projections for the exposed GDP in 2050, according to the SSP scenarios.

It is important to note that the SSP scenarios only reflect the expected growth of population and GDP, and are projected onto the current spatial distribution of population over Afghanistan. The scenarios do not reflect how the projected population expansion will occur spatially. For example, it is plausible that populations will move away from avalanche-prone areas, nominally because avalanches concentrate in high mountain regions where living conditions are overall more difficult. Such demographic trends cannot be reflected in the results for 2050 projected avalanche exposure displayed in Figure 4-18, Figure 4-19, and Figure 4-20.

References

Chapter 4

Ammann, W. J. 2003. Snow, avalanches, protection measures. Lecture notes, ETH Zürich, 300 pp.

Bartelt, P., Buser, O., and Platzer, K. 2007. Starving avalanches: Frictional mechanisms at the tails of finite-sized mass movements Geophys. Res. Lett. 34.

Bartelt, P., Bühler, Y., Buser, O., and Ginzler, C. 2013. Plume formation in powder snow avalanches. In: Naaim-Bouvet, F., Durand, Y., and Lambert, R. (eds) International Snow Science Workshop 2013, October, 2013, 7–11. Proceedings. ISSW. Grenoble—Chamonix Mont Blanc. Grenoble, ANENA. 576–582.

Buehler, Y., Hueni, A., Christen, M., Meister, R., and Kellenberger, T. 2009. Automated detection and mapping of avalanche deposits using airborne optical remote sensing data, Cold Reg. Sci. Technol. 57, 99–106.

Bühler, Y., Kumar, S., Veitinger, J., Christen, M., and Stoffel, A. 2013. Automated identification of potential snow avalanche release areas based on digital elevation models. Nat. Hazards Earth Syst. Sci. 13: 1321–1335.

Castebrunet, H., Eckert, N., Giraud, G., Durand, Y., and Morin, S. 2014. Projected changes of snow conditions and avalanche activity in a warming climate: the French Alps over the 2020–2050 and 2070–2100 periods. *The Cryosphere*, 8, 1673–1697.

Chabot D., and Habibi H. 2015. Panjshir Valley Avalanches 25 February, Avalanche Site Investigation 15 June Report pp. 1–7.

Chirico, P. G. and Barrios, B. 2005. Void-Filled SRTM Digital Elevation Model of Afghanistan *Geological Survey* (U.S.).

Christen, M., Bartelt, P., amd Kowalski, J. 2010. Back calculation of the In den Arelen avalanche with RAMMS: Interpretation of model results, *Ann. Glaciol.*, 51, 161–168.

Christen, M., Bühler, Y., Bartelt, P., Leine, R., Glover, J., Schweizer, A., Graf, C., McArdell, B.W., Gerber, W., Deubelbeiss, Y., Feistl, T., and Volkwein, A. 2012, Integral hazard management using a unified software environment: numerical simulation tool "RAMMS" for gravitational natural hazards. In: Koboltschnig, G., Hübl, J., and Braun, J. (eds) 12th Congress INTERPRAEVENT, 23–26 April 2012 Grenoble—France. Proceedings. Vol. 1. Klagenfurt, International Research Society INTERPRAEVENT. 77–86.

Christen, M., Bartelt, P., Buehler, Y., Deubelbeiss, Y., Schneider, M., Schumacher, L., and Salz, M., 2013. RAMMS::AVAL User Manual v1.5 Avalanche, update March 7, 2013, WSL Institute for Snow and Avalanche research SLF p. 110.

Feistl, T., Bebi, P., Christen, M., Margreth, S., Diefenbach, L., and Bartelt, P. 2015. Forest damage and snow avalanche flow regime. *Nat. Hazards Earth Syst. Sci.* 15, 6: 1275–1288.

Feistl, T., Bebi, P., Teich, M., Bühler, Y., Christen, M., Thuro, K., and Bartelt, P. 2014, Observations and modeling of the braking effect of forests on small and medium avalanches. J. *Glaciol.* 60, 219: 124–138.

IPCC. 2013. Summary for Policymakers. In: Climate Change 2013: The Physical Science Basis. Contribution of Working Group I to the Fifth Assessment Report of the Intergovernmental Panel on Climate Change. Stocker, T. F., D. Qin, G.-K. Plattner, M. Tignor, S. K. Allen, J. Boschung, A. Nauels, Y. Xia, V. Bex, and P. M. Midgley (eds.). Cambridge University Press, Cambridge, United Kingdom and New York, NY, USA.

Jonas, T., Marty, C., and Magnusson, J. 2009. Estimating the snow water equivalent from snow depth measurements in the Swiss Alps. *Journal of Hydrology*, 378(1-2), 161–167, doi: 10.1016/j.jhydrol.2009.09.021

Jonkman, S. N. and Schweckendiek. 2015. Flood Defences, Delft University of Technology lecture notes: https://surfdrive.surf.nl/files/index.php/s/jn9SGBT82hEf22X

Kern, M. A., Bartelt, P., Sovilla, B., and Buser, O. 2009. Measured shear rates in large dry and wet snow avalanches J. Glaciol. 55, 327–338.

Kravtsova, V. I. and Bondareva, T. A. 1993. *Mapping the Avalanche Hazard for Mountainous Areas of Afghanistan Mapping Sciences and Remote Sensing,* 30, 137–150.

McClung, D. 2000. Predictions in Avalanche Forcasting, *Annals of Glaciology,* 31, 377–381.

McClung, D., and Lied, K. 1987. Statistical and Geometrical Definition of snow avalanche runout, *Cold regions Science and Technology, 13 107–109, Elsevier Science Publishers B.V., Amsterdam.*

McClung, D., and Schaerer, P. 2006. The Avalanche Handbook, The Mountaineers Books, p. 342.

Pielmeier, C., Techel, F., Marty, C., and Stucki, T. 2013. Wet snow avalanche activity in the Swiss Alps—trend analysis for mid-winter season. In: Naaim-Bouvet, F., Durand, Y., and Lambert, R. (eds) International Snow Science Workshop 2013, October, 2013 7–11. Proceedings. ISSW 2013. Grenoble—Chamonix Mont Blanc. Grenoble, ANENA. 1240–1246.

Schmucki, E., Marty, C., Fierz, C., and Lehning, M. 2015. Simulations of 21st century snow response to climate change in Switzerland from a set of RCMs. I*nternational Journal of Climatology,* John Wiley & Sons, Ltd. 35, 3262–3273.

Sovilla, B., Schaer, M., Kern, M., and Bartelt, P. 2008. Impact pressures and flow regimes in dense snow avalanches observed at the Vallée de la Sionne test site. *J. Geophys. Res.* 113.

Vera Valero, C., Wikstroem Jones, K., Bühler, Y., and Bartelt, P. 2015. Release temperature, snow-cover entrainment and the thermal flow regime of snow avalanches. *J. Glaciol.* 61, 225: 173–184.

Veitinger, J., Sovilla, B., and Purves, R. S. 2014. Slab Avalanche Release Area Estimation: A new GIS Tool. In: International Snow Science Workshop 2014. A merging of Theory and Practice. September 29–October 3, 2014. Banff, Alberta, Canada. Proceedings. ISSW. Banff, ISSW. 256–262.

Photo: PhotoTalk.

CHAPTER 5

Earthquake

This chapter focuses on the risk of ground shaking caused by seismic activity. The modeling of the earthquake shaking is undertaken with the open source CAPRA software. A summary of the modeling environment can be read from Daniell et al. (2014).

Using the programs CRISIS2007[1] and CAPRA,[2] the hazard, exposure, and vulnerability modules are combined to create the risk results.

5.1 Hazard

5.1.1 Approach

A probabilistic seismic hazard approach is undertaken to produce the stochastic event set and hazard maps for Afghanistan. Estimating earthquake hazard and its uncertainties is the first step in earthquake risk analysis and loss estimation. Earthquake hazard can be analyzed from the beginning at the source, to the production of waves traveling through the earth, to the site on the earth's surface where damage occurs.

The shaking which is felt at the site is a function of duration, amplitude, and frequency of the ground motion; distance from the fault; rupture length of the fault; and local site conditions. A ground motion prediction equation (GMPE) or attenuation relationship can be used to predict the ground motion at specified locations given the site conditions, magnitude, location, and fault mechanisms of an earthquake. Depending on the availability of data, a probabilistic or a deterministic analysis of earthquake hazard can be carried out. A probabilistic analysis calculates the probability of exceeding all levels of ground shaking from all potential seismic sources in the area, instead of a single postulated source as in the case of a deterministic analysis. In the stochastic approach undertaken here, all possible single events are considered in order to produce a probabilistic exceedance of a certain shaking.

The process undertaken to create the hazard outputs is as follows:

1. Importing of historic earthquake data and source models (zones and faults);
2. Computing of data completeness and declustering (explained below) of earthquake catalogue;
3. Selection of fault and source model;

[1] http://www.ecapra.org/crisis-2007
[2] http://ecapra.org/software

4. Selection of GMPEs;
5. Calculation of ground motion through logic tree analysis;
6. Estimation of site and topographic effects;
7. Stochastic calculation of a model catalogue; and
8. Ground motion sensitivity analysis.

5.1.2 Initial modeling of the hazard components

Historic earthquake data and the source model were assembled and imported from existing databases, including the work undertaken by Daniell and Schaefer for Afghanistan, creating the ECA catalogue as well as the EMME catalogue (Zare et al., 2014). In particular, Ambraseys and Bilham (2003) provide data on the key earthquakes in Afghanistan, reassessed in a consistent methodology from the year 800.

A component called 'declustering' is undertaken to remove the earthquakes which are either foreshocks (earthquakes before the main earthquake) or aftershocks (earthquakes after the main earthquake) in order to have a catalogue of independent events.

5.1.3 Final hazard maps

The intensity of an earthquake can be quantified using the spectral acceleration, which represents for each shaking frequency the acceleration imparted by the earthquake on an object. The hazard maps were derived for various ground spectral accelerations for shaking periods of 0 to 2 seconds, with return periods (RPs) of 10, 50, 100, 250, 500, 1,000 and 2,500 years using the CRISIS2007 model. As an example, Figure 5-1 shows the map of the peak ground acceleration (PGA) measured in g (the earth's gravity acceleration) with a 500-year RP.

The PGA for Kabul was calculated as 0.26 g for the 500-year RP, and 0.47 g for the 2,500-year RP, which indicate a significant hazard. A comparison of the seismic hazard in Kabul with some other locations using GSHAP (Global Seismic Hazard Assessment Program) is reported in Table 5-1.

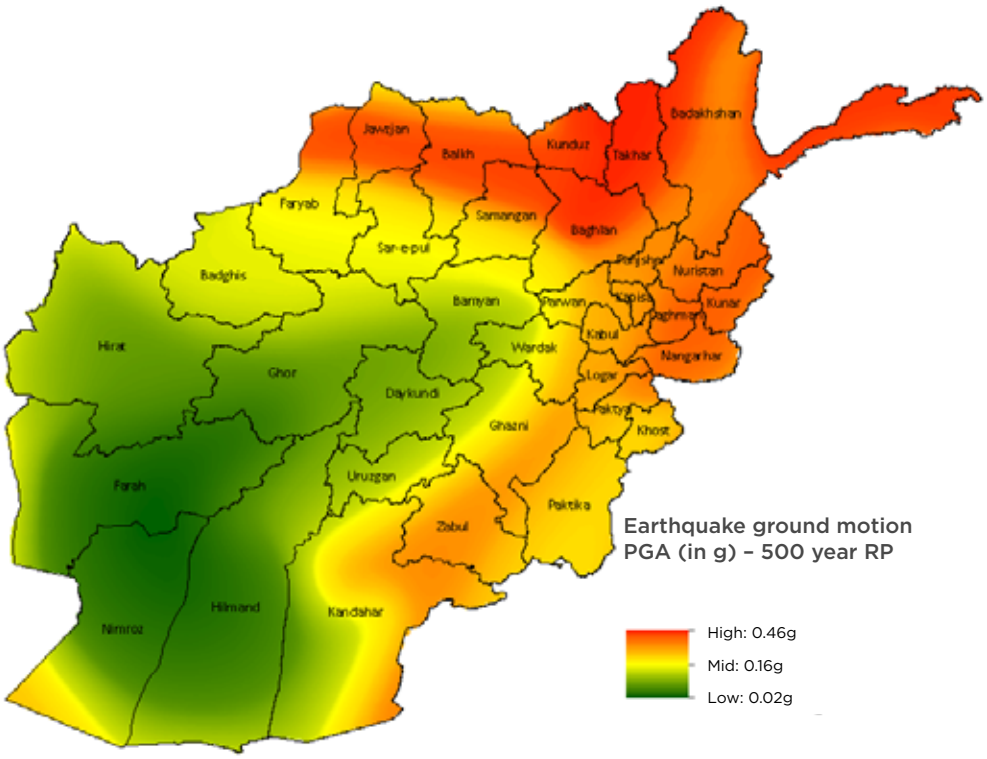

Figure 5-1

500-year RP earthquake ground motion—PGA (peak ground acceleration) measured in g.

Table 5-1

Comparison of the seismic hazard for Kabul obtained in this study with values for other cities obtained by the GSHAP.

City	Country	PGA (475/500 year) in g
Kabul	**Afghanistan**	**0.260**
Lisbon	Portugal	0.131
New Delhi	India	0.139
Bucharest	Romania	0.205
Jakarta	Indonesia	0.279
Manila	Philippines	0.387
Managua	Nicaragua	0.390
Tokyo	Japan	0.508
San Francisco	United States	0.611
Lima	Peru	0.702

A similar comparison was made for the PGA intensity (in percent of g) that exceeds the 10 percent probability of occurrence in 50 years (see Figure 5-2). This shows Kabul as being within the top few cities globally within city risk studies.

5.1.4 Final hazard-exposure maps

- The hazard-exposure maps were derived for seven return periods and 48 exposure layers at a level of 0.075 g, indicative of a damaging PGA.
- RPs used: 10, 50, 100, 250, 500, 1,000, 2,500 years

Figure 5-3 shows the difference between the hazard limits for the 500-year and for the 50-year return periods, respectively.

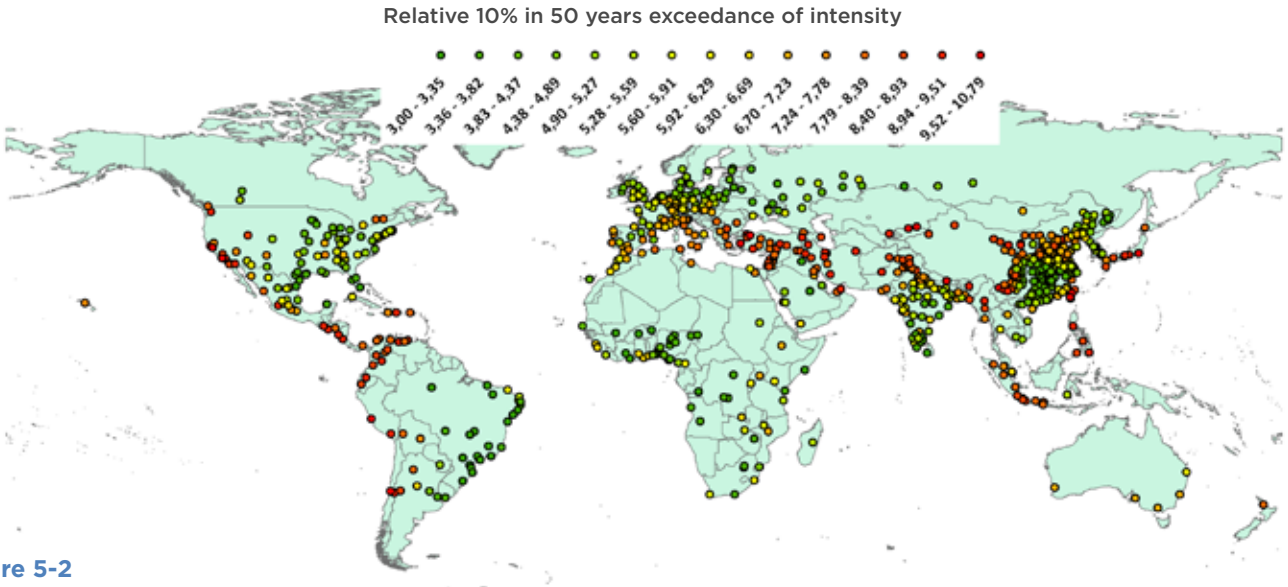

Figure 5-2

PGA intensity (in percent of g) that exceeds the 10 percent probability of occurrence in 50 years. Kabul is in the top 5 percent of major cities globally for earthquake hazard. (Daniell, 2011).

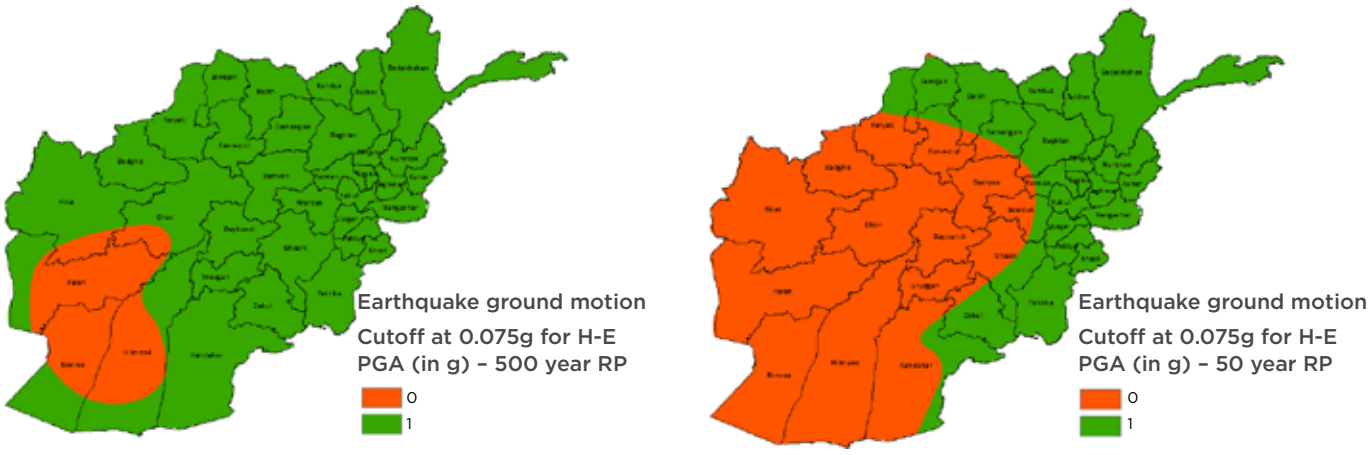

Figure 5-3

The difference of the hazard-exposure cutoff for (Left) 500-year RP and (Right) 50-year RP.

5.2 Exposure and Vulnerability

Determining vulnerability of the infrastructure and buildings to earthquakes is a complex task, yet there are some key concepts that can be used to relate the earthquake hazard to the vulnerability of structures. Fragility or vulnerability curves are an important tool that allows engineers to group buildings in different classes and estimate (based on analytical models, physical experiments, and past earthquake behavior) how the building would react to earthquake forces. However, there are many uncertainties due to the way that buildings are designed and built, especially in Afghanistan.

Table 5-2 presents the exposure to earthquakes of intensity VI (equivalent 0.075g) of roads (in km), population, residential and non-residential capital stock, respectively.

5.3 Risk

5.3.1 Event loss tables

For each scenario, the expected loss (EP) is produced, indicating the damage in USDs, or deaths which are expected to occur.

5.3.2 Loss results

5.3.2.1 National level (Afghanistan) PML and PMD

Table 5-3 reports the probable maximum loss (PML), the tail value at risk (TVaR), the occurrence exceedance probability (OEP) calculated at various return periods, and the annual average loss (AAL).

Table 5-4 shows the potential fatalities from the stochastic event set for Afghanistan in terms of probable maximum deaths (PMD), the tail deaths at risk (TDaR), the OEP calculated at various return periods, and the annual average deaths (AADs).

5.3.2.2 Province level PML

The PML for a 500-year RP is reported in Figure 5-4 for each province. Kabul clearly dominates the high period losses in Afghanistan due to the concentrated exposure.

Table 5-2

Total exposure in Afghanistan over intensity VI (equivalent 0.075 g).

Return period (years)	10	50	100	250	500	1000	2500
Roads (km)	11,769	38,729	42,692	47,547	52,290	54,074	55,664
Population (million people)	2.7	18.0	20.4	22.7	25.5	26.3	26.6
Residential capital stock (million USD)	1,662	13,317	15,459	16,526	18,375	18,983	19,212
Non-residential capital stock (million USD)	2,120	16,266	18,723	20,465	23,247	24,693	25,222

Table 5-3

Afghanistan earthquake shaking costs (does not include landslide-induced losses) detailing the AAL, the PML for seven return periods, and the relative loss versus the country capital stock and the TVaR.

Exposed Value: $45,097,973,886.00

RP	PML	TVaR	OEP as a percent of total value
10	$170,165,488	$409,462,074	0.377%
50	$519,673,959	$926,270,732	1.152%
100	$762,594,108	$1,229,967,626	1.691%
250	$1,166,363,224	$1,684,329,752	2.586%
500	$1,522,054,564	$2,048,119,915	3.375%
1,000	$1,911,917,773	$2,404,072,479	4.239%
2,500	$2,469,661,572	$2,792,214,542	5.476%
AAL	**$79,538,969.68**		**0.176%**

Table 5-4

Afghanistan earthquake deaths (does not include landslide-induced deaths) detailing the AAD and, for seven return periods, the PMD, the TDaR, and the relative loss versus the total population.

Exposed population: 27,102,565

RP	PMD	TDaR	OEP as a percent of total population
10	1,275	3,820	0.005%
50	4,690	9,745	0.017%
100	7,285	13,723	0.027%
250	12,192	20,562	0.045%
500	17,254	26,813	0.064%
1,000	23,628	33,661	0.087%
AAD	**563.27**		**0.0021%**

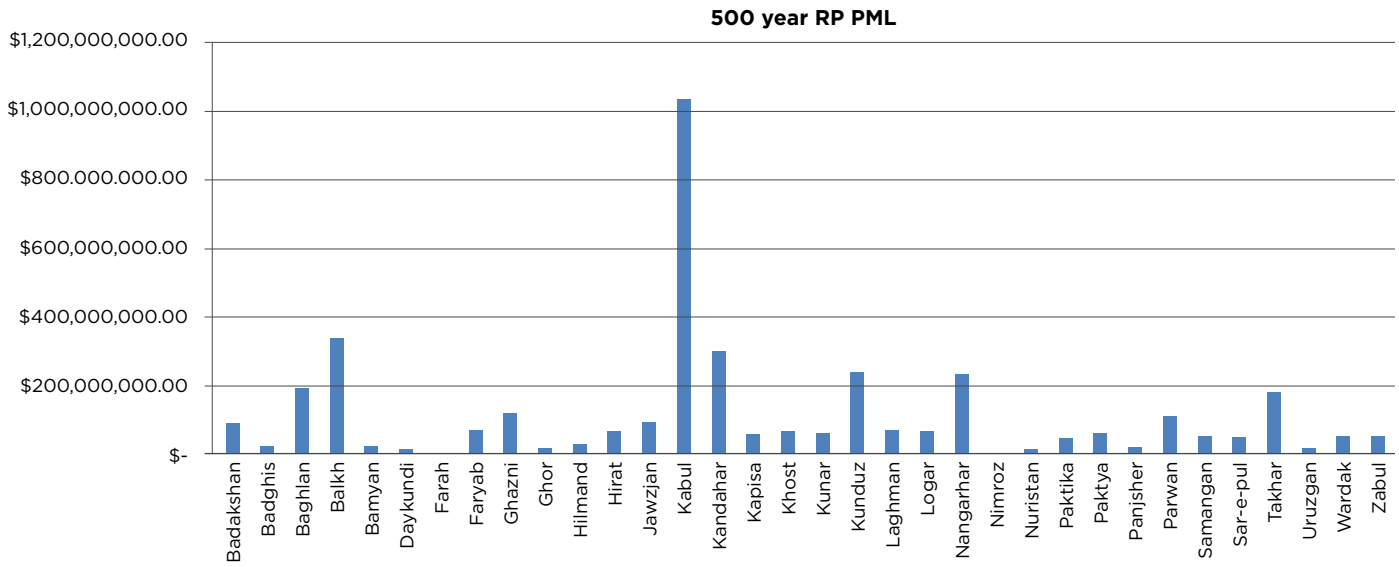

Figure 5-4

Earthquake losses expected for the 500-year return period event PML in each province.

5.3.2.3 AAL on a national, province, and district level

Figure 5-5 shows the annual average loss (AAL) on a 1 km grid resolution for the entire country.

Figure 5-6 shows the AAD (annual average number of deaths) in Afghanistan, corresponding to a total of about 400 deaths per year, in good agreement with historical records which indicate about 8,000 fatalities from earthquakes in the past 20 years.

Figure 5-7 shows that Kabul has a relative loss of 0.15 percent of capital stock, corresponding to about 40 percent higher risk than Turkey (Daniell and Schaefer, 2014). Figure 5-8 shows that Kabul has also the higher exposed value in USD.

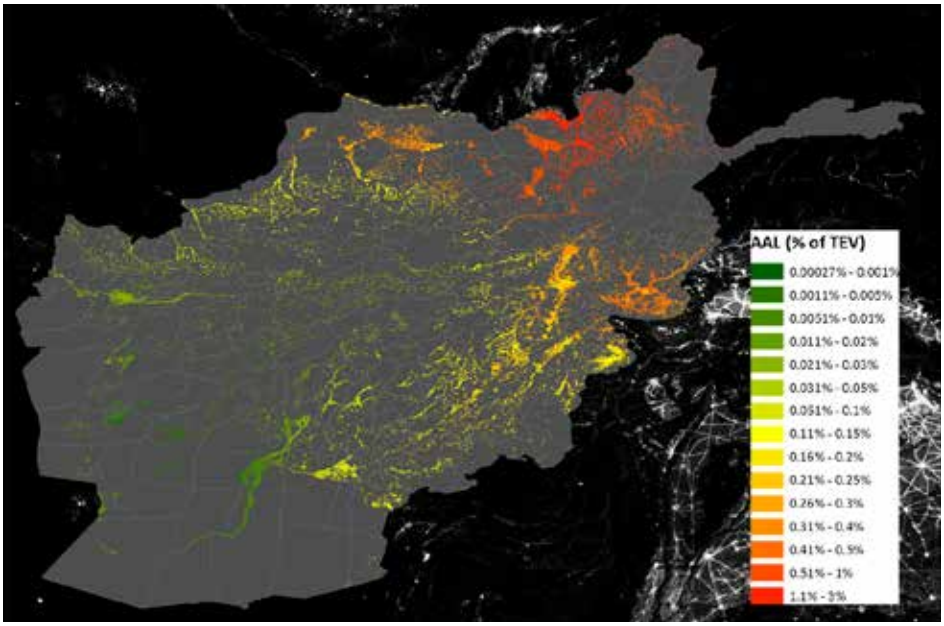

Figure 5-5

Annual average loss per square kilometer as a percent of total exposed value (TEV) due to earthquake shaking.

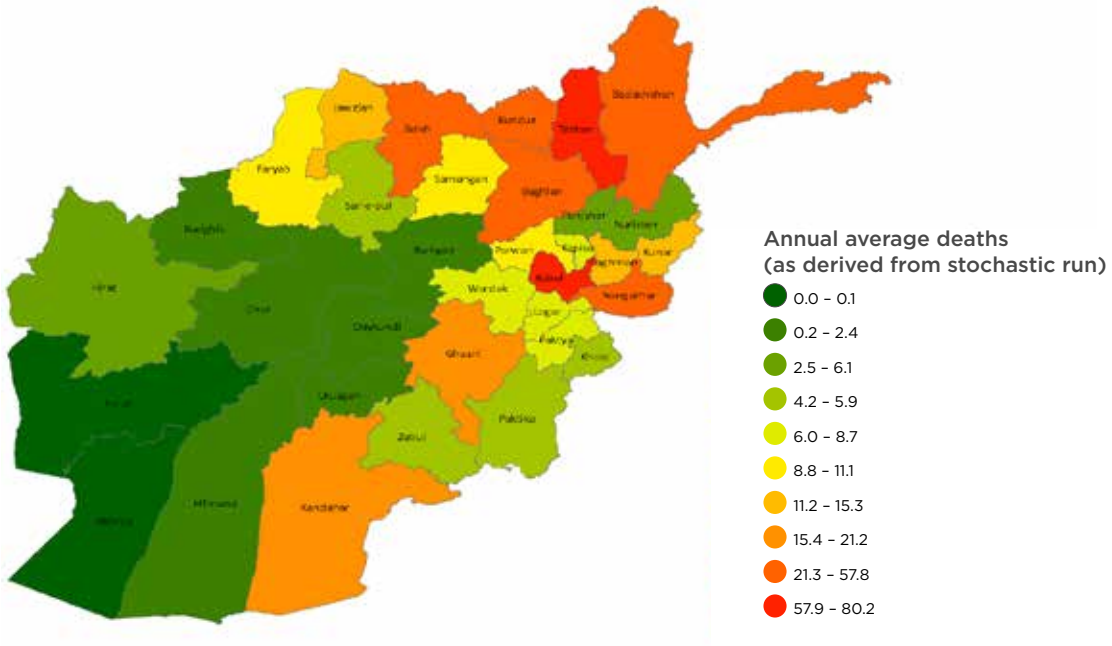

Figure 5-6

Annual average deaths as derived from the stochastic risk assessment for each province for earthquake shaking.

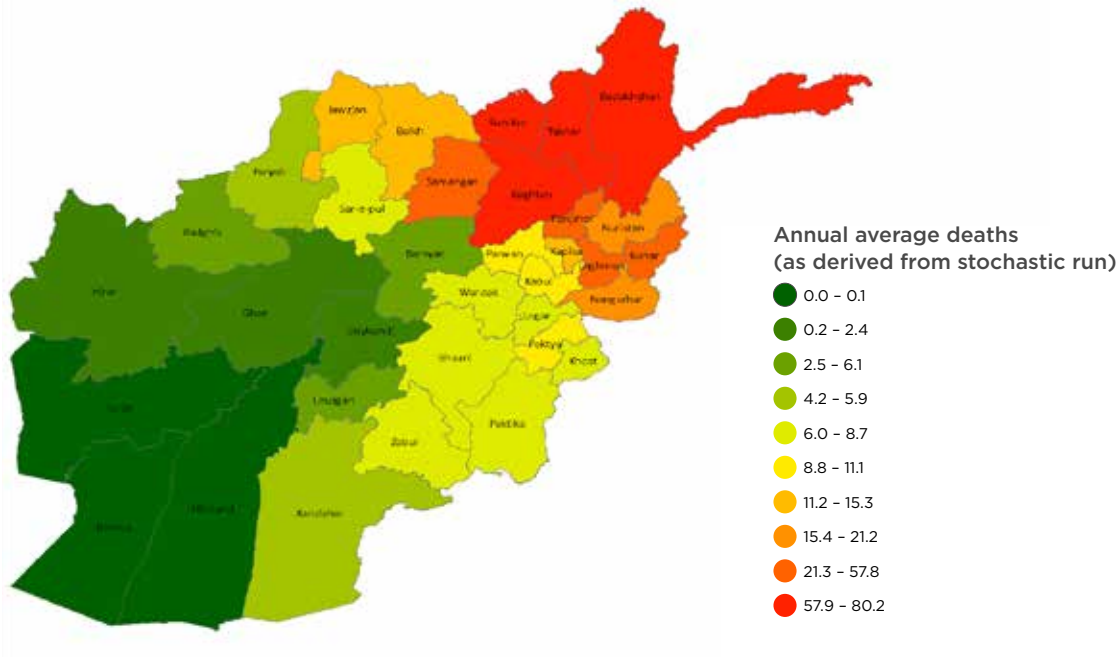

Figure 5-7

Annual average losses in relative terms as a percent of capital stock per province for earthquake shaking.

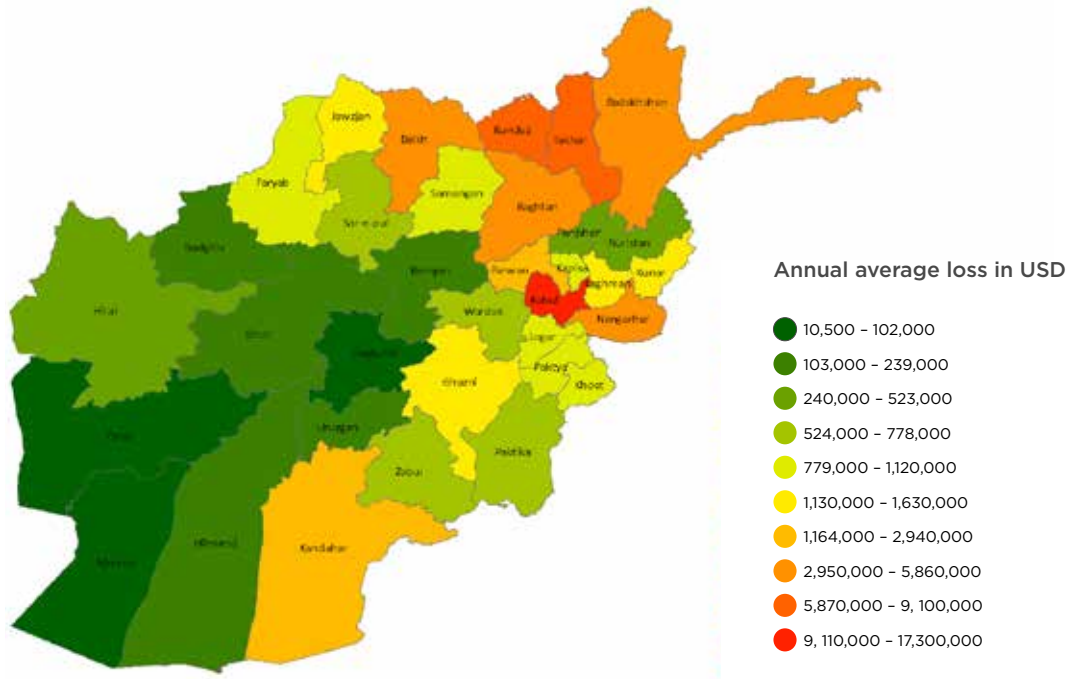

Figure 5-8

Annual average loss in absolute terms per province measured in USDs for earthquake shaking.

5.4 Earthquake-induced landslides

Landslides induced by earthquakes can come in various forms including slide, rock fall and slump, amongst others. The methodology correlates the results of Chapter 3 (Landslides) to historic earthquake loss results.

5.4.1 Relationship of earthquake-induced landslide losses

According to the CATDAT Damaging Earthquakes Database, a total of about 2,900 landslide deaths vs. about 9,000 shaking deaths have occurred from earthquakes since 1950 in Afghanistan, or a ratio of 1:3 in terms of losses.

Hazard exposure maps equivalent to a combined PGA and slope impact have been derived using a 0.1 percent cutoff as the onset of landslide density. Figure 5-9 and Figure 5-10 show the 500-year and 2,500-year return period earthquake-induced landslide risk index measured as landslide density.

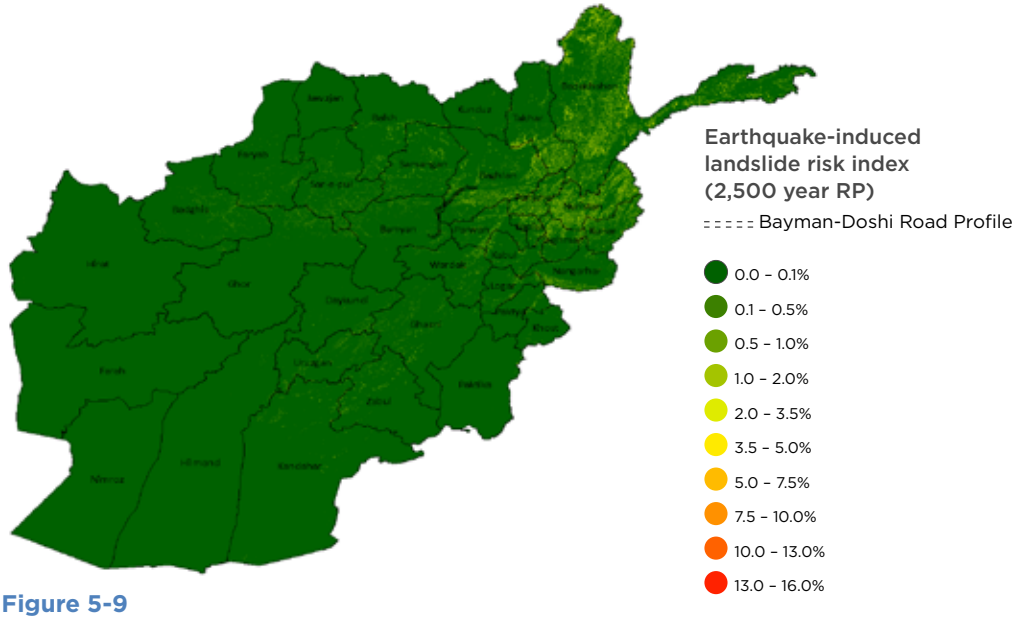

Figure 5-9

The 500-year return period earthquake-induced landslide risk index measure as landslide density in conjunction with the landslide assessment.

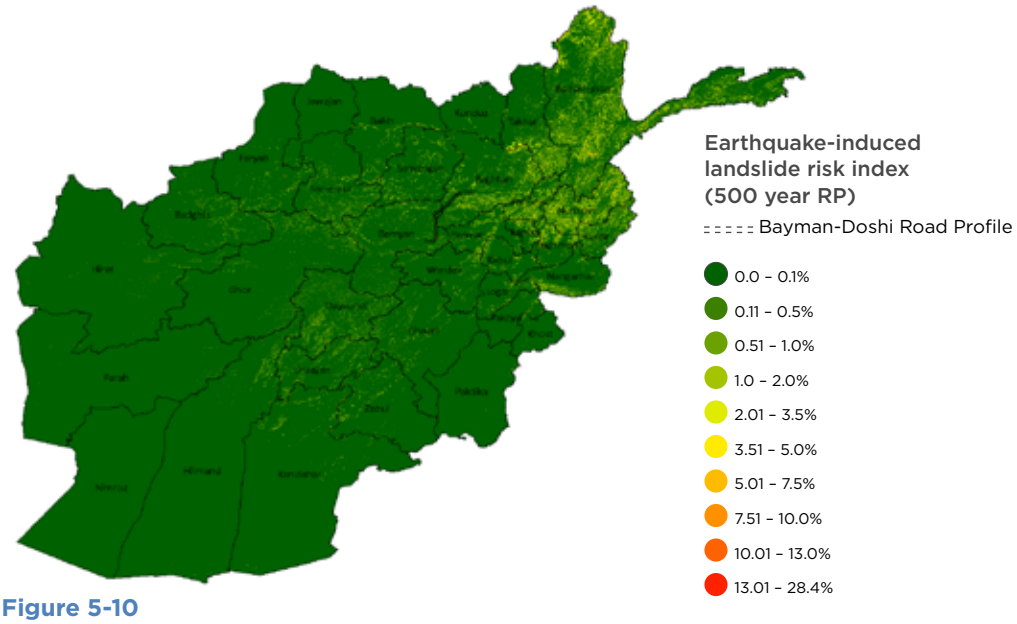

Figure 5-10

The 2,500-year return period earthquake-induced landslide risk index measure as landslide density in conjunction with the landslide assessment.

A very good correlation was observed between the index and historical earthquake landslides causing fatalities. The derivation of loss results was not possible because the necessary resolution of the rural settlement information was unavailable. A rule of thumb is that areas over about 2 percent landslide density present a substantially higher percentage of fatalities (approaching 30 percent or more), than shaking fatalities.

5.5 Case Studies for Examination of Cost-Benefit Analyses

5.5.1 Schools' case study

In the schools' case study, an earthquake risk assessment was undertaken for the base portfolio of schools, including modifications made to the building stock over time. The school typologies and vulnerabilities were considered representative of the Afghanistan school building stock, as indicated by details from the Ministry of Education, as well as other surveys of schools in Afghanistan.

Summary of the approach:

- Exposure analysis;
- Examination of previous studies on schools;
- Research building typologies of schools;
- Calculate PML and AALs for a base portfolio of schools; and
- Apply various retrofitting techniques.

5.5.1.1 Breakdown of cost components and exposure analysis

From various Bills of Quantities from schools being produced around Afghanistan, a list of expected components in a school masonry design was compiled. Costing for these components can differ by a factor of ten between the various building stocks.

Data from the Ministry of Education of Afghanistan was used to determine the number of schools. The individual school sites with geocoordinates totaled between 1,100 and 1,600, depending on the project, with inconsistent distribution across Afghanistan.

According to the Ministry of Education (EMIS 2016), in 2011–2012 there were 16,584 schools (15,701 schools are government and the rest private) in Afghanistan with at least 8,303 of these having buildings. This is in good agreement with the Afghan Central Statistics Organization (CSO) data from 2003–2005 shown in Figure 5-11. The value of schools distributed across Afghanistan is shown in Figure 5-12.

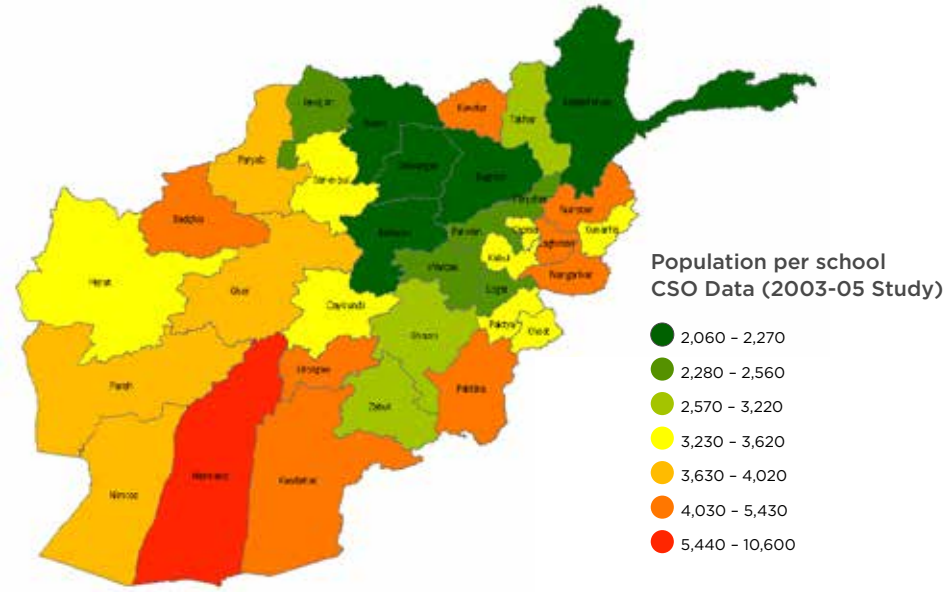

Figure 5-11
Population per school in province from CSO data (2003–2005).

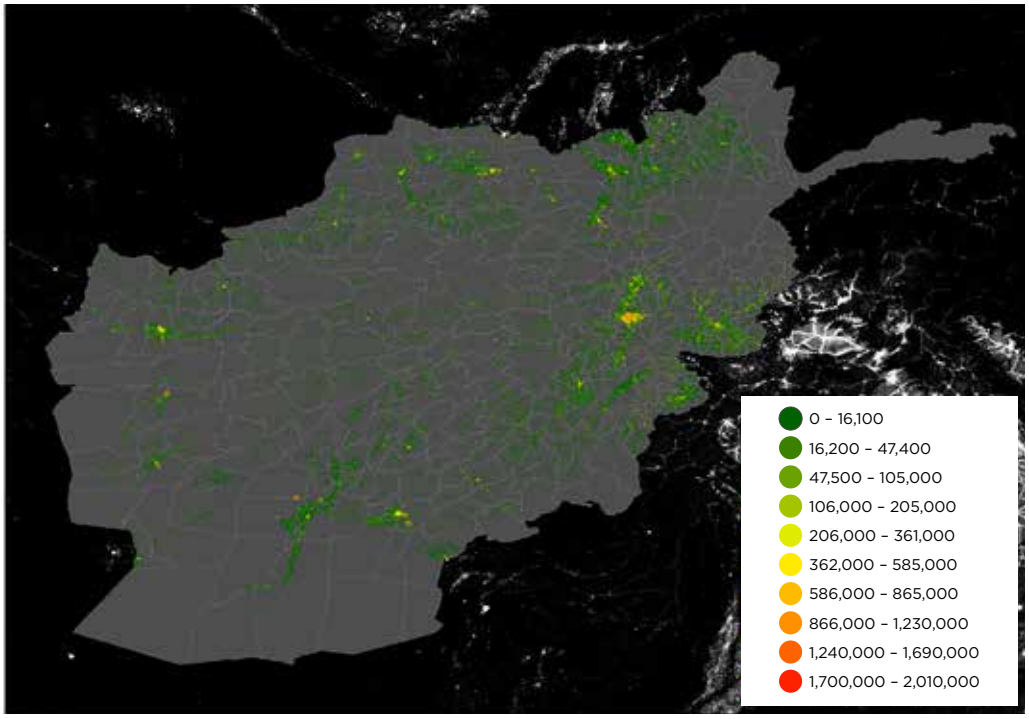

Figure 5-12

Values of Afghanistan schools distributed across Afghanistan. Total = 1.67b USD.

5.5.1.2 PML and AAL analysis of schools in Afghanistan

Using the 8,300 schools with buildings distributed across the nonresidential exposure, the base school portfolio was produced. A proportionate amount of two-story infrastructure was examined, as well as studies examining schools, including technical drawings. The vulnerability classes were distributed evenly nationwide.

The PML, TVaR, and AAL are shown in Figure 5-14 and Table 5-5 for the distributed base school portfolio in Figure 5-13. The PML250 for the schools' portfolio is around 3 percent, meaning that for a 250-year event, a likely loss of 3 percent of the building stock associated with schools will be damaged. Close to the epicenter schools will likely collapse, whereas further afield minor damages are expected. It should be noted that this study does not consider universities.

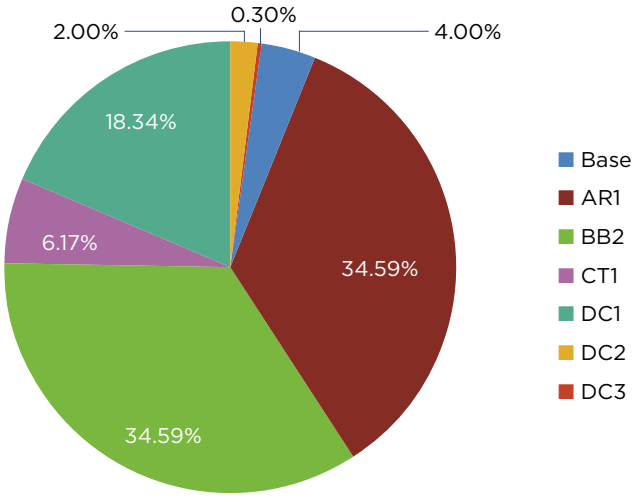

Figure 5-13

Relative percentage of building typologies for schools in Afghanistan currently.

Note: Base = improved masonry (engineered), BB2 = brick masonry (horizontal reinforcement or otherwise), CT1 = timber frame—heavy infill masonry, DC1 = in-situ reinforced concrete (RC) frame with nonstructural cladding, DC2 = RC frame with infill masonry, DC3 = in-situ RC frame with shear wall.

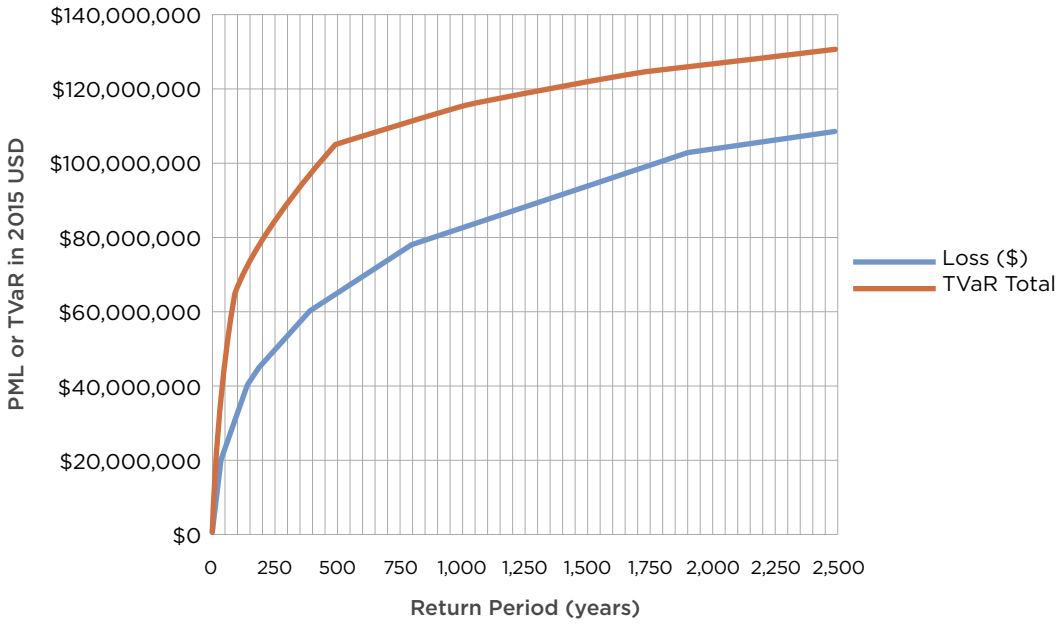

Figure 5-14.

PML and TVaR curve for Afghanistan schools as a current base portfolio in Afghanistan from 10 to 2,500 years from a TEV of around 1.67 billion USD.

Table 5-5

Afghanistan earthquake shaking costs for the school portfolio currently in Afghanistan (does not include landslide-induced losses) detailing the AAL, PML for seven return periods and the relative loss versus the country capital stock. The TVaR (tail value at risk) also provides a good basis that much of the risk is potentially mostly covered by a 2,500-year return period given the ratio of around 1.3:1.

Exposed value: $1,669,238,999.24

RP	PML	TVaR	OEP as a percent of total value
10	$7,599,026	$19,421,659	0.455%
50	$22,921,572	$46,801,692	1.373%
100	$33,270,659	$66,305,884	1.993%
250	$49,771,178	$85,319,587	2.982%
500	$65,111,627	$105,457,322	3.901%
1,000	$82,825,791	$115,788,097	4.962%
AAL	$3,311,319		0.198%

The AAL of $3.3 million per year may seem quite inconsequential compared to the GDP of Afghanistan ($20 billion), but in a single event a value of $50 million would not be uncommon for the school system. However, impacts include interruption of education, and fatalities. If all earthquakes hit during school time, around 4.94 million school students would be exposed in school buildings (around 55 percent of students are expected to be in schools with buildings). With the base portfolio, around Afghanistan, the total annual school student death toll expected would be around 144 students in schools. Given that the school time only makes up around 23 percent of a week, this would correspond to an annual average loss of around 33 students per year with average stock schools.

A 100-year event would cause a PML of $33 million of the $1.67 billion school building stock value (with significant uncertainties) but would kill an estimated 1,860 students in unsafe school buildings if it occurred during school time.

Table 5-6

Scenario 1–5 for schools' improvement.

Scenario 1	Adjusting masonry in rural and bad quality to better quality
Scenario 2	Adjustment to rural concrete (RC) (low code) stock from masonry
Scenario 3	Adjustment to RC (moderate code) from masonry
Scenario 4	Improvement of stock to code
Scenario 5	Rural school Improvement to better classes and AR1 class removal

5.5.1.3 Retrofitting and benefit ratio estimation

Cedillos et al. (2012) and Smyth et al. (2004) detail successful retrofitting of schools in different environments around the world. The price of retrofitting is often around 8–20 percent the value of the structure where only minor changes are required but would improve life safety far more than that. The base AAL for schools is approximately 0.2 percent across Afghanistan, which is slightly higher than the total AAL (around 0.15–0.16 percent). This indicates the vulnerable nature of poorly built masonry schools. Five scenarios are set out (Table 5-6) to examine the impact of reducing the vulnerability of the school stock.

Figure 5-15 shows the AAl for each building type, and for each scenario, where

Base = Improved masonry (engineered)
AR1 = Rubble masonry, adobe, mud, or other vulnerable masonry construction
BB2 = Brick masonry (horizontal reinforcement or otherwise)
CT1 = Timber frame—heavy infill masonry
DC1 = In-situ RC frame with nonstructural cladding (to low code levels)
DC2 = RC frame with infill masonry (to moderate code levels)
DC3 = In-situ RC frame with shear wall (to high code levels)

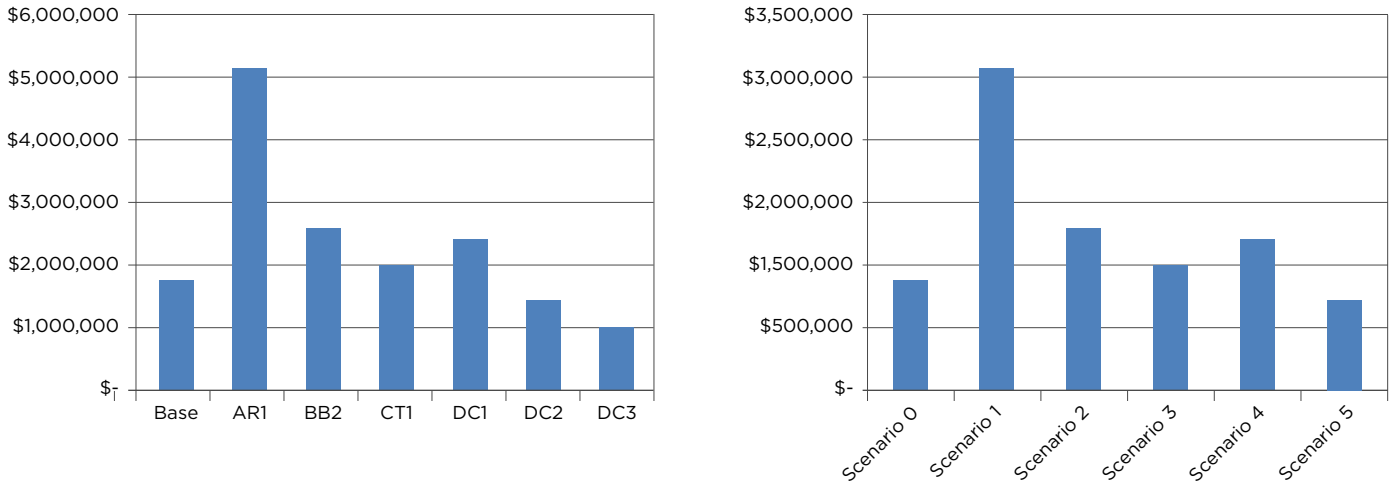

Figure 5-15. Left: AAL for each building type using a base portfolio of all this building type; Right: AAL for each of the six scenarios (five scenarios [1–5], and base scenario [0]).

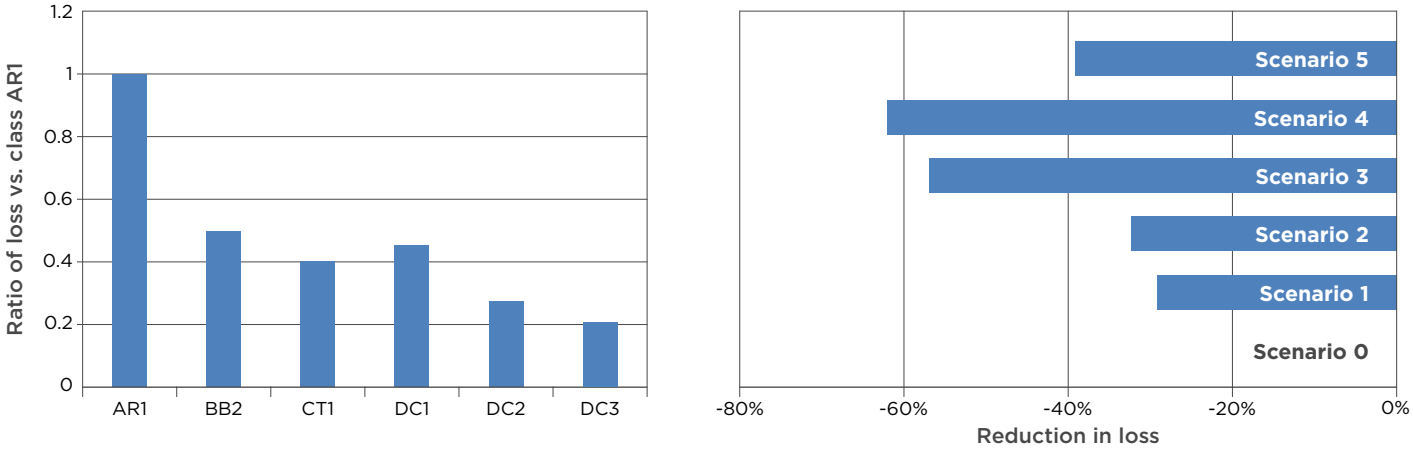

Figure 5-16

Left: Relative loss vs. vulnerability class AR1, showing the reduction in vulnerability from alternate classes of buildings vs. vulnerable masonry as measured from annual average loss; Right: The savings in AAL (not considering cost of program) from the five scenarios vs. the initial stock.

The human impact would likely be reduced by an even higher amount with the reduction of fatalities from the brittle collapse of buildings occurring mainly in the AR1 and BB2 classes (Figure 5-16).

For the purposes here, the fatalities as an annual average are shown in Table 5-7

The costs associated with each component are based on expert opinions from previous retrofitting studies in other countries and the associated costs of new construction from the residential building costs.

5.5.1.4 Recommendations

- The cost of a nationwide upgrading is prohibitive. However, an inventory of vulnerabilities to seismic safety of each school building should be produced using the Ministry of Education database of schools.
- Bad quality building stock out of mud, masonry, or badly built reinforced concrete (RC) should be earmarked for retrofitting in high and moderate seismic regions in the country (i.e., locations where the 100-year earthquake exceeds 0.075 g) or simply the provinces in the east and north of the country as this will show the maximum benefit.
- Unreinforced masonry (URM) and adobe buildings are most vulnerable.
- Either Scenario 1 or Scenario 5 are most feasible, given the large difficulties associated with the other options.
- Up to 90 percent of fatalities could be prevented by employing a school seismic safety scheme.

Table 5-7

Scenarios 0–5 showing the benefit in terms of AAL vs. a zero-cost assumption.

		AAL	Savings in AAL	Fatalities (annual avg.)	Reduction in fatalities
Scenario 0	Average	$3,311,320	0%	32.87	0%
Scenario 1	Adjusting masonry in rural and bad quality to better quality	$2,426,520	27%	21.11	36%
Scenario 2	Adjustment to RC (low code)	$2,303,303	30%	10.73	67%
Scenario 3	Adjustment to RC (moderate code)	$1,467,846	56%	4.60	86%
Scenario 4	Improvement of stock to code	$1,277,786	61%	3.71	89%
Scenario 5	Rural school improvement	$2,016,248	39%	13.39	59%

Table 5-8

Investment and capital stock in roads in Afghanistan used for the replacement cost.

Roads	km	Unit cost	Value
Total existing roads	33,864		
Asphalted roads	9,468	310,000/km	**$2,935,080,000**
Sand roofed roads	24,146	80,000/km	**$1,931,680,000**
Other roads	144	80,000/km	**$11,520,000**

5.5.2 Doshi-Bamyan Road case study

5.5.2.1 Exposure profile

A case study of the Doshi-Bamyan Road was undertaken to examine the effect of earthquakes on the potential path of the road. A shape file of the path was created for the length from Bamyan to Afghan Doshi.

The elevation profile along the road from Bamyan to Afghan Doshi drops from 2,539 m to 838 m, namely a drop of 1,701 m over around 180 km (an average gradient of 1 percent).

Table 5-8 reports investment and capital stock in roads in Afghanistan; it was compiled using a combination of datasets. The replacement cost for the Doshi-Bamyan Road is taken from Table 5-8 for asphalted roads ($310,000/km). A total of 179.33 km of roads and bridges are required. Thus, the total replacement cost to be assumed is $55.6 million.

5.5.2.2 Vulnerability

Road vulnerability functions were derived from various authors. Two methodologies were examined: the NIBS (2004) and Werner et al. (2006) functions for road pavements, and the SAFELAND methodology for roads on slopes.

5.5.2.3 Hazard

Peak ground displacement (PGD) was derived using the 2.0 sec peak ground acceleration (PGA).

The PGD and PGA have been derived for each location (Figure 5-17) along the road by using spectral response at PGA (2.0 s) and other empirical checks. Figure 518 shows the PGD nationwide.

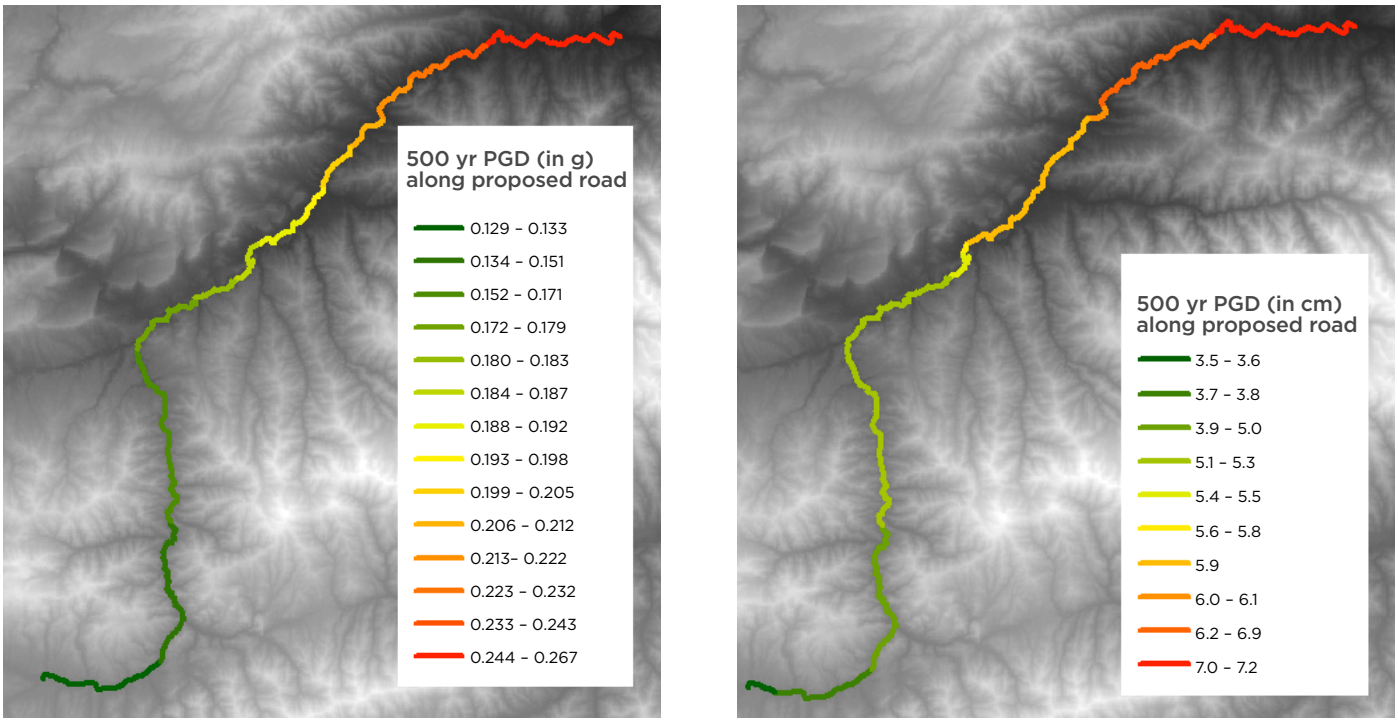

Figure 5-17

Left: 500-year PGA interpolated along the proposed road; Right: 500-year PGD interpolated along the proposed road.

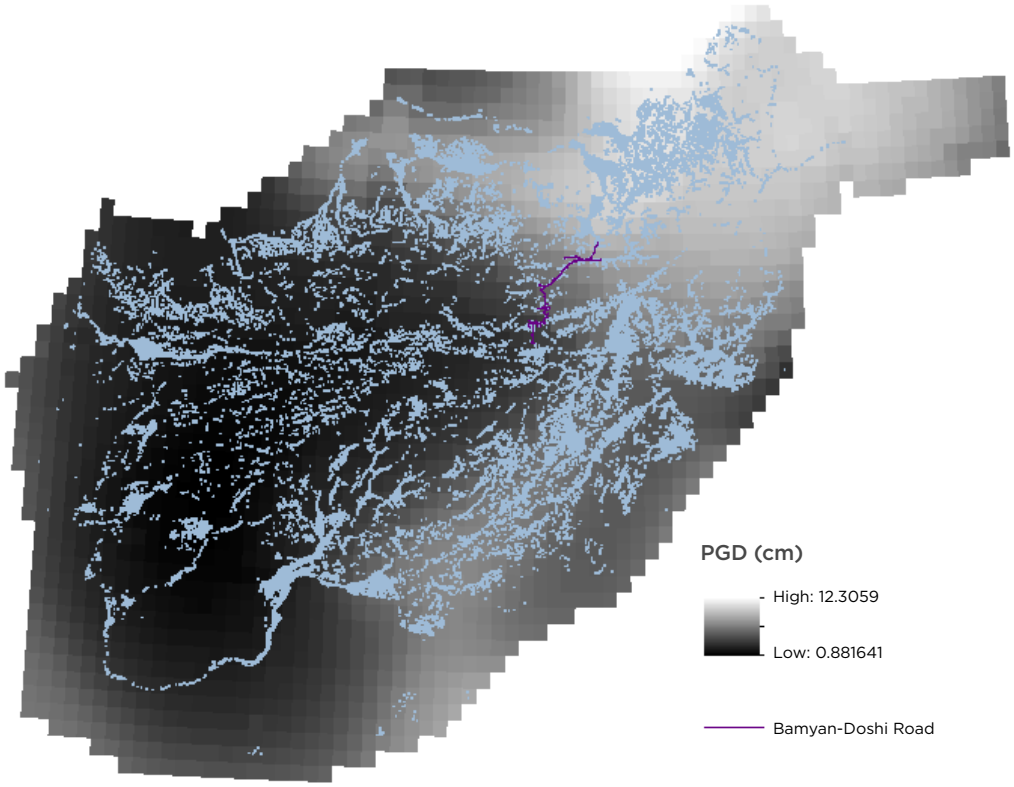

Figure 5-18

Peak ground displacement (PGD) derived for each cell on a non-interpolated grid, and the Bamyan-Doshi Road

5.5.2.4 Risk

The risk is calculated using the damage ratios of Werner et al. (2006) for the given hazard maps. The results are presented in Figure 5-19, Figure 5-20, and Table 5-9. It should be noted that if local effects are in place, the PGD may be much higher or lower than the calculated hazard, and thus there is a significant standard deviation on the loss.

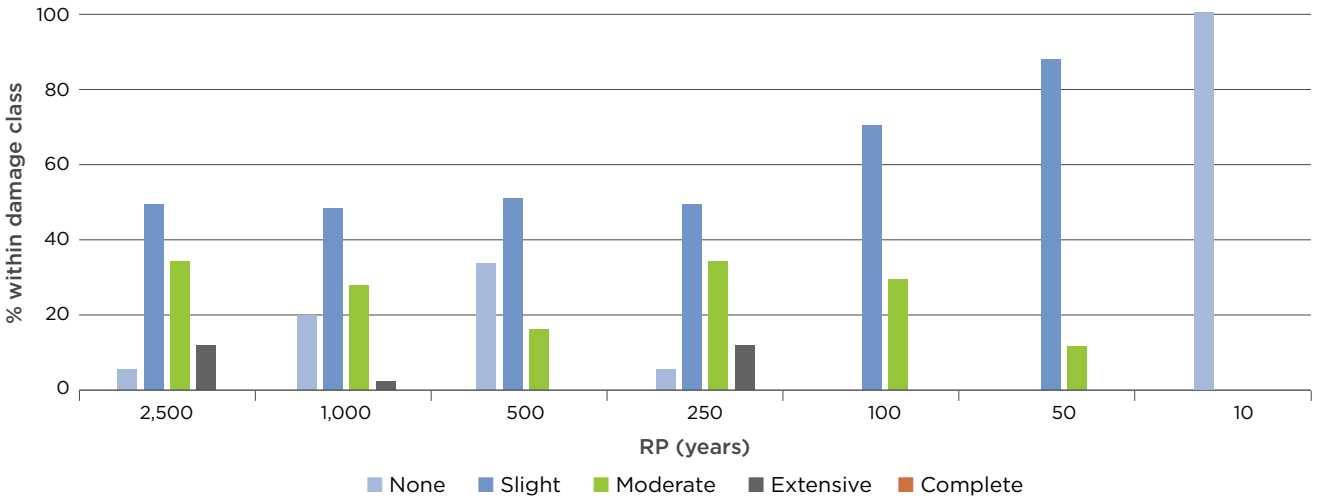

Figure 5-19

Damage percentages to the Bamyan-Doshi Road for each return period for each class.

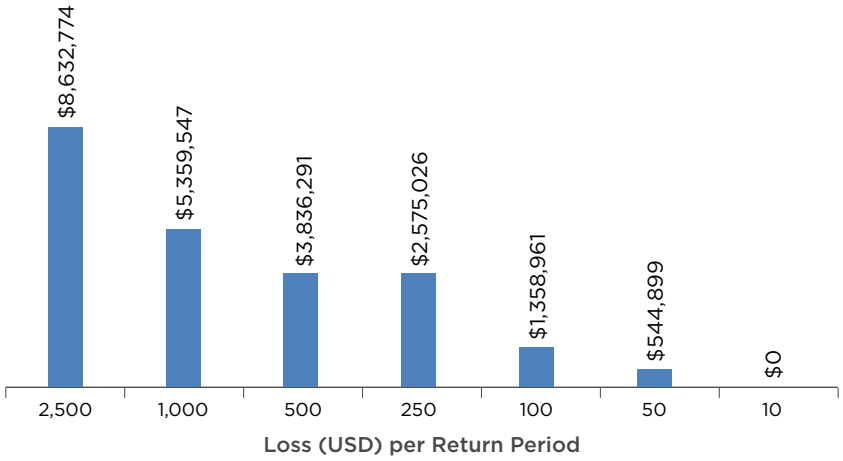

Figure 5-20

Loss (USDs) for each return period for the proposed road showing the significance of large events.

Table 5-9

Final calculated loss results for the $55.6 million road from Bamyan to Doshi.

RP (years)	Loss (USD)	MDR	km damaged
2,500	8,632,774	15.5%	27.8
1,000	5,359,547	9.6%	17.3
500	3,836,291	6.9%	12.4
250	2,575,026	4.6%	8.3
100	1,358,961	2.4%	4.4
50	544,898	1.0%	1.8
10	—	0.0%	0.0

The earthquake-induced landslide risk index is higher in the steeper sections of the profile in the first half of the road, which may mean that better stabilization of slopes is required to avoid landslides covering the road in potential earthquakes (Figure 5-21).

5.5.2.5 Costs and benefits associated with upgrading the Bamyan-Doshi Road to a higher standard to reduce damage

The construction of earthquake-resistant roads is extremely difficult, given the ground stability being a key component with additional compaction and increased strength of concrete and bitumen having no marked effect on earthquake loss.

Around the world a few methods have been used to attempt to protect roads and bridges:

- Micropiles (high-capacity rods or pipes grouted to the ground) have been used for anchoring the shoulder and the subgrade; however, this only in theory minimizes damage and would be extremely costly.
- Base isolation (a method to isolate the structure from the ground using shock absorbers) and other techniques such as dampers should be employed for the parts of the road that span the river, given that we may expect lateral spreading and/or liquefaction in the locations near the river.
- Glass or carbon fiber retrofitting in some cases could be used, but not for the entire portion of the road given the cost.
- Embankments and bridges can be designed through the geotechnical engineering process to have a higher factor of safety. This can be achieved through soil replacement, shotcreting, compaction, and/or reinforcement, and thus is generally more stable in a minor earthquake event, reducing minor losses. This is the most important method of road stabilization in a big earthquake event.

The increased cost associated with a better factor of safety, better ground conditions studies, earthquake-resistant design in the retaining walls, geotechnical make-up of the road, and other cases is in the order of 20–30 percent of the design cost. It is expected that up to 75 percent of the damage may be able to be reduced by better building practices, up to around 0.2 m displacement; however, beyond that, the benefits would be markedly reduced (from empirical evidence). Thus, the most benefit would be for the slightly and moderately damaged portions of the road.

Over 150,000 people would be serviced by the road, bringing a likely increase of 50 percent of their income based on the road being active. That transfers to close

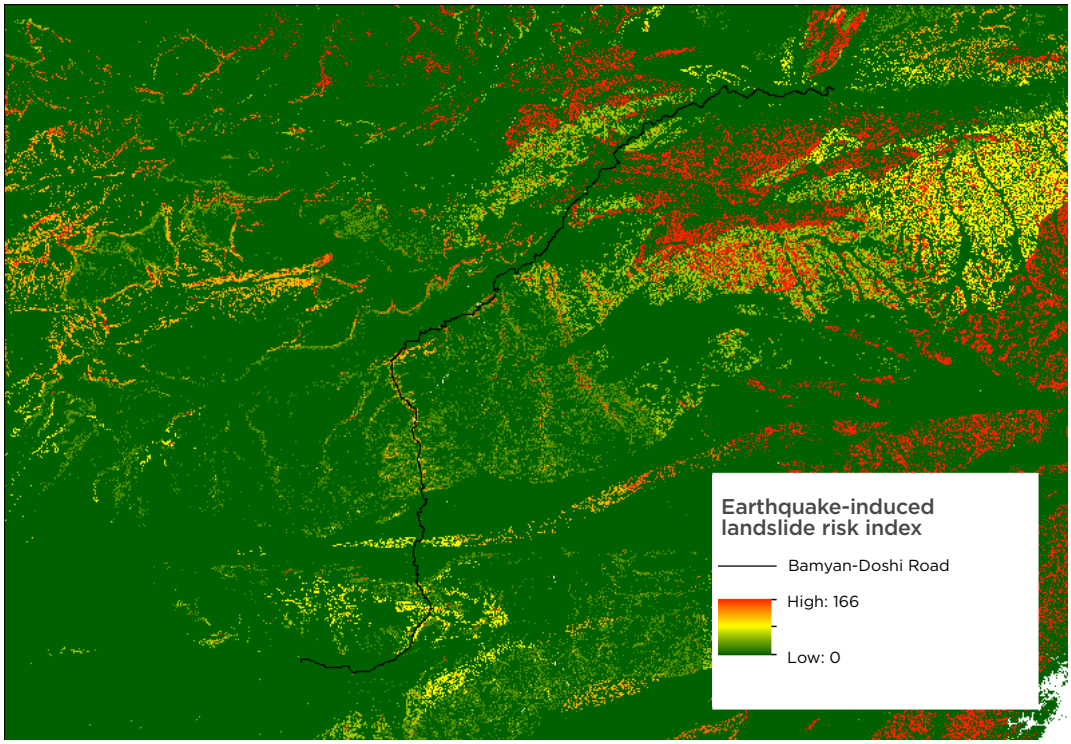

Figure 5-21

The location of the Bamyan-Doshi Road with respect to the earthquake-induced landslide risk index. Red = high risk; green = low risk.

Table 5-10

The cost in days and dollars downtime associated with loss results for the scenario events.

RP (years)	Loss (USD)	MDR	km damaged	Minimum downtime (to previous standard) (days)
2,500	8,632,774	15.5%	27.8	485 ($159 m)
1,000	5,359,547	9.6%	17.3	188 ($62 m)
500	3,836,291	6.9%	12.4	95 ($32 m)
250	2,575,026	4.6%	8.3	39 ($13 m)
100	1,358,961	2.4%	4.4	13 ($4.3 m)
50	544,898	1.0%	1.8	5 ($1.7 m)
10	—	0.0%	0.0	0.0

to $8 million per month, in addition to reduced freight costs. (A 15-day downtime assumption per km moderately damaged is used.) A value of 30 days for extensively and completely damaged kilometers are used, given the cleanup and design needed post-event. For slight damage, a value of five days is used per kilometer.

5.5.2.6 Recommendations

- Earthquakes are a key issue in Afghanistan, and the Bamyan-Doshi Road will be likely subjected to an earthquake during its design lifetime. A proper earthquake-sensitive design should be undertaken for the road, especially toward Doshi.
- Retrofitting or redesigning versus usual road design is not cost effective, and the increased road cost would be prohibitive, even versus the economic impact for the region.
- Detailed geotechnical work should be undertaken, as there may be cost-effective solutions to improving stability against earthquakes. It is likely that additional money invested into geotechnical design and build will also increase service life of the road.

- The road could have a damage fund set up, rather than unnecessarily building beyond the usual engineering effort, as the likelihood of slight damage is very high, whereas the chance of a major rebuild is very low. This could then aid with repairs of the road over the design life due to smaller earthquakes, as well as aid with maintenance of the road.
- Earthquake-induced landslides, without detailed information as to road cutting and soil testing, are not possible to include in a preliminary analysis; however, they should be examined as part of the road building design.

References

Chapter 5

Afghan Tax Office. 2015. http://www.trade.gov/static/AF_Tax_Guide20.pdf - Afghan Tax Office

Ahmad, N. 2011. Seismic risk assessment and loss estimation of building stock of Pakistan. Diss. PhD Thesis, ROSE School-IUSS Pavia, Pavia, Italy.

Allen, T. I., and Wald, D. J. 2007. "Topographic slope as a proxy for global seismic site conditions (VS30) and amplification around the globe," U.S. Geological Survey Open-File Report 2007-1357.

Ambraseys, N. N., and Simpson, K. A. 1996. Prediction of vertical response spectra in Europe. Earthquake Engineering and Structural Dynamics, 25(4), 401–412.

Ambraseys, N. N., and Melville, C. P. 1982. A History of Persian Earthquakes: Cambridge, Cambridge University Press, 219 p.

Ambraseys, N., and R. Bilham. 2003. Earthquakes in Afghanistan, Seism. Res. Lett., 74(2), 107–123.

Ambraseys, N. N. 1958. *The Seismic Stability of Earth Dams*, PhD Thesis, Imperial College London.

Ambraseys, Nicholas, and Bilham, Roger. 2003a. Earthquakes in Afghanistan: Seismological Research Letters, v. 74, pp. 107–123 (includes electronic supplement on the web site of the Seismological Society of America, http://www.seismosoc. org/publications/SRL/SRL_74/srl_74-2_ambraseys_esupp1. Html)

Ambraseys, Nicholas, and Bilham, Roger. 2003b. Earthquakes and associated deformation in northern Baluchistan: Bulletin Seismological Society America, v. 93, pp. 1573–1605.

Cedillos, V., Tucker, B., Blondet, M., Carpio, J., Quispe, J., Rondon, S., and Sanchez, M. 2012. Towards Creating Earthquake-Safe Communities: Seismic Retrofit of an Adobe School Building in Rural Peru Using Geomesh, 15WCEE, Lisbon.

Central Statistic Organization (Islamic Republic of Afghanistan). 2016. http://cso.gov.af/en

CSO. 2009. "Integrated Business Enterprise Survey," http://www.adb.org/sites/default/files/project-document/63965/37047-01-afg-dpta.pdf

CSO. 2011. Afghanistan Multiple Indicator Cluster Survey 2010–2011.

CSO. 2014. "Afghanistan living conditions survey (ALCS) 2013–14 or National Risk and Vulnerability Assessment (NRVA) 2013–14." http://cso.gov.af/en/page/1500/1494/nrav-report

CSO. 2014. Central Statistics Organization of Afghanistan Kapisa HIGHLIGHTS Socio-Demographic and Economic Survey.

CSO. 2015. Central Statistics Organization of Afghanistan Kabul Socio-Demographic and Economic Survey.

CSO Afghanistan. 2015. http://countryoffice.unfpa.org/afghanistan/drive/afghanistan_sdes_bamiyan_final_report_24_april_2013.pdf. SDES Bamiyan.

CSO Afghanistan. 2015. http://countryoffice.unfpa.org/afghanistan/drive/Kabul_Socio-demographic-Economic-Survey_English.pdf .SDES Kabul.

CSO Afghanistan. 2015. http://countryoffice.unfpa.org/afghanistan/drive/SDES-Ghor-English-Low-Resolution-Version.pdf .SDES Ghor Province.

CSO Afghanistan. 2015. http://cso.gov.af/Content/files/Afghanistan%20SDES%20Bamiyan%20Final%20Report%20-%2024%20April%202013.pdf .Bamiyan Socio-Demographic and Economic Survey.

CSO Afghanistan. 2015. http://cso.gov.af/Content/files/ALCS%202013-14%20Main%20Report%20-%20English%20-%2020151221.pdf .ALCS 2013–14.

CSO Afghanistan. 2015. http://cso.gov.af/Content/files/ALCS%202014%20Half-year%20Report%20-%20141208%20BdB.pdf .Afghanistan Living Conditions Survey 2014 Mid-term results.

CSO Afghanistan. 2015. http://countryoffice.unfpa.org/afghanistan/drive/afghanistan_sdes_daykundi_highlights_2014.pdf; http://countryoffice.unfpa.org/afghanistan/drive/SDES-DaikundiReport-Part1-pag-1-50.pdf;http://cso.gov.af/Content/files/Daikundi%2051-84.pdf. 2012 Socio-Demographic and Economic Survey in Daykundi.

CSO Afghanistan. 2015. http://cso.gov.af/Content/files/SDES%20Kapisa%20Report%20-%20Final.pdf. SDES Kapisa Province.

CSO Afghanistan. 2015. http://cso.gov.af/Content/files/SDES%20Parwan%20Report%20-%20Final.pdf .SDES Parwan Province.

Daniell, J. E. 2010. Earthquake Risk Analysis Course; Eds: Khazai, B., Daniell, J. E., Apel, H. 2010. "Risk Analysis Course Manual," The World Bank Institute, Washington DC.

Daniell, J. E., Wenzel, F., and Khazai, B. 2010. The cost of historic earthquakes today–economic analysis since 1900 through the use of CATDAT. In Proceedings of the Australian Earthquake Engineering Society Conference.

Daniell, J. E. 2014. "Development of socio-economic fragility functions for use in worldwide rapid earthquake loss estimation procedures," Doctoral Thesis, Karlsruhe Institute of Technology, Karlsruhe, Germany.

Daniell, J. E., and Schäfer, A. 2014a. "Making an Australian brick house more earthquake-resistant for $100 or less: Ideas, Practice and Loss Analysis," Australian Earthquake Engineering Society Conference, Lorne, Victoria.

Daniell J. E., Schäfer A. M. 2014b. Eastern Europe and Central Asia Risk Profiling for Earthquakes, World Bank, Washington DC, 147 pp.

Daniell, J. E., Simpson, A., Gunasekara, R., Baca, A., Schaefer, A., Ishizawa, O., Murnane, R., Tijssen, A., Deparday, V., Forni, M., Nunez, A., Himmelfarb, A. 2014. Review of Open Source and Open Access Software Packages Available to Quantify Risk from Natural Hazards, Understanding Risk Report, GFDRR, 72 pp.

Daniell, J. E., and Wenzel, F. 2014d. The Economics of Earthquakes: A reanalysis of 1900–2013 historical losses and a new concept of capital loss vs. cost using the CATDAT Damaging Earthquakes Database.

Daniell J. E., Wenzel F., Khazai B., Santiago J. G., and Schäfer A. 2014e. "A worldwide seismic code index, country-by-country global building practice factor and socioeconomic vulnerability indices for use in earthquake loss estimation," Paper No. 1400, 15th ECEE, Istanbul, Turkey.

Daniell, J. E. 2015. "Global View of Seismic Code and Building Practice Factors," eds. Michael Beer, Edoardo Patelli, Ioannis Kougioumtzoglou and Ivan Siu-Kui Au in "Encyclopaedia of Earthquake Engineering." Springer.

Daniell, J. E., Schäfer, A., and Wenzel, F. 2015. "The value of life in earthquakes and other natural disasters: historical costs and the benefits of investing in life safety," Australian Earthquake Engineering Society Conference, Sydney, Australia.

Daniell, J. E., Schaefer, A. M., Vervaeck, A., and Skapski, J-U. 2016. "Intensity Relations from historic Afghan earthquakes," in press.

Deltares, Global Risk Forum Davos, Karlsruhe Institute of Technology, National Agency for New Technologies, Energy and Sustainable Economic Development, Omran Technical Company—Afghanistan, 2015: Afghanistan—Multi-hazard risk assessment, cost-benefit analysis, and resilient design recommendations; inception report.

EERI. 2016. https://www.eeri.org/projects/schools/resources/seismic-school-safety-by-country/

EMIS. 2016. http://www.emis.af/content/download/datasets/dataset%201393/

Envotech. 2015. http://www.envotechinc.com/foam-home/

FAOSTAT, FAO of the UN, Accessed on August 12, 2014. http://faostat.fao.org/site/377/default.aspx#ancor

Field, E. H. 2005. Probabilistic seismic hazard analysis (PSHA): A primer. http://www.opensha.org/sites/opensha.org/files/PSHA_Primer_v2_0.pdf

Grünthal, G. (ed.), Musson, R., Schwarz, J., and Stucchi, M. 1998a. "European Macroseismic Scale 1998 (EMS-98)," Cahiers du Centre Europeen de Geodynamique et de Seismologie, Vol. 15, Luxembourg.

Gunasekera, R., Ishizawa, O., Aubrecht, C., Blankespoor, B., Murray, S., Pomonis, A., and Daniell, J. 2015. Developing an adaptive global exposure model to support the generation of country disaster risk profiles. Earth-Science Reviews, 150, 594–608.

Haldar, P, Singh, Y., Lang, D. H., and Paul, D. K. 2013. Comparison of seismic risk assessment based on macroseismic intensity and spectrum approaches using 'SeisVARA', Soil Dynamics and Earthquake Engineering.

HAZUS-MH—FEMA. 2003. "HAZUS-MH Technical Manual", Federal Emergency Management Agency, Washington, DC, U.S.A.

Heuckroth, L. E., and Karim, R. A. 1970. Earthquake history, seismicity and tectonics of the regions of Afghanistan. Seismological Center, Kabul University.

ILO. 2012. Afghanistan: Time to move to Sustainable Jobs Study on the State of Employment in Afghanistan, May 2012.

IMF. 2015. "World Economic Outlook Database October 2015" URL. https://www.imf.org/external/pubs/ft/weo/2015/02/weodata/index.aspx

Jaiswal, K. S., and D. J. Wald. 2008. "Developing a global building inventory for earthquake loss assessment and risk management." In Proceedings of 14th World Conference on Earthquake Engineering.

Jarvis, M., Lange, G. M., Hamilton, K., Desai, D., Fraumeni, B., Edens, B., and Ruta, G. 2011. *The changing wealth of nations: measuring sustainable development in the new millennium.*

Joya, O., and Ansari, M. T. 2012. "Estimating Business Fixed Investment in Afghanistan," http://www.aisa.org.af/Content/Media/Documents/Estimating-BFI-Afghan81120141314464825533 25325.pdf

Khan, S. A., Qureshi, M. A., and Scholar, P. G. 2014. Seismic Risk Assessment of Khyber Pakhtunkhwa Province Pakistan. Life Science Journal, 11(2s).

Khazai, B. 2004. GIS Approach to Seismic Slope Stability. Civil Engineering. UC Berkeley. PhD.

Malan, L. M. 2010. Sustainable construction in Afghanistan (Doctoral dissertation, Monterey, California. Naval Postgraduate School).

Maqsood, S. T., and Schwarz, J. 2008. Seismic vulnerability of existing building stock in Pakistan. In Proceedings of the Fourteenth World Conference on Earthquake Engineering, Beijing, China.

Maqsood, S. T., and Schwarz, J. 2011. Estimation of Human Casualties from Earthquakes in Pakistan—An Engineering Approach. Seismological Research Letters, 82(1), 32–41.

Maqsood, T., and Schwarz, J. 2008. Seismic Vulnerability of Existing Building Stock in Pakistan, 14th World Conference on Earthquake Engineering, October 12–17. 2008, Beijing, China.

Meinen, G., Verbiest, P., and de Wolf, P. P. 1998. Perpetual inventory method. Service lives, discard patterns, and depreciation methods. Heerlen-Voorburg: Statistics Netherlands.

Meunier, P., Hovius, N., and Haines, A. J. 2007. Regional patterns of earthquake-triggered landslides and their relation to ground motion. Geophysical Research Letters, 34(20).

Mohadjer, S., Ehlers, T. A., Bendick, R., Stübner, K., and Strube, T. 2015. A Quaternary Fault Database for Central Asia, Nat. Hazards Earth Syst. Sci. Discuss., 3, 5599–5632, doi:10.5194/nhessd-3-5599-2015.

Nehru, V., Swanson, E., and Dubey, A. 1995. A new database on human capital stock in developing and industrial countries: Sources, methodology, and results. *Journal of development Economics*, 46(2), 379–401.

National Institute of Building Sciences (NIBS) 2004. HAZUS-MH: Users's Manual and Technical Manuals. Report prepared for the Federal Emergency Management Agency, Washington, D.C.

Parker, R. 2013. Hillslope memory and spatial and temporal distributions of earthquake-induced landslides (Doctoral dissertation, Durham University).

Pitilakis et al. 2010. Physical vulnerability of elements at risk to landslides: Methodology for evaluation, fragility curves and damage states for buildings and lifelines. Deliverable 2.5 in EU FP7 research project No 226479 SafeLand: Living with landslide risk in Europe: Assessment, effects of global change, and risk management strategies.

Regional Rural Economic Regeneration Strategies (RRERS)—Provinces (34).

Ruleman, C. A., Crone, A. J., Machette, M. N., Haller, K. M., and Rukstales, K. S. 2007. Map and Database of Probable and Possible Quaternary Faults in Afghanistan, United States Geological Survey Open-File Report, 2007-1103, available at: http://pubs.usgs. gov/of/2007/1103/ (last access: July 2015).

Samangan Socio-Demographic and Economic Survey (SDES). 2015. http://cso.gov.af/Content/files/Samangan%20Report%20English%20V1_Reza_13Dec2015_webquality.pdf

Schaefer, A. M., Daniell, J. E., and Wenzel, F. 2016. The Smart Cluster Method—adaptive earthquake cluster identification and its application for declustering, in press.

Shebalin et al. 1978. Kondorskaya N. V. and Shebalin N.V. (eds). 1982. New Catalogue of strong earthquakes in the USSR from Ancient Times through 1975. 2nd edition, Boulder, Colorado, 608 pp. (1st edition, 1977, Moscow, 536 pp., in Russian).

Smyth, A. W., Deodatis, G., Franco, G., He, Y., and Gurvich, T. 2004. Evaluating earthquake retrofitting measures for schools: a cost-benefit analysis. School Safety and Security Keeping Schools Safe in Earthquakes, 208.

Social Assessment Profile Fact Sheet. 2012. (NHLP)—Provinces (34).

Socio-Economic and Demographic Profile Report. 2003–2005. Provinces (34).

Sovilla, B.; Schaer, M.; Kern, M., and Bartelt, P. 2008. Impact pressures and flow regimes in dense snow avalanches observed at the Vallée de la Sionne test site *J. Geophys.* Res., 113.

Spence, R., Coburn, A. W., and Pomonis, A. 1992. "Correlation of Ground Motion with Building Damage: The Definition of a New Damage-Based Seismic Intensity Scale," Proceedings of the Tenth World Conference on Earthquake Engineering, Madrid, Spain, Vol. 1, pp. 551–556.

Steiniger, S., and Hunter, A. J. S. 2011. "Free and open source GIS software for building a spatial data infrastructure." In E. Bocher and M. Neteler (eds): Geospatial Free and Open Source Software in the 21st Century: Proceedings of the first Open-Source Geospatial Research Symposium, 2009, LNG&C, Springer, Heidelberg, pp. 247–261.

Szabo, A., and Barfield, T. J. 1991. Afghanistan: an atlas of indigenous domestic architecture. Thomas Barfield.

Szeliga, W., Bilham, R., Kakar, D. M., and Lodi, S. H. 2012. Interseismic strain accumulation along the western boundary of the Indian subcontinent. *Journal of Geophysical Research: Solid Earth* (1978–2012), 117(B8).

Szeliga, W., R. Bilham, D. M. Kakar, and S. H. Lodi. 2012. Interseismic strain accumulation along the western boundary of the Indian subcontinent, *J. Geophys. Res.*, 117, B08404, doi:10.1029/2011JB008822.

Takhar Province Socio-Demographic and Economic (SDES)—August 2015.

UNFPA. 2015. Kabul Province Socio-Demographic and Economic Survey Highlights 2015.

UNHCR http://www.unhcr.org/449aa7912.pdf

USAID. 2014. The State of Telecoms and Internet in Afghanistan (2006–2012) https://www.usaid.gov/sites/default/files/documents/1871/The%20State%20of%20Telecoms%20and%20Internet%20%20in%20Afghanistan%20(2006-2012)%20Low-Res.pdf)

USAID. 2009. Bamyan-Dushi Road Socioeconomic Baseline Study, Final Report.

Vervaeck, A., Daniell, J. E., Vitton, G., Skapski, J., Robles, C., and Kanal, A. 2010–2016. Earthquake-report.com: The best independent earthquake reporting site in the world.

WBI. 2015. "World Bank Indicators" URL: data.worldbank.org/indicator

Werner, S. D., Taylor, C. E., Cho, S., Lavoie, J-P., Huyck, C., Eitzel, C., Chung, H., and Eguchi, R. T. 2006. REDARS 2: Methodology and Software for Seismic Risk Analysis of Highway Systems MCEER-06-SP08.

Ye, L., Ma, Q., Miao, Z., Guan, H., and Zhuge, Y. 2013. Numerical and comparative study of earthquake intensity indices in seismic analysis. The Structural Design of Tall and Special Buildings, 22(4), 362–381.

Yeats, R. S., and Madden, C. 2003. Damage from the Nahrin, Afghanistan, earthquake of 25 March 2002. Seismological Research Letters, 74(3), 305–311.

Youngs, R. R., Chiou, S. J., Silva, W. J., and Humphrey, J. R. 1997. Strong ground motion attenuation relationships for subduction zone earthquakes. Seismological Research Letters, 68(1), 58–73.

Zare, M., Amini, H., Yazdi, P., Sesetyan, K., Demircioglu, M. B., Kalafat, D., and Tsereteli, N. 2014. Recent developments of the Middle East catalog. Journal of Seismology, 18(4), 749–772.

The geographical location of Afghanistan and years of environmental degradation in the country make Afghanistan highly prone to intense and recurring natural hazards such as flooding, earthquakes, snow avalanches, landslides, and droughts. These occur in addition to man-made disasters resulting in the frequent loss of live, livelihoods, and property. The creation, understanding and accessibility of hazard, exposure, vulnerability and risk information is key for effective management of disaster risk. Assuring the resilience of new reconstruction efforts to natural hazards, and maximizing the effectiveness of risk reduction investments to reduce existing risks is important to secure lives and livelihoods.

So far, there has been limited disaster risk information produced in Afghanistan, and information that does exist typically lacks standard methodology and does not have uniform geo-spatial coverage. To better understand natural hazard and disaster risk, the World Bank and Global Facility for Disaster Reduction and Recovery (GFDRR) supported the development of new fluvial flood, flash flood, drought, landslide, avalanche and seismic risk information in Afghanistan, as well as a first-order analysis of the costs and benefits of resilient reconstruction and risk reduction strategies. This publication describes the applied methods and main results of the project.

THE WORLD BANK
IBRD • IDA | WORLD BANK GROUP

GFDRR
Global Facility for Disaster Reduction and Recovery